Study and Therapeutic Interference of T Cell Function in Pressure Overload-induced Heart Failure

Thesis

Study and therapeutic interference of T cell function in pressure overload-induced heart failure

Elisa Martini

A thesis submitted for the degree of

DOCTOR OF PHILOSOPHY

The Open University

April 2017

CONTENTS

Declaration

The work described in this dissertation was performed in the IRCSS Istituto Clinico Humanitas (ICH), between February 2013 and February 2017. I declare that this dissertation has not been submitted in part or in whole to any other academic institution.

The work reported here was carried out entirely by the author, unless otherwise indicated. The results here discussed generated a paper that was recently accepted for publication in Nature Communications (Kallikourdis et al., **Nature Communications**. 2017, Mar 6; 8:14680. doi: 10.1038/ncomms14680).

Acknowledgements

I would like to thank my internal supervisor Dr Marinos Kallikourdis for his help, suggestions and guidance over these 4 years. But most of all I thank him for sharing his wisdom and for teaching through his example.

I am thankful to Prof. Condorelli for the helpful suggestions, to Mr Carullo and Dr Sardi for the technical help and good advices.

I thank my external supervisor Dr Alex Betz for his availability and for useful advice.

I thank Dr Bonecchi for providing the *Il10* KO mice.

I am thankful to present and past Kallikourdis lab members for the time spent together.

Abbreviations

Ab: Antibody

AKT: AMP-activated protein kinase

AKT-tg: AKT transgenic

AngII: angiotensin-II

ANP: atrial natriuretic peptide

APC: Antigen Presenting Cell

αSMA: smooth muscle α-actin

AT1R: angiotensin receptor 1

autoAb: auto-antibodies

β-AR: β-adrenergic receptor

BCR: B cell receptor

BMP: bone morphgenic protein

BNP: brain natriuretic peptide

Breg: regulatory B cell

Cam: calmodulim

CIA: collagen-induced arthritis

CTLA4: cytotoxic T-lymphocyte–associated antigen 4

DCM: dilated cardiomyopathy

EAE: experimental autoimmune encephalomyelitis

ECM: extracellular matrix

ET-1: endothellin-1

FOXP3: forkhead box P3

GPCR: G-protein-coupled receptors

HF: Heart Failure

HFpEF: Heart Failure with preserved Ejection Fraction

HFrEF: Heart Failure with reduced Ejection Fraction

IDO: indolemine 2,3-dioxygenase

IGF-1: insulin-like growth factor-1

IL-1b: interleukin-1

IL-6: interleukin-6

IL-10: interleukin-10

IL-17: interleukin-17

IPEX: immune dysregulation, polyendocrinopathy, enteropathy, X-linked

IRS-1: insulin receptor substrate

IS: immunological synapse

iTreg : inducible Treg

JAK/STAT: Janus Kinase Y signal transducer and activator of transcription

LV: left ventricle

MAPK: mitogen-activated protein kinase

myoFb: myofibroblasts

MHC: major histocompatibility complex

MHC-α: myosin heavy chain-alpha

MHC-β: myosin heavy chain-beta

MI: myocardial infarction

MMPs: matrix metalloproteinases

mTOR: mammalian target of rapamycin

NFAT: calcineruin-nuclear factor of T cells

nTreg: natural Treg

PD-1: programmed death-1

PI3,4P: phosphatidylinositol 3,4 bisphosphate

PI3,4,5P: phosphatidylinositol 3,4,5 triphosphate

PO: pressure overload

RA: rheumatoid arthritis

ROS: Reactive oxygen species

sIL-6R: IL-6 soluble receptor

SkA: skeletal α-actin

TAC: Transverse Aortic Constriction

T-bet (or TBX21): T-box protein

TCR: T cell receptor

TGFβ: transforming growth factor beta

TF: Transcription Factor

Th: T helpers

TLR: Toll-like receptor

TNFα: tumor necrosis factor alpha

Treg: Regulatory T cell

tTreg: thymus Treg

Publications obtained during the course of this thesis

Benedusi, V., **Martini, E.**, Kallikourdis, M., Villa, A., Meda, C. & Maggi. A. "Ovariectomy shortens the life span of female mice". **Oncotarget** 2015, May 10;6(13):10801-11

Garetto*, S., Trovato*, A. E., Lleo*, A., Sala*, F., **Martini*, E.**, Betz, A. G., Norata, G. D., Invernizzi, P. & Kallikourdis, M. "Peak inflammation in atherosclerosis, primary biliary cirrhosis and autoimmune arthritis is counter-intuitively associated with regulatory T cell enrichment". **Immunobiology**. 2015 Aug;220(8):1025-9 ***Equally contributed**

Tortarolo, M., Vallarola, A., Lidonnici, D., Battaglia, E., Gensano, F., Spaltro, G., Fiordaliso, F., Corbelli, A., Garetto, S., **Martini**, **E.,** Pasetto, L., Kallikourdis, M., Bonetto, V. & Bendotti, C. "Lack of TNF-alpha receptor type 2 protects motor neurons in a cellular model of amyotrophic lateral sclerosis and in mutant SOD1 mice but does not affect disease progression". **Journal of Neurochemistry**. 2015, Oct;135(1):109-24

Garetto*, S., Sardi*, C., **Martini**, **E.,** Roselli, G., Morone, D., Angioni, R., Cianciotti, B. C., Trovato, A. E., Franchina, D. G., Castino, G. F., Vignali, D., Erreni, M., Marchesi, F., Rumio, C. & Kallikourdis, M. "Tailored chemokine receptor modification improves homing of adoptive therapy T cells in a spontaneous tumor model." **Oncotarget**. Jul 12;7(28):43010-43026
***Equally contributed**

Sardi, C., Luchini, P., Emanuelli, A., Giannoni, A., **Martini**, **E.,** Manara, L. M., Sfondrini, L., Kallikourdis, M., Sommariva, M. & Rumio, C. "Three months of western diet induces small intestinal mucosa alteration in TLR KO mice." **Journal of Microscopy Research and Technique.** 2017 Jan 17. doi: 10.1002/jemt.22831

Kallikourdis*, M., **Martini***, **E.,** Carullo*, P., Sardi, C., Roselli, G., Greco, C. M., Vignali, D., Riva, F., Ormbostad Berre, A. M., Stølen, T. O., Fumero, A., Faggian, G., Di Pasquale, E., Elia, L., Rumio, C., Catalucci, D., Papait, R. & Condorelli+, G. "T cell costimulation blockade blunts pressure overload-induced heart failure". **Nature Communications**. 2017, Mar 6; 8:14680.
***Equally contributed**

AIM OF THE STUDY

Heart failure (HF), which is the end-stage of pathological cardiac hypertrophy, is a leading cause of hospitalization and mortality. Cardiac remodeling, hypertrophy and fibrosis characterize HF. These pathological hallmarks are accompanied by systemic inflammatory response and immune cell infiltration and activation. As clinical trials targeting pro-inflammatory cytokines in HF were unsuccessful, possibly due to redundant functions of individual cytokines, we attempted to better target cardiac inflammation in order to develop an immunotherapy for HF.

Characterizing the inflammatory response in the myocardium of the gold-standard mouse model of HF, as well as in biopsies of patients with different forms of HF, we were able to link T cells with the progression of HF. As T cells are responsible for chronic and lost-lasting immune responses we decided to use them as therapeutic target. To do so we blocked T cell costimulation through FDA-approved rheumatoid arthritis drug CTLA-4Ig (abatacept, BMS). The therapeutic effects obtained with the administration of abatacept enforced the hypothesis that T cells are involved in the pathogenesis of HF thus electing them as potentially relevant therapeutic target for patients with HF.

INTRODUCTION

Note to the reader:

This thesis describes an *immunological* study of cardiac pathology. In order for the reader to follow the work discussed, it was deemed useful to include, in the introduction, a substantial segment introducing basic concepts of cardiac pathology.

Part 1 – *Characteristics and definitions of cardiac hypertrophy and heart failure*

1.1 *Brief overview of cardiac anatomy and physiology*

The primary energetic source of eukaryotic cells is the oxidative metabolism of glucose.

Approximately 90% of the oxygen intake in eukaryotic organisms is utilized through oxidative phosphorylation (Taylor et al., 2007).

In order to distribute oxygen to all their cells, multicellular organisms have evolved cardiovascular systems. The cardiovascular system (from *Kardia* [heart] + *vasculum* [small vessel, pod]) is composed of the heart and blood vessels. The heart is a hollow muscular organ that acts as a pump allowing the circulation of a fluid, the blood, through a web of tubes that are the vessels. The muscular tissue composing the heart is the involuntary striated muscle; it is formed by sarcomeres, which are its component contractile units. Sarcomeres are, in turn, constituted by filaments of actin and myosin. Actin and myosin create, respectively, the thin and thick filaments. During contraction, the thin and thick filaments, that normally overlap, slide on each other, shortening the entire fiber.

Macroscopically, the heart is composed of four chambers separated by 4 valves: right atrium, right ventricle, left atrium and left ventricle, separated in the center by the septum. The valves

open and close in response to changes of pressure that occur during a cardiac cycle; in this way the direction of blood flow through the 4 chambers is controlled. The valves between the ventricles and the atria are called atrial-ventricular valves (AV valves) and the valve between the ventricle and the arteries are called semilunar valves.

The right atrium receives blood from peripheral tissues that subsequently pass to the right ventricle, enter the pulmonary circulation through the pulmonary artery, and thus reach the lungs. Once it arrives in the lungs, the blood uptakes oxygen and releases carbon dioxide. It then moves into the left atrium and the left ventricle, before leaving the heart through the aorta, to replenish with oxygen all the peripheral tissues.

In the duration of one heartbeat, the heart completes a cardiac cycle, which includes systole and diastole. The systole refers to the contraction phase of the myocardium, whilst the diastole is the phase during which the myocardium is relaxed. Since blood flow follows a pressure gradient from a low-pressure area to a high-pressure area, the contraction of the myocardium increases the pressure. The cardiac cycle is composed of 5 phases:

1- atrial and ventricular diastole; the atria are relaxed and receive blood from the veins whilst the ventricles have just ended the contraction phase. As long as the ventricles relax, the valves between atria and ventricles open and let the blood flow in the ventricles.
2- Atrial systole; although the majority of the blood enters the ventricles passively thanks to atrial relaxation, an extra 20% enters in consequence of atrial contraction (atrial systole).
3- Isovolumic ventricular contraction; this is the beginning of ventricular contraction (systole). The muscles start to contract from the heart apex (the lower end of the heart), the pressure inside the chamber rises and the AV valves close. The muscular fibers of the atria start to relax.
4- Ventricular ejection; the ventricles' contraction generates a pressure inside the chamber sufficiently high to open the semilunar valves. The blood is ejected into the arteries; the

high pressure of the blood freshly ejected from the ventricles makes the blood already present in the vessels move.

5- Isovolumic ventricular relaxation; at the end of the ventricular ejection, the ventricles start to relax and the pressure in the ventricles falls, blood flows back and this imposes the closure of the semilunar valves. When the ventricular pressure is lower then the atrial pressure, AV valves open and the blood accumulated inside the atria during the ventricular contraction fills the ventricles, so that a new cardiac cycle can start (Silverthorn, 2007).

1.2 *Definition of cardiac hypertrophy*

"Hypertrophy" (noun) derives from the Greek words *hyper* (above) and *trophe* (nutrition); in medical terminology it is commonly used to indicate the enlargement of an organ in consequence of the increased size of its own cells (Berenji et al., 2005). The term hypertrophy, as applied to cardiology, comprises numerous pathophysiological conditions in which, in response to different stimuli, a cardiac enlargement occurs (Dorn et al. 2003). Cardiac enlargement is an adaptive and compensatory mechanism of the myocardium to overcome increased demands of cardiac work and reduce ventricular wall tension in response to stimuli of different origin (Hunter and Chien, 1999; Samak et al., 2016). In the late 19th century the Swedish physician S. Henschen first discovered, in cross-country skiers, that excessive exercise causes an enlargement of the heart accompanied by what must be inferred to be improved heart functionality. Henschen defined this condition as "athlete's heart" (Rost, 1997; Forteza-Alberti et al., 2016).

Indeed we now know that cardiac enlargement is considered physiological when it develops during exercise training, development and pregnancy; in these cases it is a mild and/or reversible condition characterized by increased maximal cardiac output and stroke volume, decreased resting heart rate and electrocardiographic changes in conduction (Mihl et al., 2008; Berenji et

al., 2005). In the same period as Henschen, Sir William Osler observed that cardiac hypertrophy can evolve from adaptive to maladaptive. Osler identified cardiac hypertrophy as the base of the development of heart failure. Whilst athlete's heart is characterized by increased heart functionality, heart failure was thus associated with decreased heart functionality. More specifically, it was linked to a reduction in the function of the cardiac ventricles (Forteza-Alberti et al., 2016). Although the hypertrophic cardiac growth is a compensatory adaptation of the myocardium in order to overcome the increased workload, in presence of chronic stimuli myocardium remodeling is irreversible. The presence of excessively increased ventricular dimensions and reduced ventricular functionality distinguish pathological cardiac growth from physiological hypertrophy**.** Eventually the myocardium pump function, which is the main means of the organisms to provide oxygen to peripheral tissues, is too compromised and heart failure develops (Grossman et al., 1975; Samak et al., 2016).

Thus, in current clinical practice, cardiac hypertrophy is classified as:

- concentric remodeling, characterized by normal cardiac mass with increased relative wall thickness
- concentric hypertrophy, when there is an increase in both relative wall thickness and cardiac mass with no changes or decrease in the chamber dimension; this is associated with increased cardiac afterload as consequence of aortic stenosis or hypertension (Gjesdal et al., 2011)
- eccentric hypertrophy, which typically evolves from increased preload conditions i.e. valvular insufficiencies, presents increased cardiac mass as well as chamber dimension whilst relative wall thickness may be normal, decreased, or increased. Developmental and physiological hypertrophies are also included in this category (Heineke and Molkentin, 2006; Berenji et al. 2005; Gjesdal et al., 2011).

Concentric and eccentric hypertrophy can be anatomically distinguished according to the orientation of newly added sarcomeres. In concentric hypertrophy sarcomeres are added in

parallel and cell growth occurs in width rather than in length. On the other hand, in eccentric hypertrophy sarcomeres are added in series to lengthen the cell. Sarcomeres are also added in series when pathological cardiac hypertrophy produces a cardiac dilation phenotype with eccentric hypertrophy and dilatory cardiac growth (Heineke and Molkentin, 2006; Gjesdal et al., 2011). The different cardiac hypertrophies can also be classified according to the type of hemodynamic stress that the myocardium undergoes: "volume-overload" usually triggers an eccentric hypertrophy whilst "pressure-overload" is more typical of concentric hypertrophy (Dorn et al., 2003; Grossman and Paulus, 2013).

1.3 *Characteristics of physiological cardiac hypertrophy*

As outlined above, physiological cardiac hypertrophy is an adaptive response to increased demands of blood and oxygen. To satisfy the augmented needs of the body the heart increases in size and often also in functionality (Shimizu and Minamino, 2016; Kemi et al., 2008; Kong et al., 2005). During the development from early age to adulthood, there is a 3-fold increase of cardiomyocyte diameter in human hearts. The increase of heart weight during this period is almost exclusively attributed to cardiomyocyte enlargement; heart weight and body weight are inherently connected (Shimizu and Minamino, 2016).

The mechanisms that activate an adaptive or a maladaptive phenotype of cardiac hypertrophy are still unknown. Considering that the physiological stress stimuli are usually discontinuous it is possible that the chronicity of the stimulus could be critical for the development towards physiological or pathological hypertrophic response (Perrino et al., 2006). Studies on animal models showed that intermittent pressure overload induces a milder hypertrophic response compared to chronic persistence of the stimulus; the same results were obtained when physical training was applied in order to induce physiological hypertrophy. Thus the cardiac hypertrophy phenotype, pathological or physiological, is depending on the nature of the stress signal,

respectively pressure-overload versus exercise training, whilst the duration is responsible for the severity (Perrino et al., 2006).

Studies on gene expression in rat models show that there is differential gene activation according to the hypertrophy phenotype. For instance in physiological hypertrophy there is an increased expression of genes involved in cell growth and metabolism, whilst on the other hand in pathological conditions there is an increased expression of genes involved in the oxidative stress response (Kong et al., 2005).

1.3.1 *Molecular pathways involved in physiological hypertrophy*

Cardiac remodeling in physiological hypertrophy differs from pathological hypertrophy also in the absence of fibrosis. This makes physiological hypertrophy a harmless and reversible condition. Physiological hypertrophy progresses via growth hormone signals and mechanical forces. Growth hormones, including thyroid hormone and insulin-like growth factor-1 (IGF-1), activate signaling pathways throughout phosphoinositide 3-kinase (PI3K), AMP-activated protein kinase (AKT) and mammalian target of rapamycin (mTOR). Signal transduction of these pathways induces cardiac growth (Shimizu and Minamino, 2016). IGF-1 has short-term insulin-like effects and long-term growth-factor effects on cell metabolism. IGF-1 activity is mediated via the binding of IGF-1 receptor; IGF-1 receptor phosphorylates the insulin receptor substrate (IRS-1 and IRS-2) initiating the intracellular signal transduction. The IGF-1 signal activates MAP kinases that trigger transcription factor activity. The effects of IGF-1 signaling in the myocardium include increased DNA and protein synthesis, reduced protein degradation and anti-apoptotic effects. IGF-1 has rapid and long-lasting effects on the cardiac tissue; in normal conditions in rat hearts this signaling improves heart functionality (Ren et al., 1999). Overexpression of IGF receptor-1 in transgenic mice induces cardiac enlargement as a consequence of an increase cardiomyocyte size and increased ventricular function. This response

was PI3K-dependent and resembles the physiological cardiac hypertrophic response (McMullen et al., 2004). Besides IGF-1 signaling, Akt/mTOR pathway is also activated in the heart during the response to training. The pathway is deactivated in pathological hypertrophy. Thus the Akt/mTOR pathway may have a key role in the differentiation between the two phenotypic hypertrophic responses (Kemi et al., 2008). Akt is a serine-threonine kinase activated by PI3K, which is activated through ligation of transmembrane receptors (including IGF-1). After activation PI3K generates phosphatidylinositol 3,4 bisphosphate (PI3,4P) and phosphatidylinositol 3,4,5 triphosphate (PI3,4,5P). Phospholipids generated from PI3K activation directly bind Akt and recruit it from the cytoplasm to the cell membrane; at this point Akt can be phosphorylated and fully activated. Activated Akt has anti-apoptotic effects and protects cardiomyocytes from cell death both in *in-vivo* ischemia-reperfusion models and in *in-vitro* cultured myocytes in serum-deprivation conditions (Fujio et al., 2000). Akt involvement in cardiomyocyte growth in physiological hypertrophy has been demonstrated in a transgenic mouse model overexpressing a constitutively cardio-specific active form of Akt (E40K mutant Akt). Transgenic Akt (Akt-tg) mice develop heart hypertrophy with increased myocardial mass and ameliorated heart functionality and contractility (Condorelli et al., 2002).

1.4 *Pathological cardiac hypertrophy*

1.4.1 *Causes and types*

Pathological cardiac hypertrophy will eventually lead to dilated cardiomyopathy (DCM); the final stage of the latter is heart failure. Heart failure occurs when the myocardium loses the capability to satisfy systemic blood and oxygen demands (Heineke and Molkentin, 2006). The causes of heart failure are several and different nature; according to the mechanisms that drive the development of HF, they can be classified in 4 categories. The first category includes both

traditional risk factors, such as hypertension and ischemic injury after myocardial infarction, coronary artery disease and metabolic syndrome, including diabetes mellitus, hyperlipidemia and obesity. The second category includes all the genetic alterations and congenital defects. Third are mechanical causes due to valve disorders, the most common of which is aortic stenosis. Aortic stenosis will induce a pressure-overload stress that initially induces cardiac hypertrophy and at the end progresses into left ventricle dysfunction. All these 3 categories are not immune-mediated but activate an inflammatory response after an initial insult. The last category of heart failure causes includes the immune-mediated factors: viral or bacterial infections or autoimmune responses (Dick and Epelman, 2016). General symptoms of heart failure are palpitations, dyspnea, fatigue, confusion, appetite loss, chronic wheezing and coughing (Latronico et al., 2008).

Patients with HF are classified according to their heart functionality; HF can be defined as HF with reduced left ventricle ejection fraction (HFrEF) whilst patients with preserved EF are classified as suffering from HFpEF. HFrEF and HFpEF patients have similar degree of cardiac impairment in terms of inability to fulfill the blood supply needs of the organism (Van Tassell et al., 2014).

As mentioned above for physiological hypertrophy, hypertrophic growth signals alter gene expression, increase protein synthesis and block protein degradation but -conversely to physiological conditions- compensatory mechanisms will lead to cardiomyocyte loss and secondary heart damage (Heineke and Molkentin, 2006; Latronico et al., 2008). Causes and effects of pathological cardiac hypertrophy are summarized in **Figure A**.

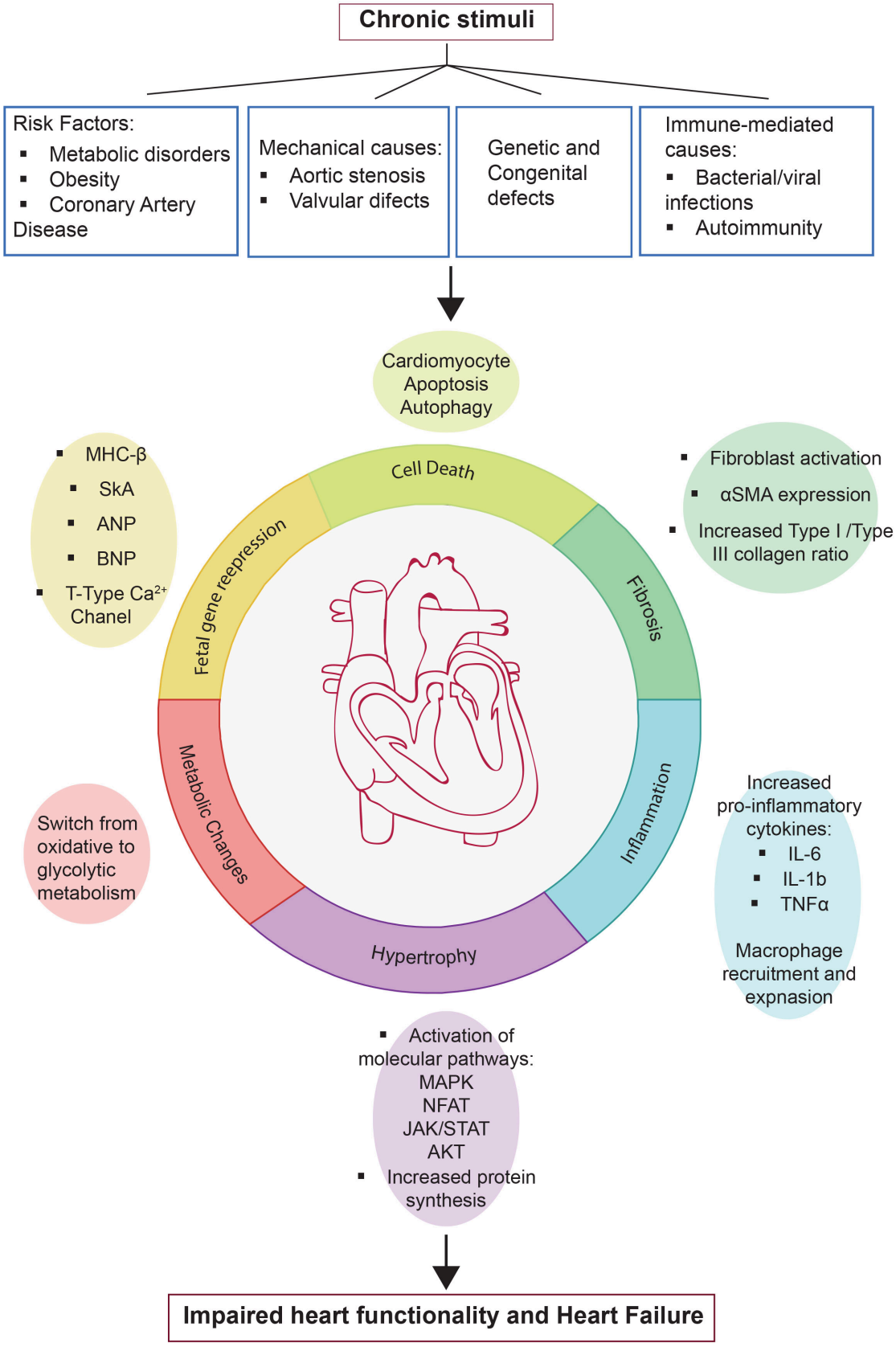

Figure A: Summary of the causes of HF and its pathological hallmarks. Chronic stimuli, including risk factors, mechanical stress, genetic alterations and infections, drive the development of HF. In pathological conditions cardiac hypertrophy is mediated by activation of specific molecular pathways (MAPK, AKT, JAK/STAT) and induces increase protein synthesis. In parallel fetal genes are re-expressed and cardiomyocyte metabolism switches from oxidative to glycolytic. Fibroblasts are activated and induce production o collagen therefore formation of fibrosis. Cardiac stress induces also production of pro-inflammatory cytokines and expansion of macrophages. These pathological hallmarks together with cardiomyocyte apoptosis and autophagy lead to impaired heart functionality and HF.

1.4.2 *Molecular pathways involved in pathological hypertrophy*

Pathological cardiac hypertrophy, besides showing alterated protein synthesis and gene expression, is characterized by cardiomyocyte metabolic changes and alterated calcium handling, cardiomyocyte apoptosis and autophagy as well as fibrosis formation in the myocardium and angiogenesis (Latronico et al., 2008; Tham, et al., 2015).

The most well-studied mediators of cardiac hypertrophy are MAPK (mitogen-activated protein kinase), NFAT (calcineruin-nuclear factor of T cells) and IGF-1-phosphatidylinositol 3-kinase (PI3K)-AKT. IGF-1 signaling is mostly associated with physiological cardiac hypertrophy, although it has been reported that activation of this pathway is present in the initial compensatory phase of pathological cardiac hypertrophy (Tham et al., 2015).

One of the main molecular pathways that induce HF progression goes through G-protein-coupled receptors (GPCR)-activating molecules such as thyroid hormones, angiotensin-II (AngII), endothellin-1 (ET-1) and α-adrenergic agonists (e.g., noradrenaline). Elevation of calcium ions (Ca^{+2}) downstream of $G\alpha_{q/\alpha11}$ subunit activates calmodulim (Cam) that can binds to NFAT, inducing its translocation into the nucleus and activation of the expression of hypertrophic genes (Tham et al., 2015; Samak et al., 2016). Activation of $G\alpha_{q/\alpha11}$ can also induce activating signals on MAPK pathways with downstream activation of p38, JNKs and ERKs. MAPK signaling promotes the gene expression of hypertrophic genes (Heineke and Molkentin, 2006).

Further, activation of Janus Kinase signal transducer and activator of transcription (JAK/STAT) has different effects on cardiac hypertrophy. Activation of the JAK/STAT pathway initially, in acute phase, promotes anti-apoptotic pathway but its chronic activation promotes inflammation and oxidative stress (Terrell et al., 2006; Shi and Wei, 2012).

1.4.3 *Hypertrophic genes*

The increase in size of cardiomyocytes is accompanied by an altered gene expression similar to that observed during fetal cardiac development; for this reason this characteristic feature of pathological hypertrophy is defined as a reactivation of fetal gene programs. This altered gene expression is considered, both in humans and in animal models, causative of the maladaptive phenotype development (Dorn et al., 2003; Samak et al., 2016; Dirkx et al., 2013). The fetal genes that are reexpressed during HF are involved in different cellular pathways: contractility, calcium handling and cellular metabolism (Dirkx et al., 2013). Contractile protein cardiac myosin heavy chain-alpha (MHC-α), which is the adult predominant isoform, is substituted by myosin heavy chain-beta (MHC-β) and skeletal α-actin (SkA), which are both fetal isoforms. Indeed SkA is one of the principal components of adult skeletal thin muscles and the actin isoform of fetal heart. Normally the fetal isoforms of contractile proteins decrease after birth, in particular the gene encoding for SkA in healthy adult myocardium is completely silenced. In ventricles of mouse models of HF, the ratio α- to β-MHC is reduced and SkA expression is increased. Similarly to SkA, smooth muscle α-actin (αSMA), the principal actin isoform of the vascular and respiratory systems, is expressed in fetal heart and absent in adult cardiomyocytes. Ventricular expression of αSMA can be induced by hypertrophic stimuli. (Samak et al., 2016; Kuwahara et al., 2012; Dorn et al., 2003) Atrial and brain natriuretic peptide (ANP and BNP) are two peptides that mediate vasodilation, inhibition of renin and are anti-mitogenic; both these peptides are increased at mRNA and protein levels and can be used as marker of cardiac pathology and stress (Maisel, 2001). Finally T-type Ca^{2+} channels are abundantly expressed in fetal myocardium, normally absent in adult hearts and its expression is restricted to conduction system. In adulthood, cardiac expression of T-type Ca^{2+} channels, which can be induced in hypertrophic conditions and failing hearts, is a hallmark of arrhythmias and ventricular dysfunction (Kuwahara et al., 2012). ANP and BNP increase in hearts with depressed ventricular

functionality independently from hypertrophy; whilst αSA increases in hypertrophic mouse models during progression towards heart failure (Dorn et al., 2003).

Hypertrophic gene expression and fetal genes reactivation are regulated by transcription factors such as NFAT, MEF2, GATA4. Fetal gene activation is regulated by epigenetic changes and modifications, which potentially offer new therapeutic targets (Kuwahara et al., 2012; Dirkx et al., 2013).

1.4.4 *Animal models*

Animal models are essential to study the pathogenesis of a disease and to develop new therapeutic strategies. For cardiovascular disease studies, animal models for myocardial infarction, hypertension, HF, cardiac hypertrophy and fibrosis have been developed. For HF research, mammals of several sizes can be used: bovine, sheep, dog, pig, rabbit, rat, guinea pig, turkey, cat, and hamster. Animal models for heart failure and cardiac hypertrophy have limitations or advantages depending on the aim of the study they are used for; as for all animal models, the similarity with the human pathology needs to be taken in consideration (Hasenfuss, 1998; Rai et al., 2016). In the past, rats were extensively used for HF and cardiac hypertrophy studies. For studies on the transition from hypertrophy to HF, the three main rat models are: spontaneous or Dahl salt-sensitive hypertension models that develop reduced myocardial functionality as a consequence of hypertension, and, finally, the binding of suprarenal aorta model (Hasenfuss, 1998). Hypertension models have been developed also in mice, using chronic intravenous infusion of renin and AngII (Carnevale et al., 2014).

Thanks to the development of microsurgical procedures, in 1991 a pressure-overload (PO) induced HF mouse model was created, the Transverse Aortic Constriction (TAC) mouse model. This is currently used as gold-standard model for HF studies (Rockman et al., 1991). TAC-operated mice have a high surgical survival rate, develop left ventricle hypertrophy, reduced

cardiac functionality, increased fibrosis, and increased expression of fetal gene (i.e. ANF and Mhy7). Besides TAC, other PO mouse models are used and they include ascending aortic binding, abdominal aortic constriction, and TAC with distal left anterior coronary ligation (Rockman et al., 1991; Rai et al., 2016). PO induces early morphological changes in cardiomyocytes as soon as 2 days after TAC, with increased cardiac hypertrophy (measured as relative wall thickness as well as heart weight to body weight) and reduced endothelial cell population together with increase acute inflammatory response. After 1 week, TAC mice have increased collagen deposition and myocyte width; after 4 weeks, TAC mice present a marked heart dysfunction (Souders et al., 2012). Finally, genetic models have been developed to study the function of single genes in specific pathophysiological process such as cardiac fibrosis or hypertrophy independently from cardiac dysfunction (Rai et al., 2016).

1.5 *Fibroblasts: differentiation and functions*

The heart of vertebrates is constituted by cellular and acellular components. The cellular compartment is represented by cardiac myocytes and non-myocytes surrounded by the acellular compartment that is the extracellular matrix (ECM), which provides scaffold for individual myocytes and for the whole heart. (Gourdie et al., 2016; Baudino et al., 2006).

The acellular component, ECM, is composed by interstitial collagen, proteoglycans, glycoproteins that form a 3D network that interconnects with the cellular components. In addition to providing scaffold for both myocytes and non-myocytes, ECM also has a role in distributing mechanical forces throughout the whole heart, as well as transmitting mechanical signals to individual cells via cell surface receptors (mechanotransduction). Finally in ECM growth factors, cytokines and proteases can also be found. The ECM also participates in movement of the extracellular environment (Baudino et al., 2006; Gourdie et al., 2016).

Non-myocyte cellular components include endothelial cells, mast cells and fibroblasts. Although the bulk of myocardial volume is represented by cardiomyocytes, cardiac fibroblasts, in terms of numbers, are the most frequent cell type and have a key role in cardiac tissue. Indeed in a healthy heart 60-70% of the cells are fibroblasts and only the remaining 30-40% is composed of cardiomyocytes (Van Linthout et al., 2014). According to more detailed studies on animal models, the murine adult heart is composed by 56% cardiomyocytes, 27% fibroblasts, 7% endothelial cells and 10% vascular smooth muscle cells (Fujiu and Nagai, 2013). In adult rat hearts, 64% are fibroblasts, 30% cardiomyocytes, endothelial cells, and vascular smooth cells and only 6% are immune cells (Fujiu and Nagai, 2013).

Fibroblasts are cells of mesenchymal origin, essential for tissue remodeling. They generate and maintain the connective tissues by production of interstitial collagen (Gourdie et al., 2016; Baudino et al., 2006). The name itself *"fibroblasts"*, which derives from the Latin word *fibra (*fiber or filament*)* and from the Greek word *blastos (*germ or sprout*)*, suggests the main function of this cellular population. Fibroblasts, besides collagen production, have biochemical, paracrine and juxtacrine interactions with cardiomyocytes; and due to their ability to respond to mechanical, electrical and chemical stimuli fibroblasts have an active role in preservation of cardiac function (Kakkar and Lee, 2010; Gourdie et al., 2016; Fujiu and Nagai, 2013; Kohl et al., 2005). The interaction between fibroblasts and cardiomyocytes is essential in physiological development and remodeling as well as in response to tissue damage and under pathological conditions (Van Linthout et al., 2014; Gourdie et al., 2016). In fact, in response to stress, quiescent cardiac fibroblasts change phenotype and differentiate into myofibroblasts (myoFb). MyoFb are spindle-shaped fibroblast-smooth cell hybrid with dendritic-like processes, contractile properties and ability to produce collagen (Davis and Molkentin, 2014; Gourdie et al., 2016). MyoFb differentiation is a two-step process. Initially fibroblasts develop into proto-myofibroblasts, which express cytoplasmic actin fibers and small adhesion molecules. Thanks to adhesion molecules, proto-myofibroblasts can migrate to the wounded area where they start to

secrete collagen. Cytokines and mechanical stress induce proto-myofibroblasts to acquire a mature phenotype. Proto-myofibroblasts are highly sensitive to proinflammatory cytokines, such as interleukin-1 (IL-1), interleukin-6 (IL-6), tumor necrosis factor alpha (TNFα) and transforming growth factor beta (TGFβ); as well as vasoactive peptides such as AngII, ANP and BNP (Porter and Turner, 2009). The newly acquired phenotype can be distinguished by expression of αSMA and super-adhesion cadherin-2 and 11 proteins. At this point myoFb capability to migrate towards damaged tissue area is enhanced thank to their fully active contractile activity (Davis and Molkentin, 2014).

1.5.2 *Collagen synthesis*

Acute injury and tissue damage are usually followed by a scaring process called fibrosis, during which the deposition rate of new collagen fibers and of non-collagenous ECM is higher then the degradation (Daskalopoulos et al., 2016; Van Linthout et al., 2014). In fact, cardiac fibrosis is part of the structural remodeling that the myocardium undergoes, during several pathologies such as myocardial infarction, pathological cardiac hypertrophy and heart failure. Cardiac fibrosis has a variety of consequences. Above all, it leads to myocardium stiffness, responsible for reduced organ functionality (Kong et al., 2014; Gourdie et al., 2016; Van Linthout et al., 2014). Fibrosis formation in myocardium has two main patterns: reparative fibrosis and reactive fibrosis. Reparative fibrosis is the formation of a focal fibrotic scar and it is present mostly in myocardial infarction (MI). On the other hand, end-stage HF reactive fibrosis is a diffuse fibrosis formation in interstitial and perivascular spaces (Heymans et al., 2015). Irrespective of its etiology, cardiac fibrosis is characterized by increased deposition of both type I and type III interstitial fibrillar collagen (Van Linthout et al., 2014). The amount of collagen but also the degree of cross-linking of the fibers directly correlates to myocardial stiffness (Badenhorst et al., 2003; Daskalopoulos et al., 2016).

Collagen is a protein with a 90-120 day half-life, and can divided into 18 types. The most abundant collagen type in human connective tissues is type I; 85% of cardiac ECM is composed of type I collagen and 11% of type III collagen with a small presence of type IV and VI. The main difference between type I and type III is the level the crosslinking between the fibers: type I forms thicker fibers with more crosslinking. In cardiac fibrosis type I/ type III ratio increases (de Jong et al., 2011); in myocardial infarction animal models, type I has a more sustained upregulation compared to type III collagen. Even if it is not the most abundant collagen form, non-fibrillar type VI collagen can activate fibroblasts as well as induce *in-vitro* transdifferentiation from fibroblasts to myoFb. Type VI collagen effects in vivo are still controversial as it has also been shown to disrupt the fibrotic process and improve cardiac function after myocardial infarction (Naugle et al., 2006; Kong et al., 2014).

1.5.3 *Regulation of cardiac fibroblast activation and fibrosis*

Exposure to stress induces fibroblast proliferation and differentiation; in fact hypoxia, mechanical stress (hypertension) and inflammation can trigger fibrosis. AngII, TGFβ, and other molecules can stimulate fibroblast differentiation and consequently lead to cardiac fibrosis.

TGF-β is a class of cytokines that includes 3 isoforms. TGFβ is produced by platelets, immune cells such as macrophages, injured epithelial cells and fibroblasts in response to inflammation (Tomasek et al., 2002). Among the several activities in which they are involved, we can list regulation of inflammatory response, ECM deposition, cell proliferation and differentiation (Dobaczewski et al., 2011).

TGF-β in cardiac injuries has a plethora of effects. First of all, together with collagen VI deposition, it can control fibroblast phenotype, inducing αSMA expression (Kong et al., 2014). Even though αSMA expression in myoFb can be directly increased also by mechanical stress, TGFβ presence is essential to fully trigger myoFb differentiation (Kong et al., 2014). TGFβ

induces focal adhesions and stress fibers, important for the transition from pro-myoFb to mature myoFb (Tomasek et al., 2002).

TGFβ increases ECM synthesis, inhibits Matrix Metalloproteinase (MMP) activity and induces tissue inhibitors of metalloproteinases (TIMPs) (Dobaczewski et al., 2011). MMPs are zinc-dependent proteases synthetized mainly by fibroblasts and existing in more than 20 types. MMP-1, MMP-8 and MMP-13, also known as collagenase, cleave type I and III collagen into 2 fragments that will denature at physiological conditions and be digested by MMP-2 and MMP-9, known as gelatinases. MMP-9 can also induce profibrotic pathways and increase collagen accumulation in ECM. MMP activity is regulated by a class of enzymes known as tissue inhibitors of metalloproteinases (TIMPs). There are 4 identified types of TIMP family enzymes. TIMPs bind the catalytic site of MMPs, abolishing their cleavage activity. Furthermore TIMPs can also induce fibroblast differentiation into myoFb, induce collagen synthesis and cell proliferation. The interaction between TIMPs and MMPs is crucial in all collagen-related disease but also in tumor metastasis process (de Jong et al., 2011). TGFβ is secreted as inert form and needs to be activated after secretion; MMP-2 and MMP-9 can cleave the inert form of TGFβ (Dobaczewski et al., 2011; Berk et al., 2007).

Therapeutic attempts in order to regulate cardiac fibrosis formation have been conducted in myocardial infarction animal models. Considering the importance of TGFβ signaling has been developed an orally active TGFβ Type 1 receptor (ALK5) inhibitor. ALK5 inhibitor was able to reduce collagen accumulation and cardiac hypertrophy, and improved systolic function (Tan et al., 2010).

Part 2 - *The immune system*

The immune system is a sophisticated and complex system that includes several cell populations and molecular effectors; it has evolved in order to defend the organism from pathogen infections. Vertebrates have two branches of immune defense: innate immunity, that activates a rapid defense reaction immediately after the appearance of a pathogen, and adaptive immunity that generates a highly specific response at a subsequent timepoint, which can efficiently eliminate pathogens and provides long-lasting protection. Innate immunity is composed of macrophages, neutrophils, dendritic cells (DC), mast cells, natural killer cells (NK), basophils and eosinophils. Besides cellular mediators, innate immunity acts also via activation of the complement cascade and production of inflammatory cytokines and chemokines. One of the major functions of innate immunity is to activate adaptive immunity. The latter is composed of two classes of lymphocytes: B lymphocytes (B cells) and T lymphocytes (T cells). B cells are generated in the bone marrow and are responsible for the secretion of antibodies, which are small proteins of the immunoglobulin family. On the other hand, T cells, which originate in the thymus, are divided into different classes that can either enhance the activity of other immune cells or directly eliminate infected cells (Alberts et al., 2007).

2.1 *T lymphocytes*

T cells are divided in two categories: cytotoxic T cells and T helper cells. Cytotoxic T cells are mainly responsible for the killing of infected cells while T helper cells support the activity of other cells of the immune system through cytokine production. T helper cells sustain B cell activation and antibody production; help DC to activate T cells and macrophages to eliminate pathogens, and recruit and activate cytotoxic T cells. Cytotoxic and T helper cells can be

distinguished by the expression of surface markers CD8 in cytotoxic T cells (CTL) and CD4 in T helper cells (Th) (Janeway et al., 2001).

2.1.1 *T helper cells*

CD4 Th cells are divided into several subsets: Th1, Th2, Th17, Th22, Th9 and T follicular help (Thf). The different Th classes are distinguished by their cytokine production profile, different homing chemokine receptors and specific transcription factors. The first identified and cloned classes of Th are Th1 and Th2, classified on the basis of different cytokine production (Mosmann et al., 1986). Th1 cells mainly produce INFγ, IL-2 and TNFα whilst Th2 produce IL-4, IL-5, IL-9 and IL-13. Th1 activate macrophages and respond against intracellular pathogens (Zhu and Paul, 2010). Th2 are involved in allergic reaction and asthma, inducing IgE production, elimination of extracellular pathogens such as helminths, alternative activation of macrophages and can also affect epithelial cells (Zhu, 2015). The later discovered Th17, which are generated in response to IL-6 and IL-23, produce IL-17a, IL-17f, IL-21 and IL-22 (Zhu and Paul, 2010). Th17 are involved in many autoimmune diseases and in the defense against extracellular pathogens. Other subsets are Th22 that activate response against Gram-negative bacteria, Th9 that are involved in asthma, and Tfh that have essential functions in germinal centers (Cosmi et al., 2014). The classes of T helper cells are distinguished by the expression of master transcription factors. Each class is involved in different aspects of the immune response, producing different cytokines and utilizing different chemokines and chemokines receptors to migrate to the site of infection (Janeway et al., 2001). Indeed T helper cells differentiate from naïve $CD4^+$ T cells in response to cytokines present in the microenvironment, which differ according to the nature of the pathogen. The naïve T cells upregulate specific transcription factors, which are crucial for the differentiation of each class (Zhu and Paul, 2010). T-box protein (T-bet or TBX21) is the transcription factor that mediates Th1 differentiation (Szabo et

al., 2000). T-bet binds to *Infg* promoter and induces IFNγ production; T-bet expression can redirect Th2 polarized cells into Th1 and absence of this transcription factor leads to failure of Th1 differentiation (Szabo et al., 2000; Oh and Hwang, 2014). IFNγ binding to its receptor enhances Tbet expression and activates STAT1 (Oh and Hwang, 2014). Th2 develop in response to IL-4 and IL-4R signaling activating GATA-3 and STAT6. GATA-3 is the lineage transcription factor for Th2 and regulates the expression of type-2 cytokines together with STAT6, which is necessary for chromatin remodeling of the IL-4/IL-13 locus (Szabo et al., 2000; Zhang et al., 1997).

Besides cytokine production, lymphocyte trafficking is another way to control immune responses. Recruitment of T cells in different tissues interferes with their differentiation and therefore with their functions. Upon differentiation into polarized Th subsets, the migration of the T cells is mediated by differential expression of chemokine receptors, which respond to cognate chemokines. Th1 cells express CCR2, CCR5, CXCR3 and CXCR5 thus respond to chemotactic gradients created by CCL2, CCL5, CXCL9, CXCL10 and CXCL11. Th2 express CCR3, CCR4 and CCR8 (Sallusto et al., 1998).

2.1.2 *T cell Activation and Costimulation. Role of CD80/86 and CD28.*

T cells need to be fully activated via two signals in order to function. The first is the activation of the T cell receptor (TCR) by recognition of an antigen and the second is the costimulation that occurs independently from the antigen recognition (Frauwirth and Thompson, 2002; Alberts et al., 2007). The antigen recognition by a TCR is mediated by antigen presentation from a host cell, acting as an Antigen Presenting Cell (APC), which could be dendritic cells, B cells, or macrophages. Firstly the innate immune system is activated via pattern recognition receptors that can detect microbial and viral products or microorganism-mediated metabolic changes. Activated APCs increase the amount of major histocompatibility complex (MHC) molecules on

their cell surface. MHC complexes are glycoproteins and are divided into two classes: MHC class I are expressed on the majority of the cells, except for erythrocytes, whilst MHC Class II (in mice) is expressed only on APC. MHC Class I molecules present pathogen-derived antigens on the surface of infected cells. MHC Class II molecules present antigens from pathogens that have been endocytosed by APC. For the pathogen proteins to be presented to T cells, the proteins need to be processed and a small peptidic sequence (the antigen) are bonded to the MHC. APC migrate to peripheral lymphoid organs to activate naïve T cells (Janeway et al., 2001; Alberts et al., 2007; Josefowicz et al., 2012). Yet, in order to be fully activated, T cells need to receive a second costimulatory signal. If TCR receives a very strong signal, it is possible to activate T cells in absence of costimulation. Costimulation is nonetheless critical for cell proliferation, differentiation and cytokine production; in absence of costimulation T cells undergo antigen-specific unresponsiveness (anergy) and/or apoptosis (Sharpe, 2009). Costimulation occurs via the binding of costimulatory molecules during interactions between T cells and APC. Costimulatory proteins on the surface of the APC can activate either negative or positive signals in matching receptors on the T cells. The balance between negative and positive costimulatory pathways (which may not necessarily appear concurrently) is crucial both to maximize immune responses and maintain immune tolerance. The most extensively-studied pathway for positive costimulation is via B7-1(CD80)/B7-2(CD86)-CD28. Murine T cells constitutively express CD28, whilst CD86 is constitutively expressed at low levels on the majority of APC and is quickly upregulated after APC activation; CD80 requires APC activation to be expressed. The different timing for the expression of these two receptors suggests that CD86 may be more important (Sharpe and Freeman, 2002). *Cd28*-gene deficient mice have reduced T cell activation even though not completely abrogated (Walker and Sansom, 2011). After TCR and CD28 have been engaged, T cells form stable immunological synapses (IS), necessary for the complete activation of the T cell (Sharpe, 2009). The T cell itself, after activation, exerts a costimulatory effect on the DC, reinforcing the ability of the DC to present the antigen, inducing production of

pro-inflammatory cytokines and expression of costimulatory molecules. Activated Th can proceed to expand, to induce class-switched antibody production by B cells, and induce macrophages to kill pathogens (Janeway et al., 2001). CD28 intracellular signals amplify the activation of NFkB and NFAT that is initiated by TCR signaling (Rudd et al., 2009). Besides CD28, other costimulatory molecules, such as ICOS can induce T cell differentiation and activation. ICOS ligand is expressed in many cell types, such as B cells, monocytes and DC under IFNγ stimulation (Sharpe and Freeman, 2002).

2.1.3 *Pathways inhibiting costimulation*

Immune regulation is essential for the maintenance of peripheral tolerance and to limit no-longer required immune responses. There exists a class of $CD4^+$ T cells, termed regulatory cells (Treg) that will be extensively presented in the next section. Besides the functions of Treg, immune responses are regulated via immune checkpoints and co-inhibitory receptors that can induce T cell unresponsiveness and block immune responses (Murakami and Riella, 2014). Within the B7-CD28 superfamily there are the two principal co-inhibitory receptors: programmed death-1 (PD-1) and cytotoxic T-lymphocyte–associated antigen 4 (CTLA4) (Sharpe and Freeman, 2002).

2.1.3.1 *PD-1*

PD-1, also known as CD279, was first identified on the cell surface of T cells during programmed cell death. PD-1 is an inhibitory receptor expressed on exhausted T cells, B cells and myeloid cells; it shares structural similarities with CD28 and its ligands are PD-L1 and PD-L2. PD-L1 is constitutively expressed on macrophages, resting T and B cells; its presence can also be detected on non-hematopoietic cells such as endothelial cells in the myocardium and in the placenta. Most importantly, many different tumor types express it. PD-L2 expression can be

induced on professional APC. PD-1 signaling inhibits Th and cytotoxic T cell function and induces peripheral Treg maturation (Sharpe and Freeman, 2002; Murakami and Riella, 2014). PD-1 negative function is exerted in the periphery by negatively regulating previously activated T cells, as well as blocking T cell proliferation and production of IL-2 and IFNγ. Interestingly, the binding of the two ligands seems to have opposite effects, as PD-L2 has been shown to enhance Th2 responses (Buchbinder and Desai, 2016).

2.1.3.2 *CTLA4*

CTLA4 binds CD80/CD86 in a competitive way with CD28 and with higher affinity (Buchbinder and Desai, 2016); the importance of this molecule for the maintenance of immune homeostasis is supported by the fact that *Ctla4*$^{-/-}$ mice die within 3 weeks of age because of massive organ infiltration and damage in consequence of lymphoproliferation (Waterhouse et al., 1995). CTLA4 is localized in intracellular compartments such as endosomes, Golgi network and lysosomes and is continuously internalized; thus the surface expression is very low. CTLA4 expression on the cell surface is induced by TCR ligation to MHC-peptide complexes, with the exception of Treg, which express it constitutively (Walker and Sansom, 2011). Several mechanisms of action have been proposed for CTLA4-mediated inhibitory effects on T cell activation. The described molecular mechanisms of action of CTLA4 include competitively binding to CD80/CD86 (with higher affinity than CD28), and activating indoleamine-2,3-dioxygenase (IDO) in DC, which via consumption of tryptophan and production of kynurenine inhibits DC maturation and Teff proliferation (Grohmann et al., 2002).

2.2 *Regulatory T cells*

In order to maintain immune homeostasis and control unwanted inflammatory responses, organisms have developed several regulatory mechanisms. The key mediator of these mechanisms in mammals (Andersen et al., 2012) is a class of immunosuppressive cells: regulatory T cells (Treg) (Vignali et al., 2008). Treg are characterized by the expression of CD4 and CD25 as surface markers and their differentiation is driven by and dependent on the expression of forkhead box P3 (FOXP3) transcription factor. Treg represent 10% of peripheral CD4 T cells (Wing and Sakaguchi, 2010; Hori et al., 2003). Gershon first identified an immunoregulatory T cell population in 1970, and defined them suppressor T cells (Gershon and Kondo, 1970). Suppressor T cells were at that time identified as CD8a+ cells and thus could not be distinguished from CD8 cytotoxic T cells; there were also several ambiguities in identifying genetic markers for suppressor T cells (Aluvihare et al., 2005). In 1995 Sakaguchi identified a CD4+CD25+ suppressive population of T cells; this population was able to block autoimmune responses. In fact depletion of $CD4^+$ $CD25^+$ or transfer of $CD4^+$ $CD25^-$ T cells in nude (T cell-less) mice was sufficient to induce organ-specific and systemic autoimmune responses; the reconstitution of the $CD25^+$ population was sufficient to block this effect (Sakaguchi et al., 1995). In 2001 the genetic mutation that causes the IPEX (immune dysregulation, polyendocrinopathy, enteropathy, X-linked) syndrome was identified (Bennett et al., 2001). The syndrome is caused by a mutation in the *Foxp3* gene. The orthologous gene of *Foxp3* was first identified in scurfy mice. Scurfy mice have a mutated form of Foxp3 that induces the development of an IPEX-like syndrome. IPEX is characterized by severe autoimmune syndrome in endocrine organs, manifested as diabetes and thyroiditis, hyper-IgE syndrome, exfoliative dermatitis and systemic inflammation (Bennett et al., 2001). Foxp3 is a transcription factor belonging to the *forkhead box winged helix* (Fox) transcription factors: Foxp1, Foxp2 and Foxp4. The Forkhead (FKH) domain is responsible for the nuclear localization of the protein, the DNA-

binding and for the interaction with NFAT (Andersen et al., 2012). Foxp3 expression in $CD4^+$ $CD25^-$ cells induces phenotypic and functional conversion into of effector T cells into Treg. Foxp3 presence is essential for the development and maintenance of Treg (Hori et al., 2003). The chronic ablation of Treg in diphtheria toxin receptor ($Foxp3^{DTR}$) knock-in mice causes death within a few weeks and induces a scurfy-like phenotype. The effects caused by depletion of Foxp3+ cells demonstrated that expression of Foxp3 in Treg is crucial for the maintenance and function of Treg, and that Treg are essential for immune homeostasis (Lahl et al., 2007). Although Foxp3 is a specific marker for murine Treg, in humans its expression is not as rigidly specific for Treg cells, as a small percentage of activated T cells can also express it. Indeed human Treg are usually identified using markers as $CD4^+CD25^+CD127^{low}$ in order to circumvent the problem of non-exclusive Foxp3 expression (Vignali et al., 2008).

2.2.1 *Treg development, nTreg, pTreg and iTreg*

$Foxp3^+$ Treg principally develop in the thymus and are referred as tTreg (thymus Treg) or nTreg (natural Treg). Yet Treg can also develop in the periphery, from $Foxp3^-$ conventional Th cells; these Treg have been termed pTreg (peripheral Treg); moreover since *in vitro* Treg can be generated by Il-2 and TGGF-b from naïve T cells, these have been termed iTreg (inducible Treg) (Shevach and Thornton, 2014). nTreg develop in the thymus, possibly from $CD4^+$ T cells that recognize self-antigens with higher avidity. Usually thymocytes that bind with high avidity self-antigens undergo negative selection and cell death in order to avoid the generation of self-reactive T cells (Gratz et al., 2013). $CD4^+$ that interact with self-antigens with intermediate strength may be those cells that will express Foxp3 and become nTerg. The TCR repertoire of nTreg is distinct from pTreg thus suggesting that the differentiation of pTreg occurs in a different way. It has been suggested that pTreg differentiation is driven by recognition of non-self antigens with high affinity together with suboptimal costimulation. Under homeostatic non-

inflammatory conditions, chronic exposure to non-self antigens, such as those from commensal bacteria, in the presence of high amounts of TGFβ, support the generation of pTreg (Josefowicz et al., 2012). It has also been reported that PD-1 can induce pTreg amplification: its expression on DC can induce naïve T cell differentiation into pTreg. PD-1 is then expressed on pTreg and promotes APC anergy (Murakami and Riella, 2014).

2.2.2 *Mechanisms of action of Treg*

The understanding of Treg suppressive mechanisms is crucial in order to take advantage of their capability to control immune responses. Mechanisms of suppression of Treg can be classified into 4 categories, even though studies on this question are still ongoing:

1- suppression by soluble factors
2- suppression by cytolysis
3- suppression by interference with cell metabolism
4- suppression by cell-to-cell contact with DC (Vignali 2008).

The suppression by soluble factors includes two different mechanisms. The high expression of CD25, which is the a-chain of IL-2R, on Treg cell surface is responsible for a high IL-2 consumption by Treg, therefore inducing a cytokine-deprivation-induced apoptosis in T effector cells (activated Th or CTL) (Pandiyan et al., 2007). Further, secretion of inhibitory cytokines, including IL-10, TGF-b and IL-35, mediates Treg suppressive function (Wing and Sakaguchi, 2010). IL-10 production by Treg is essential in allergic responses and asthma to control this type of immune response, as well as in inflammatory bowl diseases (Vignali et al., 2008). IL-10 deletion in Treg results in increased inflammatory responses in colon, lung and skin. This suggests that IL-10 produced by Treg is essential to block immunological hyperreactivity (Rubtsov et al., 2008).

The cytolysis of target cells by Treg is mediated in a granzyme-dependent manner. Human Treg

can express granzyme A and kill in a perforin-dependent manner activated T effector cells. Murine Treg, on the other hand, express granzyme B and thus can induce cell death in a perforin-independent way to mediate their suppressive function. Treg lacking granzyme B have reduced suppression activity *in vitro*. Treg expression of granzyme B *in vivo* has been demonstrated only in the tumor microenvironment, where Treg mediate NK cell and CD8 cell death (Vignali et al., 2008; Shevach, 2009).

Treg can interfere with cell metabolism via CD39 and CD73. CD39 and CD73 are ectoenzymes that induce pericellular secretion of cAMP, a potent inhibitor of T cell growth. The binding of cAMP to A2A receptor, besides blocking T cell proliferation, increases production of TGFb, modulates DC maturation and decreases IL-6 release (Josefowicz et al., 2012; Vignali et al., 2008; Bopp et al., 2007).

Finally Treg can modulate DC maturation via cell-mediated suppression of the expression of surface molecules. Treg interactions with DCs inhibit the formation of stable immunological synapses (Tadokoro et al., 2006; Sarris et al., 2008). Treg downmodulate DC costimulatory molecules and their ability to present antigen to Th and CTL, thus blocking full activation of the T cells (Shevach et al., 2011). Treg, both human and murine, are the only lymphocytes that highly express CTLA4 constitutively (Wing et al., 2010; Vignali et al., 2008). Blockade of CTLA4 with monoclonal antibody inhibits Treg suppressive function and induces organ-specific autoimmunity (Takahashi et al., 2000). The key role of CTLA4 in Treg is furthermore supported by the fact that the absence of this molecule on Treg results in systemic lymphoproliferation, hyper-IgE production and autoimmune reactions (Wing et al., 2008). Another Treg surface molecule that suppresses DC maturation is LAG3 (CD223) that binds MHC Class II with high affinity. The binding of LAG3 to MHC Class II induces activation of an ITIM-mediated inhibitory pathway and leads to block of DC maturation (Vignali et al., 2008; Shevach, 2009).

2.3 *CTLA4-Ig Abatacept*

CTLA4-Ig, or abatacept (Orencia; Bristol-Myers), is a human fusion protein composed by the extracellular domain of human CTLA4 fused to Fc portion of IgG1 human immunoglobulin approved in 2005 by US FDA for the treatment of Rheumatoid Arthritis (RA) patients; abatacept binds CD80/CD86, impeding CD28-mediated costimulation T cell (Moreland et al., 2006). Abatacept administration to RA efficiently reduces the symptoms, enhances Treg activity and suppresses T cell hyperactivation (Kremer et al., 2003). Besides its clinically approved application, CTLA4-Ig has been reported to inhibit specific T cell activation in other autoimmune diseases (systemic lupus erythematous and experimental autoimmune encephalomyelitis), Graft-versus-host-disease and in organ transplantation (Wu et al., 2012).

Abatacept is overall well tolerated with few allergic reactions and few adverse side effects (Moreland et al., 2006). Since Abatacept has been used in clinic for several years many clinical trials have been conducted. Data collected form 8 phase IV clinical trials reported that treatment with Abatacept in RA patients did not increase the risk of serious infections compared to other biological modifiers generally used for RA treatment; however Abatacept cannot be used in combination with other immunomodulatory drugs in order to avoid the increase risk of infections. Frequency of malignancies in patients treated with Abatacept was comparable to the frequency of RA patients that under other therapies; especially considering that some malignancies are associated with RA itself (Weinblatt et al., 2013; Askling et al., 2009). Finally the risk of autoimmune side effects what restricted to rare manifestation of psoriasis (Weinblatt et al., 2013).

2.4 *B lymphocytes*

Humoral immunity, in contrast to cell-mediated immunity, is the part of the immune response mediated by molecules secreted in body fluids. B cells represent the principal cell population of the humoral response due to their ability to produce antibodies (Janeway et al., 2001). In most mammals there exist five classes or isotypes of antibodies: IgA, IgD, IgE, IgG and IgM. The fundamental structure of an antibody monomer includes two identical light chains (L) and two identical heavy chains (H), two identical antigen-binding sites formed by the N-terminal region of the heavy and the light chain. The heavy chain constant region (C_H) determines the antibody class as each class has its own heavy chain (α, δ, ε, γ and μ). During B cell development light and heavy chains undergo molecular rearrangement of the variable (V), diversity (D) and joining (J) gene segments. This process is called, respectively for light and heavy chain, V-J and V-D-J recombination (Manis et al., 2002; Stavnezera and Amemiya, 2004; Vazquez et al., 2015). This recombination process generates a unique B cell receptor (BCR), which is a membrane-bound antibody, and determinates the antigen that will be recognized by each B cell clone. BCR expression is essential for the maturation process of B cell precursors and for their survival; mature B cells can co-express IgM and IgD when migrate from the bone marrow to the secondary lymphoid organs where start the antigen-dependent phase of maturation. The encounter of an antigen activates naïve B cells that proliferate and differentiate (Alberts et al., 2007; Cerutti et al., 2013). Th-cell mediated costimulation of B cells then determines the secretion of the soluble form of IgM and class switch, with secretion of either IgG, IgE or IgA soluble forms (Stavnezera and Amemiya, 2004).

In recent years other functions have been attributed to B cells, such as antigen presentation and cytokine production (Mauri 2012). B cells also contribute to autoimmune diseases via production of auto-antibodies (autoAb) (Korganow et al., 1999).

Immunosuppressive B cells expressing CD1d and IL-10 were identified in chronic inflammatory bowl disease mouse model, where they contribute to the suppression of inflammatory response (Mizoguchi et al., 2002). Indeed IL-10 production confers regulatory functions to B cells; hence this population is termed regulatory B cell (Breg). It has been shown that Breg can suppress inflammatory responses in different autoimmune models such collagen-induced arthritis (CIA), EAE, multiple sclerosis mouse models and colitis (Mauri and Bosma, 2012). In a healthy mouse Breg are 1-5% of the splenic or lymph nodal B cells. Breg phenotypically can be distinguished based on cell surface markers CD19, $CD1d^{high}$ and CD5. Breg cells can expand in response to signals through Toll-like receptors (TLR), BCR and CD40 stimulation *in vitro* (Floudas et al., 2016). IL-10 produced by Breg can negatively influence DC antigen presentation and inhibits IFNγ and IL-17 production, thus reducing Th1 and Th17 differentiation. Importantly, it has been shown in several mouse models that Breg via IL-10 production can positively influence generation and maintenance of Treg via CD80/CD86 interaction. (Mauri and Bosma, 2012; Floudas et al., 2016; Mann et al., 2007; Carter et al., 2011).

Part 3 - *Inflammation in cardiac hypertrophy and HF*

Cardiac remodeling, hypertrophy and fibrosis in HF are accompanied by systemic inflammatory response and immune cell infiltration and activation (Frieler and Mortensen, 2015; Hofmann and Frantz, 2013). The first description of inflammatory mediators in HF patients is from 1990 (Levine et al., 1990) and since then, the link between inflammatory response and pathology of cardiac diseases has become a distinct and growing research field (Mann, 2002). The trigger of the inflammatory response in HF is still unknown. Among the possible causes there is the mechanical stress that cardiomyocytes undergo during PO, whilst also hypoxia, together with gemneration of reactive oxygen species (ROS), is a potent inflammatory inducer (Hofmann and Frantz, 2013). In disease progression inflammatory cytokines are involved. The immune response in MI has been extensively studied; the early phases of post-MI response are different from the chronic alterations that occur in cardiac hypertrophy and HF (Frieler and Mortensen, 2015).

Three phases characterize the inflammatory response that occurs in consequence of cardiac injury:

1- production of inflammatory mediators (cytokines and chemokines)

2- recruitment of immune cells that intervene in tissue remodeling process

3- anti-inflammatory mediators that stop the inflammatory response (Ghigo et al., 2014).

3.1 *Cytokines and chemokines in HF*

Studies conducted in recent years have extensively investigated the presence and role of cytokines in HF patients and in animal models. Increase of these cytokines in the blood indicates an immune activation inside the myocardium, which can be itself a source of the circulating cytokines. (Hofmann and Frantz, 2013) The first cytokine detected in patients with HF is TNFα

in 1990 by Levin et al; since then IL-6, IL-1b and IL-18 (Hartupee and Mann, 2013) have also been identified as being present in significantly high levels in HF patients. CCL2, CCL3 and CXCL8 chemokines are also increased in the blood of HF patients (Gullestad et al., 2012). TNFα, IL-6 and IL-1b levels in plasma directly correlate with cardiac dysfunction and disease severity. They also correlate with increased mortality of HF patients (Hartupee and Mann, 2013; Gullestad et al., 2012; Frieler and Mortensen, 2015) TNFα and IL-6 increased expression has been detected also in the myocardium in HF patients, together with chemokine receptors CCR2 and CXCR1 (Gullestad et al., 2012). In particular IL-6 and TNFα are independent predictors of mortality, together with soluble forms of TNFR1 and 2 (Hartupee and Mann, 2013).

3.1.1 *TNFα*

TNFα in the myocardium has negative effects on contractility. The downstream effect of the binding to TNFR1 in the heart is a decreased release of calcium from the sarcoplasmic reticulum and a decrease of b-adrenergic receptor (Hofmann and Frantz, 2013). TNFα increase has been associated with LV dysfunction and cardiomyocytes apoptosis (Anker, 2004). Studies on animal models have demonstrated a causative link between TNFα presence and HF progression. Systemic injections of TNFα in rats can induce a dilated cardiomyocyte-like phenotype with reduced cardiac functionality; this phenotype was reversed using a chimeric fusion protein of TNFR2 with the Fc portion of an IgG1 (TNFR:Fc) acting as TNFα antagonist (Bozkurt et al., 1998). Mice with cardiac-specific overexpression of TNFα develop dilated cardiomyopathy with LV hypertrophy, fibrosis, cardiomyocyte apoptosis and reduced EF. Transgenic mice overexpressing TNFα also show increased mortality; mice that died spontaneously presented extreme heart dilatation and increased lung weight suggesting a congestive HF-like phenotype (Kubota et al., 1997). Cardiac-specific overexpression of TNFα has been shown to induce IL-1b and IL-6 expression in the myocardium (Kubota et al., 2000; Wang et al., 2007). Infusion of

TNFα in TNFR1 KO mice failed to induce IL-6 expression but IL-1b levels remained significantly high in the myocardium, meaning that the increased expression of IL-1b is independent of TNFR1 signaling (Wang et al., 2007). Cardiomyocytes and fibroblasts can express TNFα via NFkB and Ap-1 activation (Aoyagi and Matsui, 2012).

3.1.2 *IL-1b*

IL-1b in patients is detected in blood stream independently from the cause of HF; it has been detected in ischemic cardiomyopathy, hypertensive heart disease and idiopathic cardiomyopathy. Increase of IL-1b correlates with (increased left ventricle weight/body weight) in rat models of LV hypertrophy and is primarily produced by macrophages. (Sasayama et al., 2000) As for TNFα, systemic injection of IL-1b in mice can reduce LV contractility and functionality in a reversible way; indeed 5 days after the end of injections, the heart functionality was restored (Van Tassell et al., 2014; Van Tassell et al., 2013). IL-1b has a negative effect on cardiac contractility, desensitizing the β-adrenergic receptor (β-AR) and inhibiting L-type calcium channels. IL-1b can induce nitric oxide (NO) activity, increasing the aforementioned effects (Van Tassell et al., 2014). IL-1b has a synergistic effect with TNFα on heart contractility, and is also involved in arrhythmogenesis, hypertrophy and apoptosis (Anker, 2004).

3.1.3 *IL-6*

IL-6 is involved in HF pathogenesis; its effect on cardiomyocytes is more complex than the cytokines discussed above. In dog cardiomyocytes, IL-6 can be induced by both IL-1b and TNFα, while in human IL-6 is produced by cardiomyocytes and fibroblasts. IL-6 activation can occur through two different ways. First IL-6 binds to gp80 (IL-6R), activating dimerization of the receptors and gp130 signaling; gp130 is ubiquitously expressed but IL-6R expression is only

found in specific cell types. IL-6 can also function via sIL6R (soluble IL-6R), in this case IL-6 binds sIL-6R and this complex can directly activate gp130 (Szabo-Fresnais et al., 2010). Mice overexpressing IL-6 and IL-6R show a consequent constitutive activation of gp130, leading to myocardial hypertrophy (Hirota et al., 1995). IL-6 signaling in the myocardium induces a hypertrophic response. When IL-6 binds sIL-6R, it activates cellular signaling via STAT3, whilst IL-6R signaling does not phosphorylate STAT3 and does not activate an hypertrophic cellular response. (Szabo-Fresnais et al., 2010) IL-6 infusion in rats induces concentric cardiac hypertrophy, fibrosis, and myocardial stiffness. IL-6R is expressed on fibroblasts, though the induction of collagen synthesis and myoFb maturation needs the presence of IL-6 soluble receptor (sIL-6R) (Melendez et al., 2010). Under certain stress conditions, cardiomyocytes and cardiac fibroblasts can produce IL-6. In particular, cardiomyocytes do so in response to IL-1b and fibroblasts to AngII. Human cardiomyocytes in culture produce IL-6, Il-1b and IL-11 (Ancey et al., 2002). Even though many studies indicate that IL-6 has a detrimental effect on myocardium in response to stress, AngII-infusion or PO, the absence of IL-6 is not sufficient to prevent LV dysfunction in TAC mice. *Il6* KO mice that undergo TAC surgery develop similar levels of LV fibrosis and dysfunction to WT. Fetal gene expression upregulation and apoptosis were also maintained in these mice, suggesting that the cytokine is sufficient but not necessary for the progression of pathology (Lai et al., 2012). IL-6 signaling can have different effects on tissue according to the duration of expression. Indeed, acute or chronic presence of this cytokine seems to result in different outcomes. In the heart, short-term acute IL-6 presence activates compensatory mechanisms and has an anti-apoptotic effect in cardiomyocytes; chronic presence induces maladaptive cardiac hypertrophy and, as mentioned above for IL-1b and TNFα, reduces cardiac contractility acting negatively on βAR responsiveness (Fontes et al., 2015). IL-6 signaling through STA3 induces hypertrophic response; mice with cardiac-specific overexpression of STAT3 develop cardiac hypertrophy without any stimulus (Kunisada et al., 1999).

3.1.4 *CCL2/CCR2 and other chemokines*

Chemokines, which are small chemotactic cytokines, are also found to be increased in HF patients and animal HF models. Pressure overload in rats, after suprarenal aortic constriction, induces a rapid increase of CCL2 and perivascular infiltration of macrophages within 1 day after induction of the model. Block of CCL2 with neutralizing antibodies prevents TGFβ expression and fibroblast proliferation (Kuwahara et al., 2004). CCL2 in rats with hypertension induces left ventricle hypertrophy (Sasayama et al., 2000).

Human heart, both during HF and in healthy conditions, expresses high levels of CC- and CXC-chemokines (Damas et al., 2000). In addition to CCL2, the myocardium of TAC mice 7 days after PO displays an induction of CXCL2 and CXCL10. These chemokines are thought to mediate the recruitment of inflammatory cells that contribute to the fibrosis formation and it actively modulated fibroblast phenotype (Ying et al., 2009).

3.1.5 *IL-10*

Finally in the immune system, along with pro-inflammatory soluble mediators, anti-inflammatory mediators also exist; the most potent is IL-10. IL-10 can reduce production of TNFα, IL-1b and IL-6; it can also limit production of ROS and macrophage-derived nitric oxide (Anker, 2004). IL-10 administration, in TAC mice and in mice with ISO-induced cardiac hypertrophy, diminishes mortality and prevents hypertrophy. IL-10 blocks apoptosis by acting on caspase-3 activation and NFkB. *Il10* KO mice showed a worse outcome in ISO-induced cardiac hypertrophy (Verma et al., 2012). IL-10 deficiency has similar effects on AngII-injected mice. *Il10* KO mice infused with AngII develop ventricular dilation and ventricular dysfunction, were characterized by a higher increase of proinflammatory cytokines TNFα and IL-6 but also of

BNP, which is part of the fetal reactivation program characteristic of HF, compared to WT (Kwon et al., 2016).

3.1.6 *Summary of the role of cytokines in HF*

These inflammatory mediators have an active biological role in the pathogenesis of HF; this is demonstrated by the fact that many of these cytokines are sufficient to induce HF or HF-like phenotype in animal models (Mann, 2015). According to the "cytokine hypothesis" for HF progression, HF begins with the pro-inflammatory cytokines cascade within the myocardium, which spreads to the circulation, exerting deleterious effects (Seta et al.,1996).

3.2 *Cellular mediators*

During cardiac remodeling and in response to the release of cytokines, chemokines and other mediators, immune cells are recruited, affecting cardiac function (Frieler and Mortensen, 2015).

3.2.1 *Monocytes and macrophages*

Cardiac macrophages are a heterogeneous population present in health and disease (Frieler and Mortensen, 2015). Macrophage depletion in hypertensive rats shows that macrophages are necessary for cardiac repair. Depletion of macrophages via liposomal clodronate administration in hypertensive Ren-2 rats, which develop hypertension and left ventricle hypertrophy in consequence of overproduction of AngII, accelerate the progression of the disease. Rats depleted of macrophages have a higher loss of ventricular function accompanied by greater loss of cardiomyocytes. In this study, the authors focus on the augmented infiltration of CD4 hypothesizing that are Th1 or Th17 cells and suggesting that the production pro-inflammatory

cytokines by these subsets might be responsible for the deleterious effects on rats. As in the absence of macrophages they did not detect collagen deposition, they suggest that the increased severity of heart dysfunction in macrophage-depleted rats could be due to missing collagen-deposition functions mediated by macrophages, affecting the structural integrity of the heart (Zandbergen et al., 2009). However they did not consider that cardiac macrophage subsets have different phenotypes and functional roles, whilst the methods used in the study depleted all the macrophages and peripheral monocytes, irrespective of their cardio-protective or cardio-toxic function (Frieler and Mortensen, 2015). The majority of resident macrophages at the steady state do not originate from circulating monocytes. Macrophage repopulation in some tissues, such as lung, liver, bone marrow and spleen, occurs independently of circulating monocyte recruitment, via in situ proliferation. The tissue-resident macrophages are self-renewed and originate from the yolk sac (Hashimoto et al., 2013). Kidney, pancreatic, lung and splenic macrophages seem to originate from embryonic monocyte-derived macrophages whilst liver, brain and heart contain yolk sac-derived macrophages that persist in adulthood. At the steady state, in adult hearts there are two macrophage populations. The first is an embryonic lineage from monocytes and macrophages, which are $CCR2^{-}$ $CD11c^{lo}$ $Ly6C^{lo}$. The second population is more abundant and derives from blood $CCR2^{+}$ $Ly6C^{hi}$ monocytes. Following macrophage depletion, $Ly6C^{hi}$ monocytes can enter the myocardium, expand and reestablish a long-lasting population. In parallel, after depletion resident $CCR2^{-}$ macrophages also expand. After cardiac injury, IL-1b activation drives the expansion of the $CCR2^{+}$ subsets and recruitment of $CCR2^{+}$ monocytes, which once in the myocardium can differentiate into macrophages. The detrimental effects of macrophage expansion in cardiac injury are more likely due to the recruitment of circulating monocytes (Epelman et al., 2014). In AngII-induced hypertensive mouse models, circulating $CCR2^{+}$ monocytes are expanded via AT1 signaling. In mice lacking CCR2, AngII-induced aortic inflammation and remodeling is completely abolished but no effects are seen on LV hypertrophy. These findings nonetheless suggest that $CCR2^{+}$ monocyte expansion and

recruitment in the myocardium is detrimental in the cardiac injury (Ishibashi et al., 2004). Moreover, these studies suggest that the block of circulating monocytes, together with in situ expansion of resident macrophages, would lead to better outcomes in myocardial injury (Epelman et al., 2014). Rats with superrenal aortic constriction infused with CCL2 neutralizing antibody show a reduced macrophage presence in the myocardium, attenuated fibrosis and improved diastolic function (Kuwahara et al., 2004). CCL2 KO mice were refractive to AngII induced cardiac dysfunction; in fact these mice have reduced fibrosis in the myocardium, higher EF but absence of CCL2 did not affect ventricular remodeling (Haudek et al., 2010). All these studies together suggest that different cardiac macrophage populations have different functional roles and effects on cardiac injury. The recruitment via CCL2 of $CCR2^{+}$ monocytes has a negative effect on fibrosis formation and inflammation, whilst resident population with phagocytosis capacity may be cardioprotective (Frieler and Mortensen, 2015).

3.2.2 *T cells*

The inflammatory response activated by heart stress leads, as already mentioned, to increased production of inflammatory cytokines that activate myoFb and recruitment and expand macrophages; T lymphocytes are also recruited into the myocardium and are involved in the pathophysiology of HF (Frieler and Mortensen, 2015; Fujiu and Nagai, 2013).

In recent years the involvement of immune cells in the pathogenesis of cardiovascular diseases has been intensively investigated. In TAC mice, in parallel to increased expression of chemokines such as CXCL16, CXCL10, CCL17, there is an increased infiltration of CD4 and CD8 T cells and APCs ($CD11c^{hi}$ $MHCII^{hi}$). RAG2KO mice, that lack T and B cells, as well as CD8KO, CD4KO and MHCIIKO mice do not develop cardiac dilatation and preserve cardiac functionality when TAC is performed. The absence of HF induction in RA2KO can be reversed

by T cell administration. In the myocardium of RAG2KO mice, macrophage infiltration and fibrosis are also reduced (Laroumanie et al., 2014).

T cells infiltrating TAC mouse myocardium show an increased expression of adhesion molecules ICAM-1, VCAM-1 and E-selectin. *Tcra* KO mice show a preserved heart functionality after TAC, reduced cardiac hypertrophy and reduced reactivation of fetal gene expression together with less fibrosis. Depletion of T cells with anti-CD3 antibody 48 hours after TAC led to a maintained cardiac contractility, reduced fibrosis but no effects on cardiac hypertrophy (Nevers et al., 2015).

In two different models of hypertension, AngII and DOCA-salt induced, *Rag1* KO did not develop high blood pressure. Adoptive transfer of T, but not of B cells, could restore the induction of hypertension in both models. AngII induces TNFα production and CD69 expression in T cells. Angiotensin receptor KO (*At1r* KO) T cell transfer into *Rag1* KO recipients show that AngII has a small direct effect on T cells, both in activation and infiltration. Importantly, mice lacking T cells at the steady-state do no show significant differences in the blood pressure suggesting that T cells modulate hemodynamics only in the presence of pathological stimuli (Guzik et al., 2007).

L-NAME-induced hypertension in C57BL76 mice, Balb/c and SCID show significant differences in the way the different strains respond to the model induction. C57BL/6 have a more predominant Th1 response whilst Balb/c have a Th2-biased T cell activation. Blood pressure did not significantly differ in the three strains whilst C57BL/6 SCID, that lack T cells, had the lowest heart stiffness and fibrosis; Balb/c mice showed increased fibrosis, tissue stiffness and fibrillar collagen crosslinking (Yu et al., 2006). In AngII-induced hypertension, Balb/c compared to C57BL/6 show a stronger decrease in heart functionality (EF and FS). Balb/c develop an eccentric hypertrophy in response to AngII, in contrast to C57BL/6 that develop a compensatory concentric cardiac hypertrophy. Moreover Balb/c in AngII-induced hypertension present more fibrosis in the myocardium (Peng et al., 2011). Another study of TAC-operated *Rag1* KO mice

reported that there no difference in hypertrophy but increased perivascular fibrosis (Yang et al., 2012).

All of these studies taken together suggest that T cells have an active role in the mechanism underlying the pathogenesis of HF (Frieler and Mortensen, 2015).

3.2.3 *Treg cells in cardiovascular diseases*

Driven by the numerous studies cited in the previous section on inflammation and immune responses in HF, a consequent interest to find a way to inhibit these responses has been growing. As the natural controller of inflammation are Treg, several studies investigated the effects of Treg absence and Treg transfer in different cardiovascular pathologies (Meng et al., 2015). The majority of these studies focus their attention on myocardial infarction and atherosclerosis, whilst there are, nonetheless, some indications on Treg effects in cardiac hypertrophy and HF (Matsumoto et al., 2011; Tang et al., 2012; Weirather et al., 2014).

Treg control the development of atherogenic plaques; depletion of Treg in atherosclerosis-prone ApoEKO mice leads to increased plaque inflammation and infiltration of T cells and macrophages; Treg presence also increases the stability of the plaque due to increased collagen deposition. TGFβ expression is essential for the Treg to exert their beneficial effects (Ait-Oufella et al., 2006). Hypertensive mice show an increased presence of apoptotic Treg and reduced IL-10 (Matrougui et al., 2011). Treg transfer in hypertension mouse models infused with AngII or induced with L-NAME leads to a reduction in blood pressure and an improvement in endothelial relaxation of arteries accompanied by reduced T cell infiltration (Mian et al., 2016; Barhoumi et al., 2011). Arterial relaxation in hypertensive mice is restored by IL-10 produced by Treg. IL-10 induces NADPH oxidase activity that increases eNOS activation and improves arterial relaxation. Infusion of IL-10 shows effects similar to Treg transfer in hypertensive mice (Kassan et al., 2011). In AngII-infused mice, Treg transfer not only reduces blood pressure but also

ameliorates cardiac damage, cardiac hypertrophy and fibrosis. Besides the effects on inflammation and infiltration, it is notable that Treg also have a beneficial effect on electric remodeling to which AngII mice undergo (Kvakan et al., 2009). Finally one study shows the effects of Treg transfer in TAC mice, where -similar to the hypertension models- Treg are able to reduce inflammation, fibrosis and blood pressure (Kanellakis et al., 2011).

3.4 *Immunotherapies - Clinical trails with cytokine modifiers*

Considering the importance of the inflammatory response in the pathogenesis of HF and that, despite currently available therapies, HF in patients continues to progress unchecked, in recent years there have been several attempts to interfere with the response targeting proinflammatory cytokines. The choice of cytokines as targets was made in accordance with the cytokine hypothesis mentioned above (Mann, 2002). The cytokine hypothesis may be an oversimplified synthesis of the complexity of the inflammatory response within the ailing myocardium. Nevertheless several clinical trials have been conducted (Mann, 2015). Among biological modifiers targeting proinflammatory cytokines, the most promising results came from IL1b receptor antagonist anakinra. Anakinra produced encouraging results in a mouse model of myocardial infarction (mouse with LAD- left anterior descending artery- permanent binding). In this study, anakinra prevented adverse cardiac remodeling. Two small clinical trials in HF patients showed an increased exercise performance together with more oxygen consumption, but there are no data on cardiac dysfunction effects (Frieler and Mortensen, 2015; Mann, 2015).

Effects of inflammatory mediators can be modulated via transcriptional or translational approaches, binding with soluble neutralizing antibodies or with antagonist of receptors. Clinical trials with TNFα blockers can be divided into two groups using two different types of biological modifiers: TNFα decoy receptor or a neutralizing monoclonal antibody. In the first case, circulating TNFα binds to the decoy receptors instead of TNFα-receptor attached to the cells

therefore preventing intracellular signaling; in the second approach, the neutralizing antibody eliminates circulating TNFα molecules. The decoy receptor for TNFα is etanercept: a recombinant fusion protein of the human p75 subunit of TNFα-receptor and Fc fraction of human IgG1. After short phase I trials, three different clinical trials were conducted on chronic HF patients: Randomized Etanercept North American Strategy to Study Antagonism of Cytokines (RENAISSANCE) in North America, Research into Etanercept Cytokine Antagonism in Ventricular Dysfunction (RECOVER) for Europe and Australia, and a third one, pooling together the data of both trails (Randomized Etanercept Worldwide Evaluation, RENEWAL). The trials were ended prematurely due to an evident lack of benefits, increased hazard risk for death, hospitalizing and worsening of HF. Since then, prescribing guidelines for etanercept have been changed suggesting caution when prescribing etarnercept to patients with HF (Mann, 2002; Yndestad et al., 2006). The Anti-TNFα Therapy Against CHF (ATTACH) with Infliximab, a chimeric monoclonal antibody of engineered murine Fab anti-human TNFα and human Fc from IgG1, underwent the same fatal results of the trials with etanercept. The ATTACH trial was terminated early due to increased deaths in the drug group of HF patients compared to placebo. As for etanercept, prescription guidelines now report that infliximab must be administered with caution to patients with HF. All these studies had negatively affected HF patients in dose and time-dependent manner (Mann, 2002). There are several reasons for the failure of anti-TNF therapies in clinical trails. Above all, the intrinsic cytotoxic effects of these drugs should be considered; for instance Infliximab binds to TNF and fixes complement in cells expressing TNFα, therefore causing cell death. In HF, cardiomyocytes express TNFα so infliximab could directly be cytotoxic for cardiomyocytes. Also it has been suggested that in setting such as HF, etanercept could act as agonist instead of antagonist. This hypothesis is sustained by the fact that etenercept binding TNFα stabilizes the cytokine. In rheumatoid arthritis (RA), the pathology for which etanercept has been developed, TNFα is encapsulated into the synovial joints and circulating levels are relatively low; in HF the stabilization of TNFα probably increases the

already high levels of circulating TNFα. TNFα exerts a plethora of effects on myocardium. Physiological levels of this cytokine can be cardio-protective since it is involved in tissue remodeling and repair; this could explain why the phase I trail in HF patients ended with good results (Mann, 2002; Hofmann and Frantz, 2013; Mann, 2015) The failure of these trials has brought more interest on immunomodulation as therapy for HF. The use of drugs that act on systemic inflammation show a higher therapeutic potential suggesting that targeting one single cytokine at the time is not the right approach, due to the redundancy of the functions of pro-inflammatory cytokines (Yndestad et al., 2006; Hofmann and Frantz, 2013).

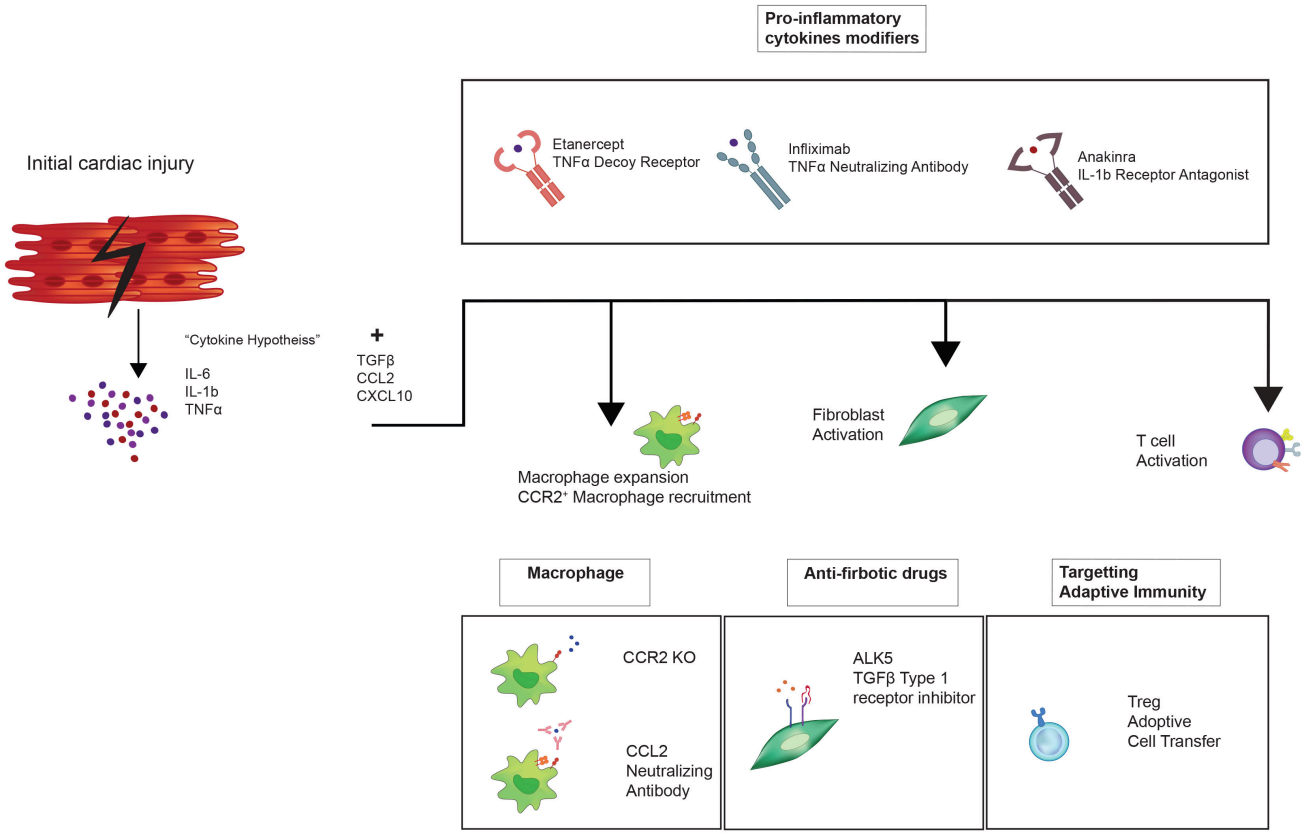

Figure B: Involvement of the immune system in the pathogenesis of HF. According to the cytokine hypothesis HF begins with the pro-inflammatory cytokines cascade that spreads to the circulation and exerts deleterious effects. Clinical trials with biological modifiers targeting TNFα and IL-1b have been conducted. Besides upregulation of pro-inflammatory cytokines, during HF there is an increase of chemokines (CCL2, CXCL10) and of TFGβ. $CCR2^{+}$ macrophages are recruited and expend, CCL2 neutralizing antibody and *Ccr2*KO mice demonstrated that the recruitment of this population is detrimental for the myocardium. Inflammation drives fibroblasts activation, TGFβ type 1 receptor inhibitor is able to block fibrosis formation. T cells infiltrate the myocardium in absence of T cells in response to stress signals myocardium show better performance. Treg cells transfer has beneficial effects on HF mouse model.

4. *MATERIALS AND METHODS*

4.1 In vivo procedures

All procedures were performed in compliance with national and EU legislation, and Humanitas Research Hospital regulations.

4.1.1 Transverse Aortic Constriction

TAC or sham for control group procedure was performed, according to (Rockman et al., 1997), on 8–10-week-old C57BL/6J male mice (Charles River, France) and on 8–10 week-old C57BL6/J *Il10* KO (Jackson Laboratories, US) male mice. All animals, prior to operation, were screened via echocardiography to establish their baseline and to eventually remove outlier subjects. Mice were anaesthetized via intraperitoneal injection of a mixture of ketamine (100mg/kg) and xilazine (10 mg/kg). In order to access the aortic arch and perform the ligation a small incision at the level of the first intercostal space was performed. With the chest cavity open it was possible to isolate the aortic arch. The ligation was performed with an 8–0 prolene suture that was placed around the aorta and with a 27G needle. The ligation was Prolene suture was performed around the needle, which was immediately removed. The removal of the needle immediately produced a stenosis in the aortic lumen. The chest cavity was then closed with one 6–0 nylon suture. All layers of muscle and skin were closed respectively with 6–0 continuous absorbable and nylon sutures. The sham control group underwent the same procedure with the exception of the final ligation. The induction of the model was then assessed measuring the differential gradient between the left and the right carotids, via echocardiography.

4.1.2 Echocardiography

Prior to echocardiography analyses mice were shaved and weighted, all the weights data were recorder and used to calculate the ratios used for the assessment of cardiac hypertrophy. Echocardiography analyses were performed on mice under anesthesia with 1.0% isoflurane.

The analyses were performed using a Vevo 2100 high-resolution in vivo imaging system (VisualSonics Fujifilm) with a MS550S probe "high frame" scanhead. Anesthetized mice were scanned for M-mode imaging. The pressure gradients were determined by echo Doppler on all animals that underwent TAC surgery and the induction of the model was considered for those animals with a gradient between 60 to 90 mm Hg.

4.1.3 Abatacept treatment

TAC and sham mice received the treatment with two different protocols.

TAC and sham mice included in the early protocol study, starting 2 days after TAC or sham surgery, were intraperitonally injected with either 100 µl PBS or 200 µg CTLA4-Ig (abatacept) in 100 µl of PBS, three times a week, for up to 4 weeks.

TAC mice included in the late protocol study, starting 2 weeks after TAC, were intraperitonally injected with either 100 µl PBS or 200 µg CTLA4-Ig (Abatacept) in 100 µl of PBS, three times a week, for up to 4 weeks. An additional group of TAC-operated mice received starting 2 days after surgery 200µg in 100µl of Human IgG Isotype Control (Novus) three times a weeks for 1 week.

An additional control group of mice did not undergo surgery and received 200 µg CTLA4-Ig (Abatacept) in 100 µl of PBS or 00µg in 100µl of Human IgG Isotype Control (Novus) three times a weeks for up to 4 weeks.

4.1.4 Adoptive transfer of wild-type B cells in *Il10* KO mice

Wild-type B cells were isolated from C57BL6/J male mice 10 weeks old. B cells were isolated via negative selection with B Cell Isolation Kit (Miltenyi Biotec). Total splenocytes were isolated; erythrocytes were lysated with Lysis Buffer (BD) and single cell suspension were counted and prepared for magnetic separation. Total splenocytes were labeled with a cocktail of biotinilated mouse antibodies for non-B cells and with anti-biotin microbeads. B cells from labeled single cell suspension were then purified on AutoMACS (Miltenyi Biotec) following "depletes" protocol. B cells were counted and purity was assessed staining with 1:100 anti-mouse CD19 (eBio1D3, eBioscience), and analyzed by flow cytometry on FACS Canto II (BD Bioscience). Purity of B cells was > 90%. On day 0 C57BL6/J *Il10* KO male mice received via intravenous injection $2 \bullet 10^6$ WT B cells. On day 1 the mice underwent echocardiographic baseline screening and on day 2 mice underwent TAC surgery. Starting 2 days after surgery, on day 4, mice were injected with 200 μg CTLA4-Ig (abatacept) in 100 μl of PBS, three times a week for 1 week.

4.1.5 Adoptive transfer of wild-type T cells in *Il10* KO mice

Wild-type T cells were isolated from C57BL6/J male mice 10 weeks olds. T cells were isolated via negative selection with Pan T Cell Isolation Kit II (Miltenyi Biotec). Total splenocytes were isolated; erythrocytes were lysated with Lysis Buffer (BD) and single cell suspension were counted and prepared for magnetic separation. Total splenocytes were labeled with a cocktail of biotinilated mouse antibodies for non-T cells and with anti-biotin microbeads. T cells from labeled single cell suspension were then purified on AutoMACS (Miltenyi Biotec) following "depletes" protocol. B cells were counted and purity was assessed staining with 1:100 anti-mouse CD3ε (145-2C11, BioLegend) and analyzed by flow cytometry on FACS Canto II (BD

Bioscience). Purity of T cells was > 90%. On day 0 C57BL6/J *Il10* KO male mice received via intravenous injection $2•10^6$ WT T cells. On day 1, mice underwent echocardiographic baseline screening and on day 2 mice underwent TAC surgery. Starting 2 days after surgery, on day 4, mice were injected with 200 µg CTLA4-Ig (abatacept) in 100 µl of PBS, three times a week for 1 week.

4.1.6 Transgenic Akt (Akt Tg) mice

Male Akt –transgenic (Akt-tg) male mice, which constitutively overexpress the active E40K Akt mutant (Akt-E40K), as previously described in (Condorelli et al., 2002) and in the discussed in introduction (Section 1.3.1) were used at 8 weeks of age. WT age-matched littler mates were used as control.

4.1.7 Exercise-trained mice

Left ventricles of exercised mice and echocardiography analyses were kindly donated by Stolen, T. O. and Ormbostad Berre A. M. Exercised and sedentary mice were BKS.Cg-m +/+ Lepdb/+db. These mice were heterozygous for the leptin receptor mutation but, when fed on a normal diet, display a wild-type metabolic phenotype. 8-week-old male mice included in the study were arbitrarily assigned to one of two groups: sedentary and exercise trained. This last group of mice was trained 80 minutes a day, 5 days a week, for 8 weeks, as previously described in (Stølen et al., 2009). Due to the difference in genetic background (BKS), all analyses of these mice were performed comparing them to their matching controls, so as to avoid genetic background-specific effects.

4.2 Human biopsies

4.2.1 Patients with laminin A/C mutations

All samples were obtained after informed consent according to the study protocols approved by the hospital's ethics committee, as described previously Roncarati, R. et al.

The severe cardiomyopathy patient samples (HF LVAD) were obtained from patients suffering from laminin A/C mutations, causing genetic form of dilated cardiomyopathy and heart failure (HF LVAD 1M). A second subset of patients carried a second mutation in titin (HF LVAD 2M), leading to a more severe dilated cardiomyopathy (Roncarati et al., 2013).

4.2.2 Patients with aortic stenosis

Ventricular samples of patients with aortic stenosis were obtained after informed consent. Samples were collected and fixed in 4% formalin at 4 °C overnight, samples were then paraffin embedded and sections of at 4μm were cut with Microtome (Microm). Sections were then used for aCD3e immunohistochemistry staining and Azan's trichrome.

4.3 Molecular biology

4.3.1 Quantitative RT-PCR analysis

Left ventricles were collected and snap frozen in liquid nitrogen, after collection samples were stored at −80°C until the RNA extraction. Tissues were homogenized in 1ml of PureZol RNA isolation reagent (Biorad) with GentleMACS and GentleMACS M Tubes (Miltenyi Biotec).

After tissue disgreagation the aqueous phase was isolated adding 200µl of chloroform (ratio chloroform/Trizol of 1:6). After collection of the aqueous phase 1.5 volumes of 100% Ethanol (EtOH) was added and immediately mixed. At this point the RNA was extracted using RNeasy Mini Kit (Qiagen) and the samples were added to the Qiagen Spin Column. RNA was then quantified with Nanodrop 2000c (Thermoscientific). The same amount of RNA was retrotranscribed with the High Capacity cDNA Reverse Transcription kit (Applied Biosystems). Real-time qPCR reactions were performed using TaqMan Probes and TaqMan Universal Master Mix on a REALTIME AB 7900HT cycler (Applied Biosystems). The following TaqMan gene expression assays were used: Rn18S (Mm03928990_g1) as internal control, *Cd3e* (Mm005996484_g1), *Foxp3* (Mm00475162_g1), *Itgam* (Mm00434455_m1), *Tnfa* (Mm00443260_g1), *Il4* (Mm00445259_m1), *Il17* (Mm00439618_m1), *Ifng* (Mm01168134_m1), *Tgfb1* (Mm01227699_m1), *Il10* (Mm00439614_m1), *Il6* (Mm00446190_m1), *Il1b* (Mm00434228_m1), *Ccl2* (Mm00441242_m1), *Ccl4* (Mm00443111_m1), Ccl5 (Mm01302427_m1), *Cxcl10* (Mm00445235_m1), *Cxcl11* (Mm00444662_m1).

Expression of genes encoding for Brain Natriuretic Peptide (*Nppb*), Atrial Natriuretic Factor (*Nppa*), and Myosin heavy chain β (*Myh7*) was assessed (IDT) using Sybr Select Master Mix (Applied Biosystems) on a ViiA7 (Applied Biosystems) instrument.

The sequences are listed in the Table:

Gene	Forward	Reverse
β-Myosin (*Mhy7*)	5'-CGCATCAAGGAGCTCACC-3'	5'-CTGCAGCCGCAGTAGGTT-3'
Brain Natriuretic Peptide (*Nppb*)	5'-GTCAGTCGTTTGGGCTGTAAC-3'	5'-AGACCCAGGCAGAGTCAGAA-3'
Atrial Natriuretic Peptide (*Nppa*)	5'-CACAGATCTGATGGATTTCAAGA-3'	5'-CCTCATCTTCTACCGGCATC-3'
18S Ribosomal RNA (18S)	5'- AAATCAGTTATGGTTCCTTTGGTC -3'	5'- GCTCTAGAATTACCACAGTTATCCAA -3'

4.4 Immunohistochemical analysis

4.4.1 Samples collection and preparation

Mouse heart samples were fixed in 4% formalin at 4 °C overnight, samples were then paraffin embedded and sections of at 4µm were cut with Microtome Leica.

4.4.2 Azan's trichrome

The slides were stained with Azan's trichrome for collagen (BioOptica). Sample sections on slides were deparaffinized and hydrated through a descending scale of alcohols. Slides were incubated in Azocarmine according to Heidenhain for 30 minutes at 56°C. Sections were washed in deionized water. Sections were than incubated in four different solutions without washing by adding 10 drops of each. At the end sections were rinsed in ascending alcohols scale. Slide images were digitalized and five fields for mouse sections and ten fields for human biopsies analyzed to quantify fibrosis, with an image analysis program (ImageJ). Cardiac fibrosis was calculated by measuring the percentage of Azan's trichrome-stained area on the total myocardial area.

4.4.3 CD3 immunohistochemistry on mouse heart samples

Sample sections on slides were deparaffinized and hydrated through a descending scale of alcohols. Antigen retrieval was performed using DIVA (Biocare Medical). Sections were cooled and then washed with 1X PBS (Lonza) + 0.05% Tween 20 (Sigma). Endogenous peroxidase were blocked by incubation with Peroxidased I (Biocare Medical) for 20 min at room temperature (RT) and nonspecific sites were blocked with Rodent Block (Biocare Medical)

20’RT. The sections were then incubated for 1h at RT with rat anti-human CD3 (Serotec) diluted 1:1000, washed, and incubated for 30 min at RT with RAT-on-mouse HRP polymer (Biocare Medical). Finally, sections were incubated with DAB (Biocare Medical), counterstained with hematoxylin, dehydrated through an ascending scale of alcohols and xylene, and mounted with coverslips using Eukitt (Fluka). All samples were observed and photographed with a microscope Olympus BX53 with a digital camera.

4.4.4 CD3 immunohistochemistry on human heart biopsies

Sample sections on slides were deparaffinized and hydrated through a descending scale of alcohols. Antigen retrieval was performed using W-Cap (Biocare Medical) at 98°C for 30 min. Sections were cooled and then washed with 1X PBS (Lonza) + 0.05% Tween 20 (Sigma). Endogenous peroxidase were blocked by incubation with Peroxidased I (Biocare Medical) for 20 min at RT and nonspecific sites were blocked with Background Sniper (Biocare Medical) 20’RT. The sections were then incubated for 1h at RT with polyclonal rabbit anti-human CD3 (Dako) diluted 1:50, washed, and incubated for 30 min at RT with Envision +System HRP anti rabbit (Dako). Finally, sections were incubated with DAB (Biocare Medical), counterstained with hematoxylin, dehydrated through an ascending scale of alcohols and xylene, and mounted with coverslips using Eukitt (Fluka). All samples were observed and photographed with a microscope Olympus BX53 with a digital camera.

4.4.5 TUNEL assay

Sample sections on slides were deparaffinized and hydrated through a descending scale of alcohols and TUNEL assay was performed (Click-it plus TUNEL assay C10617,Life technology). Slides were incubated in 4% paraformaldehyde at 37°C for 15 minutes. Slides were

then washed and permeabilized with proteinase K solution for 15 minutes. Sections were fixed for 5 minutes in 4% paraformaldehyde at 37°C. Slides were rinsed in deionized water. The terminal deoxynucleotidyl transferase (TdT) reaction was then performed. TdT enzyme incorporates dUTP at the 3'-OH ends of fragmented DNA. dUTP conjugated with Alexa-Fluor 488 was then detected and quantified. TdT Reaction buffer was added to each section, TdT enzyme and EdUTP were then added for 60 minutes at 37°C. Slides were rinsed in deionized water and washed in PBS 3% BSA 0.1% Titon X-100. Detection antibody was added and incubated. Samples digital images were acquired on fluorescent microscope Olympus IX53 with a digital camera and positive cells were counted.

4.5 Cellular biology

4.5.1 In vitro stimulation of splenocytes with Abatacept

Total splenocytes were purified from spleens of 8-week-old C57BL/6J mice. Spleens were mushed on 70µm cell strainer; erythrocytes were lysated with lysis buffer (BD Bioscience) for 5 minutes at room temperature. Plates were coated for 2 hours at room temperature with 2µg/ml of purified anti-mouse CD3ε (145-2C11, Biolegend). Splenocytes were culture with 20µg/ml Abatacept or 20µg/ml IgG isotype control (Novus) or nothing. After 72 hours of culture, Brefeldin A (eBioscience) was added during the last 4 hours of culture and splenocytes were prepared for flow cytometry analysis.

4.5.2 In vitro stimulation of splenocytes with Abatacept after T cell depletion

Total splenocytes were purified from spleens of 8-week-old C57BL/6J mice. Spleens were mushed on 70µm cell strainer; erythrocytes were lysated with lysis buffer (BD Bioscience) for 5

minutes at room temperature. Single cell suspensions were prepared for T cell isolation. T cells were depleted using Pan T Cell Isolation Kit II (Miltenyi Biotec) and AutoMACS (Miltenyi Biotec) as in 3.1.5. T cells purity and T cell depletion was assessed with 1:100 anti-mouse CD3ε (145-2C11, BioLegend) and analyzed with FACS Canto II (BD).

Splenocytes T cell-depleted were plated and activated with 2µg/ml of anti-CD3 and 5µg/ml LPS (Sigma Aaldrich). To restore T cells after depletion T cells were added to T cell-depleted splenocytes and percentage of T cells was assessed with 1:100 anti-mouse CD3ε (145-2C11, BioLegend) and analyzed with FACS Canto II (BD).

Total splenocytes or T cell-depleted splenocytes were stimulated with 2µg/ml of anti-CD3 and/or 5µg/ml LPS (Sigma Aaldrich). Splenocytes were culture with 20µg/ml abatacept or no adds. After 48 of culture, Brefeldin A (eBioscience) was added during the last 4 hours of culture and splenocytes were prepared for flow cytometry analysis.

4.5.3 *In vitro* experiments on neonatal cardiomyocytes

Hearts were collected from 1–2 day old CD1 pups and digested with 0.5% of trypsine overnight at 4°C. Cardiomyocytes were then digested in 6% of collagenase II for 5 minutes at 37°C shaking. Six subsequent digestions were performed, digested tissues were then spinned and cardiomyocytes collected. To separate cardiomyocytes from fibroblasts single cell suspensions were pre-plated twice for 1 hour. Cardiomyocytes were than plated over 0.2% of gelatin and cultured in High Glucose DMEM (Lonza) with 25% of Medium-199 (Sigma-Aldrich), 1% Penicillin-Streptomycin (Lonza), 1% glutamine (Lonza), 10% horse serum (GIBCO) and 5% of fetal bovine serum (Euroclone). Cardiomyocytes under starvation were cultured High Glucose DMEM (Lonza) with 25% of Medium-199 (Sigma-Aldrich), 1% Penicillin-Streptomycin (Lonza), 1% glutamine (Lonza). After an overnight starvation cardiomyocytes were treated with 100µM phenylephrine (PE) (Sigma Aaldrich) for 18. After 18 hours cardiomyocytes medium

was collected for ELISA assay and cells were harvested in PureZOL (Biorad) for RNA extraction and gene expression analysis of *Nppa, Nppb* and *Mhy7*.

Cardiomyocytes cultured in presence of IL-10 and IL-6 were cultured with PE for 48 hours. Four hours after the addition of PE, 10ng/ml of either murine IL-6 (R&D Systems) or murine IL-10 (Peprotech) or 20µg/ml of abatacept were added to the culture for 44 hours. Cardiomyocytes were harvested in PureZOL (Biorad) for RNA extraction and gene expression analysis of *Nppa, Nppb* and *Mhy7*.

4.5.4 IL-6 ELISA Assay

Medium from neonatal cardiomyocytes cultured with 100µM of PE for 18 hours were collected to perform Enzyme-linked immunosorbent assay (ELISA) of mouser IL-6 using Mouse Il-6 ELISA Kit (R&D System DY406). ELISA was performed on Nunc-Immuno 96-weel plates, coated with capture antibody overnight. After two washes plates were blocked adding reagent Diluent ($PBS^{-/-}$ 1% BSA) for 1 hour at room temperature. Samples and standards were added to the plates and let incubate for 2 hours at room temperature. Detection antibody and then Streptavidin-HRP were subsequently added. TMB (Thermoscientific) was added as substrate solution and to stop the colorimetric reaction H_2SO_4 2 N was added. Plates were acquired at Synergy H4 at 450nm.

4.5.5 Flow cytometry analyses

Single cell suspension were obtained form spleens and lymph nodes mushing the tissues on 70 µm cell strainers in cold $PBS^{-/-}$. Erythrocytes were removed with lysis buffer (BD Biosciences) from spleen. Cardiac infiltrate was obtained from hearts after digestion with Liberase TM (Roche). Hearts were twice digested at 37°C for 10 minutes in agitation in RPMI-1640 medium

with 0.12% of Liberase. Erythrocytes were lysated with lysis buffer (BD Biosciences). Cells from all the tissues were stained with Live/dead Aqua Fluorescent Reactive Dye (Life Technologies) diluted 1:1000 for 20 minutes at room temperature and Fc block was performed with anti-mouse CD16/32 (2.4G2, BD Pharmigen). Extracellular marker stainings were performed at 4°C for 30 minutes in 2% FBS $PBS^{-/-}$ with anti-mouse CD45 (30-F11, eBioscience), anti-mouse CD3ε (145-2C11, BioLegend), anti-mouse CD19 (eBio1D3, eBioscience), anti-mouse CD11b (M1/70, Biolegend), CD11c (Bu15, eBioscience), F4/80 (CI:A3-1, Serotec) in Figure 33, F4/80 (BM8, eBioscience) in Figure 26 and 27, Ly6C (HK1.4, eBioscience) or anti-CD25 PE (PC61.5, eBioscience).

For intracellular staining Foxp3 / Transcription Factor Staining Buffer Set (eBioscience) was used. Samples were incubated for 1 hour at 4°C with Fixation/Permeabilization buffer, and were washed twice with Permeabilization Buffer. Anti-mouse IL-10 (JES5-16E3, eBioscience) and anti-mouse FoxP3 (FJK-165, eBioscience) were incubated for 1 hours at 4°C. Samples were acquired on a FACS Canto II (BD) and analyzed with

FlowJo10.

4.6 Statistics

Statistical analysis was performed in GraphPad Prism 5 (GraphPad Software

Inc., San Diego, CA).. All data sets were tested for normal distribution prior to analyses. Normal distribution was tested using Kolmogorov-Smirnov test, D'Agostino and Pearson omnibus normality test and Sharpiro-Wilk normality test. Grubb's test was performed in order to exclude spurious outliers on data sets without normal distribution. For two groups analysis with normal distribution statistical significance was tested using unpaired t-test. Statistical significance on more then two groups with normal distribution was assessed with either one-way ANOVA with Tukey post-test or two-way ANOVA with Bonferroni post-test. Statistical significance was

tested with Mann-Whitney test in two groups without normal distribution and with one-way ANOVA with Dunn's post-test for analyses with more then two groups. Fisher's exact tests were used in the analysis of collagen deposition, testing for the presence or absence of collagen stain. P-values shown refers to the following: *, $p<0.5$, **, $p<0.01$ ***,$p<0.001$, ns = not significant ($p>0.05$).

5. RESULTS

Note:

The results described here are exclusively the work of the author; any assistance received is explicitly stated. For all cardiological mouse handling (echocardiography, TAC procedures), technical assistance was received from Mr P. Carullo of the Humanitas Cardiology Laboratory. For slide-based staining experiments (immunohistochemical staining for CD3 and Iba-1, collagen staining, TUNNEL assay) technical assistance was received from Dr C. Sardi and the Humanitas Immunohistochemistry Facility.

5.1 *Immunoprofiling of the inflammatory response in different models of cardiac hypertrophy*

It has become clear in recent years that inflammation plays an important role in the progression of HF. To better understand the pathogenesis of HF and identify potential novel therapeutic targets, we analyzed the inflammatory response in different cardiac hypertrophy models.

5.1.1 *Immunoprofiling a pathological cardiac hypertrophy model*

In order to investigate the inflammatory mediators involved in the pathological cardiac hypertrophy we utilized the TAC model, the standard model for this condition as mentioned in the Introduction (section 1.4.4). As control we utilized sham mice, both the procedures are described in Material and Methods (section 4.1.1). We analyzed the presence of cellular immune mediators and of soluble immune factors at 1 and 4 weeks after TAC surgery. 8 week-old C57BL6/J male mice underwent TAC or sham surgery after echocardiography analysis, in order to assess the heart functionality prior to disease induction, for every animal. At the moment of

sacrifice left ventricles (LV) were collected and total mRNA was extracted for gene expression analysis (**Fig.1**). As previously mentioned in the introduction, it has been shown that inflammatory cytokine production increases during cardiac hypertrophy and HF (Hofmann and Frantz, 2013); we confirmed the increase in the left ventricle at 1 week after surgery for *Il6* and *Tnfa* in TAC-operated mice compared to sham. We also analyzed the expression of several chemokines. At this early timepoint, we found a significant increase of *Ccl2*, *Ccl4*, *Ccl5*, *Cxcl10* and *Cxcl11*. The increase of these cytokines and chemokines is an indication of a type 1 (M1/Th1) polarization of the inflammatory responses. We also assessed the presence of cellular mediators; at 1 week, we found a significant increase of *Itgam* (Cd11b), which is a cellular marker for innate immune cells. Taken together, these results enable the speculation that the inflammatory response at 1 week is an innate immune even thought we cannot formally indicate which cells are mostly involved as CD11b is expressed by monocytes and macrophages. We can also speculated that is more prone towards a type 1 response as we detected an increase of TNFa, which is cytokine produced by immune cells polarized towards a type 1 response and chemokines that recruit cells that can be polarized towards a type 1 response (CCL2, CCL4, CCL5, CXCL10 and CXCL11). At 4 weeks post-TAC, we found an increase of *Il4*, which is one of the cytokines associated with a type 2 response. Moreover, we found a significant increase of *Cd3e* that is a marker for T cell presence. We speculated from these findings that at 4 weeks post-TAC, in the heart, we may have an involvement of not just innate but also adaptive immune responses. Simultaneously, the data are compatible with a switch of polarization from type 1 to type 2. The polarization of T cells towards a type 2 response has been reported to promote fibrosis formation (Wynn, 2004). The increase of *Tgfb1* at 1 week in TAC-operated mice could, indeed, be linked to fibrosis, given the role of this cytokine for fibroblast activation.

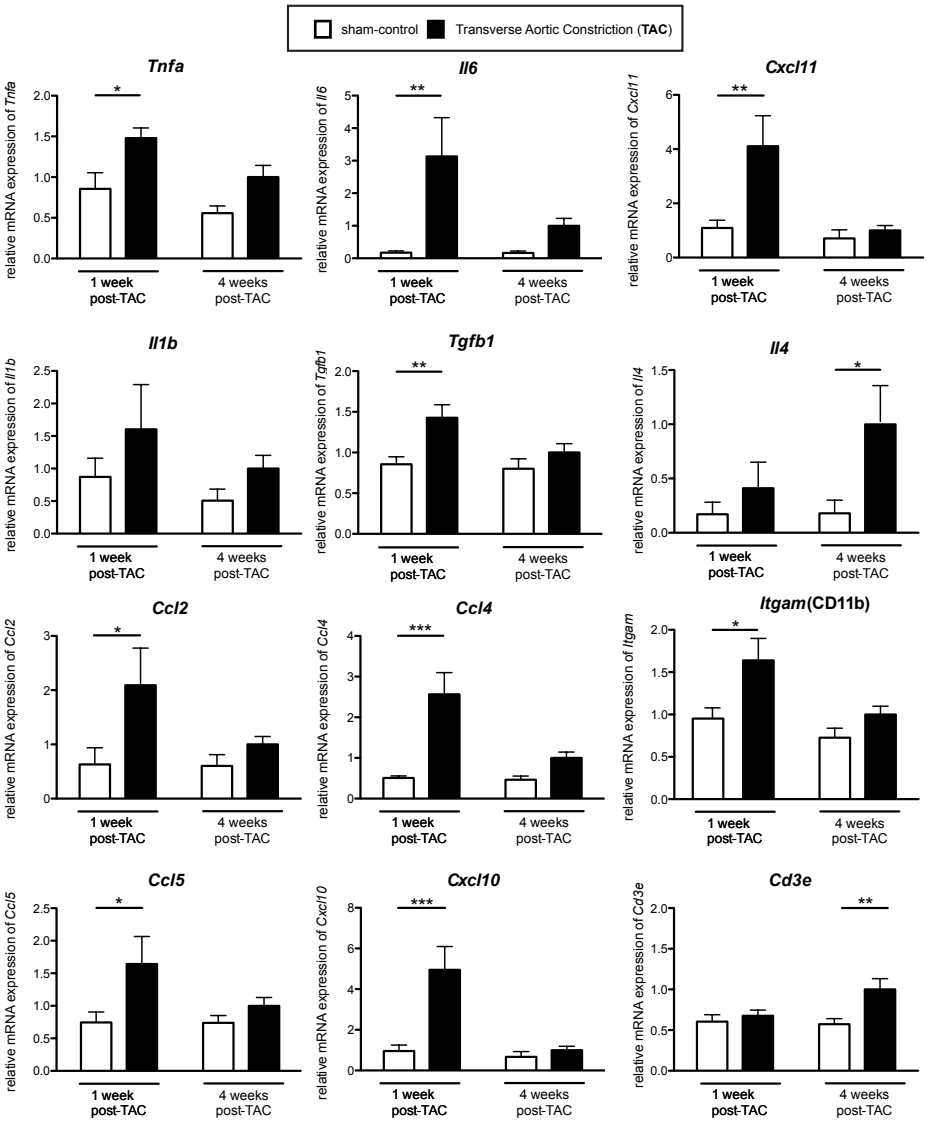

Figure 1: Characterization of the inflammatory response in left ventricle of a pathological cardiac hypertrophy model. Gene expression profile of soluble inflammatory mediators and immune cell markers in left ventricle of C57BL6/J male mice after TAC or sham surgery. Relative mRNA expression, via real-time qPCR, is normalized to 18s rRNA expression. 1 week after TAC *Tnfa, Il6, Tgfb1, Ccl2, Ccl4, Ccl5, Cxcl10, Cxcl11* and *Itgam* (CD11b) were significantly increased in the TAC group compared to sham. *Il4* and *Cd3e* were significnaly increased 4 weeks after surgery. White-bars represent sham-control mice and black bars represent TAC mice. Values are plotted as mean ± SEM (n=7-9). Two-way ANOVA, Bonferroni post-test: *, p-value <0.05; **, p-value <0.01; ***, p-value <0.001.

We also analyzed the expression of *Infg* and *Il17*, cytokines respectively associated with Th1 and Th17 responses, but we found no significant change. The same was true for *Il10* (**Fig.2**).

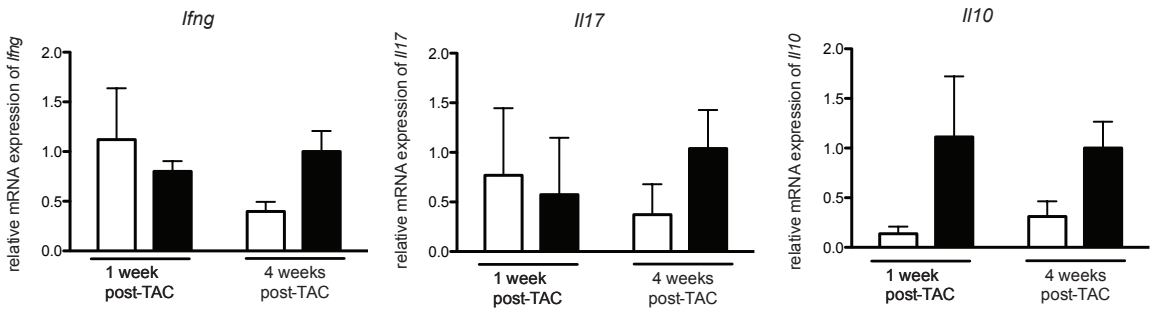

Figure 2: Characterization of the inflammatory response in left ventricle of a pathological cardiac hypertrophy model. Gene expression profile of soluble inflammatory mediators and immune cell markers in left ventricle of C57BL6/J male mice after TAC or sham surgery. Relative mRNA expression, via real-time qPCR, is normalized to 18s rRNA expression. *Infg, Il17* and *il10* were not significantly different in the TAC group compared to sham at any timepoint. White-bars represent sham-control mice and black bars represent TAC mice. Values are plotted as mean ± SEM (n=7-9). Two-way ANOVA, Bonferroni post-test.

5.1.2 *Immunoprofiling a physiological cardiac hypertrophy model*

We also analyzed the immune responses in two models of physiological cardiac hypertrophy, in order to examine their differences from pathological hypertrophy. We used a model of physiological hypertrophy induced by intense exercise and a genetic model.

5.1.2.1 *Exercise-induced physiological cardiac hypertrophy*

Physiological cardiac hypertrophy is characterized by an increase in the size of cardiomyocytes, accompanied by increased heart functionality (Stølen et al., 2009). We analyzed the gene expression of inflammatory mediators in the LV of exercised mice, compared to sedentary mice. In exercised mice we found no increase of any of the soluble mediators that characterize the inflammatory response of TAC mice (**Fig.3**). We did find a significant decrease of CCL2; as mentioned in the introduction, CCL2 in the myocardium is responsible for the recruitment of $CCR2^{+}$ monocytes that can differentiate into macrophages (Ishibashi et al., 2004; Epelman et al., 2014) and that can have detrimental effects in cardiac injury (Epelman et al., 2014). These

findings suggest that, in this model of physiological cardiac hypertrophy, not only is heart functionality increased but the inflammatory response is absent. As fibrosis absence is a hallmark of physiological cardiac hypertrophy (Daskalopoulos et al., 2016), the absence of inflammation in these mice is compatible with the role of the immune response as a main driver for fibrosis.

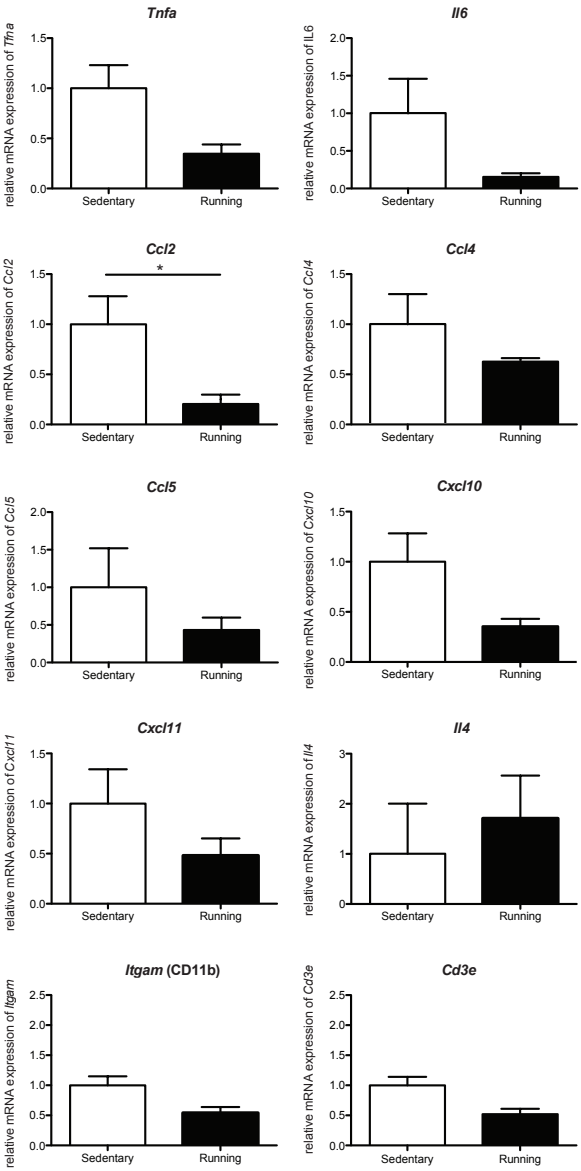

Figure 3: Characterization of the inflammatory response in left ventricle of a physiological cardiac hypertrophy model. Gene expression profile of soluble inflammatory mediators and immune cell markers in left ventricle of exercised-trained mice (running) compared to sedentary. Relative mRNA expression, via real-time qPCR, is normalized to 18s rRNA. *Tnfa, Il6, Ccl4, Ccl5, Cxcl10*, *Cxcl11, Il4, Itgam* (CD11b) and *Cd3e* were not significantly expressed in exercised-trained mice compared to sedentary. *Ccl2* significantly was decreased in the running mice. White bars are sedentary mice and black bars are exercised-trained (running) mice. Values are represented as mean ± SEM (n=3). Unpaired t-test: *, p-value <0.05.

5.1.2.2 *Characterization of the inflammatory response in Akt-transgenic mice*

Akt-transgenic mice are C57BL6/J mice overexpressing a constitutively cardio-specific active form of Akt (E40K mutant Akt). Akt mice have increased myocardial mass and ameliorated heart functionality, thus can be considered an "artificial" form of physiological hypertrophy (Condorelli et al., 2002). We performed echocardiography analysis on Akt-tg and WT littermates at 8 weeks of age. Akt-tg mice presented a marked cardiac hypertrophy. Cardiac hypertrophy was assessed at sacrifice via the calculations of 3 ratios: heart weight / body weight (HW/BW), left ventricle weight / body weight (LW/BW) and heart weight / tibial length (HW/TL). These calculations are commonly used to measure heart augmentation in relation to the size of the mouse. Akt-tg mice displayed a significant increase in all three parameters (**Fig.4**).

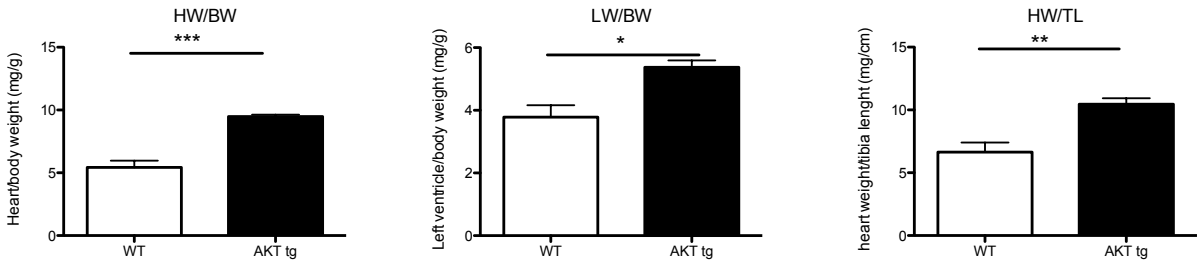

Figure 4: Assessment of AKT-transgenic mice cardiac hypertrophy.

Heart weight body weight (mg/g), left ventricle body weight (mg/g) and heart weight tibia length (mg/cm) ratios in AKT-transgenic (AKT-tg) mice compared to WT age-matched littermates display a significant increase in all these three parameters. White bars represent WT littermates and black bars represent AKT-tg mice. Values are plotted as mean ± SEM (n=6-7). Unpaired t-test: *, p-value <0.05, **, p-value <0.01; ***, p-value <0.001.

Echocardiography analysis of Akt-tg mice showed an increase in heart functionality, measured as fractional shortening (%FS) and ejection fraction (%EF) (**Fig.5**).

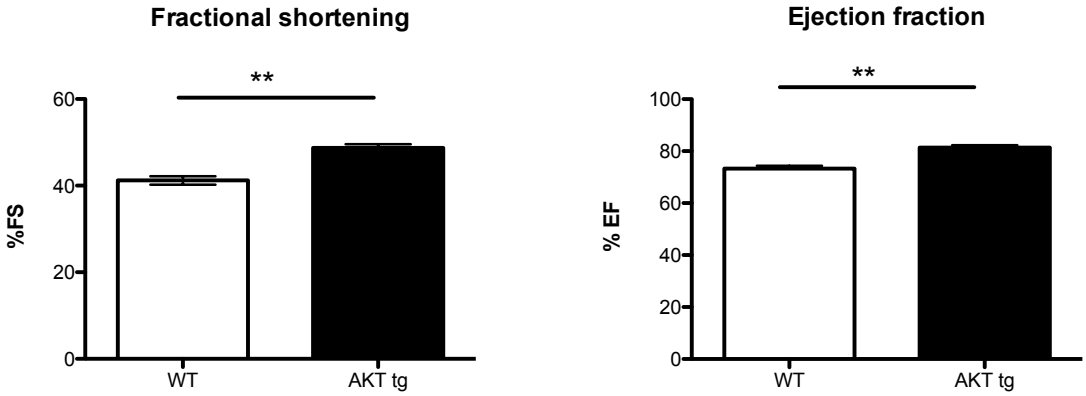

Figure 5: AKT-tg have increased heart functionality. AKT-tg mice 8 weeks old have increased heart functionality compared to age-matched WT littermates. AKT-tg (black bars) have increased fractional shortening (%FS) and ejection fraction (%EF) compared to WT (white bars). Values are plotted as mean ± SEM (n=6-7). Unpaired t-test: **, p-value <0.01.

We performed gene expression analysis for immune mediators in the left ventricle of Akt-tg mice and WT littermates (**Fig.6**). Akt-tg mice showed an increase in the expression of soluble mediators such as *Ccl4*, *Ccl5*, *Cxcl10*, *Cd3e* and *Il4*, compared to age-matched WT littermates. Akt-tg mice did also display a significant increase of cellular immune mediators. This is unlike exercise-trained mice, where a complete absence of an ongoing immune response was witnessed. This could be explained by the less "physiological" nature of the Akt-tg transgenic model (Condorelli et al., 2002) compared to the exercised mice.

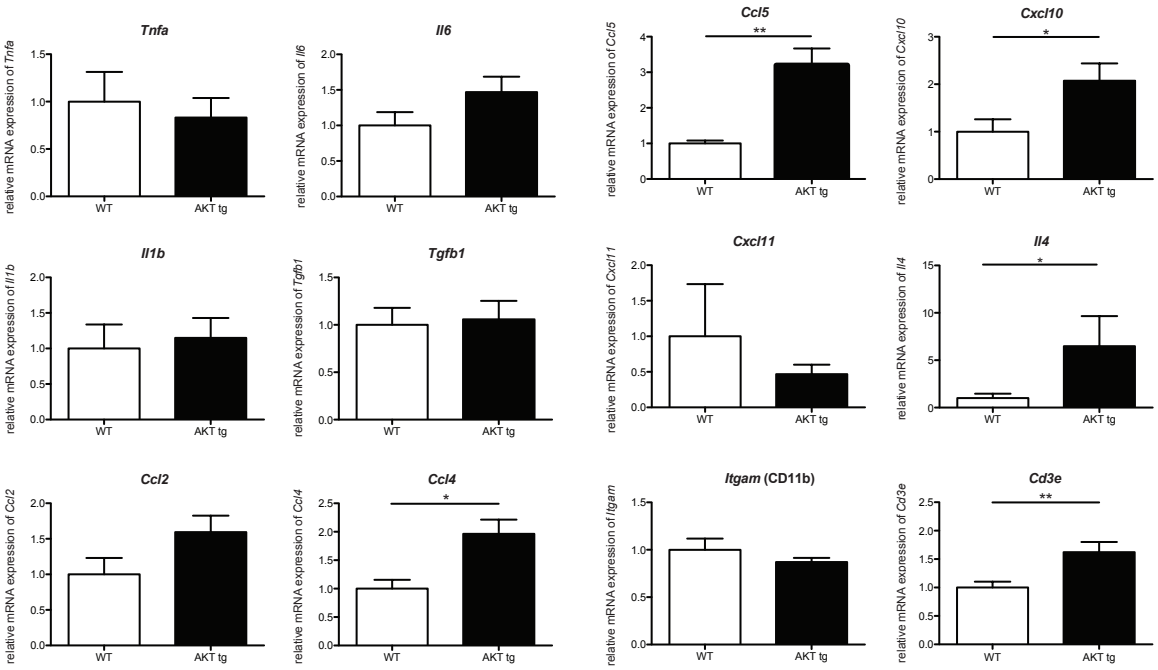

Figure 6: Characterization of the inflammatory response in the left ventricle of a physiological cardiac hypertrophy model. Gene expression profile, via TaqMan real-time qPCR, of soluble inflammatory mediators and immune cell markers in left ventricle of 8-week-old Akt transgenic mice (Akt-Tg, black bars) (n=6) compared to wild-type mice (WT, white bars) (n=7). Bars represent relative mean mRNA expression internally normalized to 18s rRNA expression. The relative expression of *Tnfa, Il6, Il1b, Tgfb1, Ccl2, Cxcl11*, and the innate cell marker *Itgam* (CD11b) did not change in AKT-tg mice, whilst *Ccl4, Ccl5, Cxcl10, Il4*, and *Cd3e* were significantly increased. Values are plotted as mean ± SEM. Mann-Whitney test: *, p-value <0.05; **, pvalue <0.01.

5.1.3 *Neonatal cardiomyocytes in presence of phenylephrine produce IL-6*

We next wondered if the inflammatory response observed in pathological hypertrophy could be the result of cardiomyocyte responses to stress conditions. The cellular stress that characterizes pathological cardiac hypertrophy could trigger expression of inflammatory cytokines. As it has already been reported in the literature that cardiomyocytes are able to produce IL-6 (Ancey et al., 2002), we first sought to confirm the expression of IL-6 in an *in-vitro* model of cardiac hypertrophy. We cultured neonatal murine cardiomyocytes (CM) with 100µM Phenylephrine (PE). PE, which is a α1-adrenergic receptor agonist, known to be potent inducer of hypertrophy. CM were cultured with PE and were collected for qPCR analysis. We found a significant

increase of IL-6 in CM after 8 hours of culture (**Fig.7A**). We also confirmed the presence of IL-6 via ELISA of the culture medium of CM (**Fig.7B**).

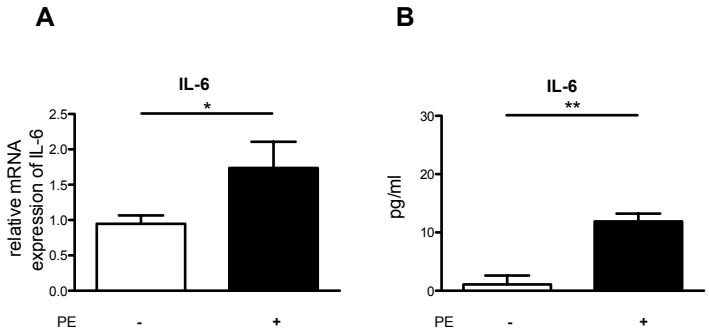

Figure 7: IL-6 production by neonatal cardiomyocytes treated with Phenylephrine. Neonatal cardiomyocytes were cultured with 100uM of phenylephrine (PE). (A) IL-6 mRNA relative expression after 8 hours of culture assessed by TaqMan real-time qPCR, internally normalized to 18s rRNA expression (n=3). (B) IL-6 protein production after 20h of culture, assayed by ELISA assay of the cell supernatants (n=6). Values are indicated as mean ± SEM. Unpaired t-tests. p value < 0.05 (*), p value < 0.01 (**).

5.1.4 *Inflammatory response in pathological cardiac hypertrophy recruits T cells into the myocardium*

5.1.4.1 *T cells infiltrate the myocardium of TAC-operated mice*

As we found a significant increase of CD3e mRNA expression in TAC mice 4 weeks after surgery, we decided to further investigate the presence of T cells in the LV of TAC-operated mice. To confirm the mRNA findings, we evaluated, via immunohistochemistry (IHC) with anti-CD3e, the presence of T cells in the myocardium of TAC- and sham-operated mice 4 weeks after surgery (**Fig.8**). We found a significant increase of T cell infiltration in TAC-operated mice compared to sham, confirming our gene expression data.

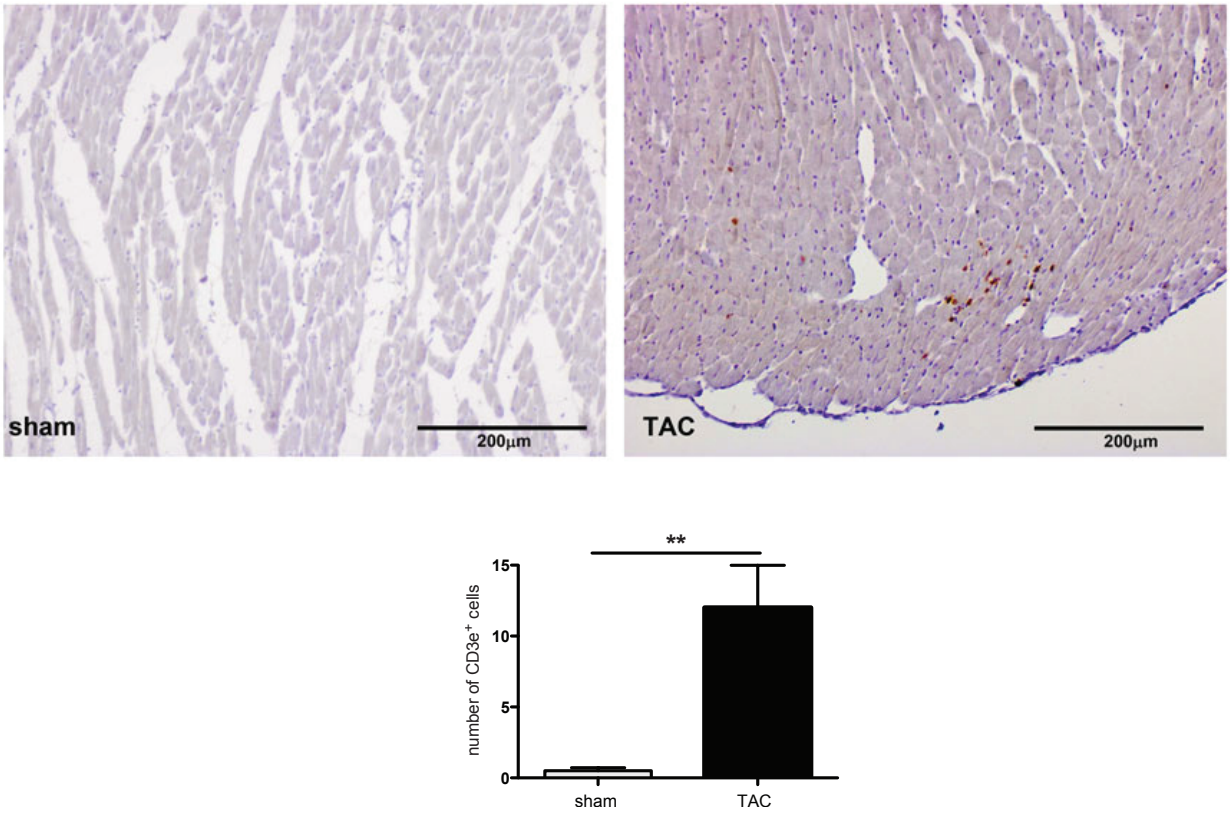

Figure 8: T cell infiltration in the myocardium of TAC-operated mice. Representative images of immunohistochemical staining (IHC) with anti-CD3e (brown color) of left ventricle of sham- and TAC-operated C57BL6/J mice 4 weeks after surgery and statistical analysis of the number of positive CD3e cells. Original magnification of the images 10X; bars = 200 µm. White bar represent sham-mice and black bar TAC-mice. Values are plotted as mean ± SEM (n=6). Unpaired t-test: **, p-value <0.01.

Having demonstrated the presence of T cells 4 weeks after the induction of the model, we hypothesized that T cells could potentially be detectable even at an earlier timepoint, even if their early presence would be too limited to lead to changes detectable by qPCR (see Fig 1). We thus assessed the presence of T cells 1 week after surgery, via IHC and we were able to detect the presence of few T cells in the myocardium of TAC-operated mice via immunohistochemistry (**Fig. 9 A**). Furthermore, we isolated infiltrating lymphocytes from single-cell cardiac suspensions via Lympholyte gradient purification, and performed flow cytometry analysis of $CD3e^+$ cells (**Fig.9 B**). We could identify a small number of $CD3e^+$ cells, thus further confirming that a small number of T cells is present as early as 1 week after TAC-surgery, before presumably expanding (or becoming further recruited) with the progression of the pathology.

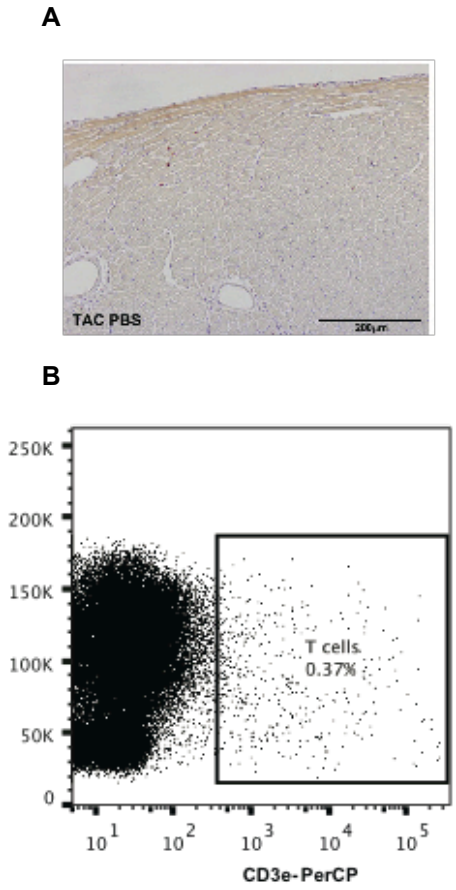

Figure 9: Presence of T cells is detectable in TAC-operated mice starting 1 week after surgery. (A) Immunohistochemical staining with anti-CD3e (brown coloration) in TAC-operated mice 1 week post-operation. Original magnification 10X; bar = 200µm (B) Representative plot of flow cytometry analysis of $CD3e^+$ cells isolated from heart of TAC mice 1 week after operation.

5.1.4.2 *Correlation between T cell presence and inflammation*

We next wondered whether the presence of inflammation correlated with T cell infiltration. Any such correlation would be compatible with the inflammation acting as the driver for T cell recruitment or expansion. To assess this, we correlated CD3e mRNA expression (as a proxy for the presence of T cells) with IL-6 mRNA expression (as a proxy for cardiac inflammation), assuming a linear regression model (**Fig.10**). TAC-operated mice 4 weeks after surgery did show a significant positive slope suggesting the existence of a correlation between inflammatory

cytokine expression and T cell infiltration in the myocardium. Each red circle represents one mouse included in the study and the red line shows the linear regression. Sham-operated mice 4 weeks after surgery also showed a significant correlation between IL-6 expression and T cell infiltration, although with lower values for both parameters. A low-grade inflammation is likely to be present in the myocardium of sham mice as a result of the (invasive, but lacking aortic ligation) sham surgery. This would confirm that sham-operation is the correct control for the

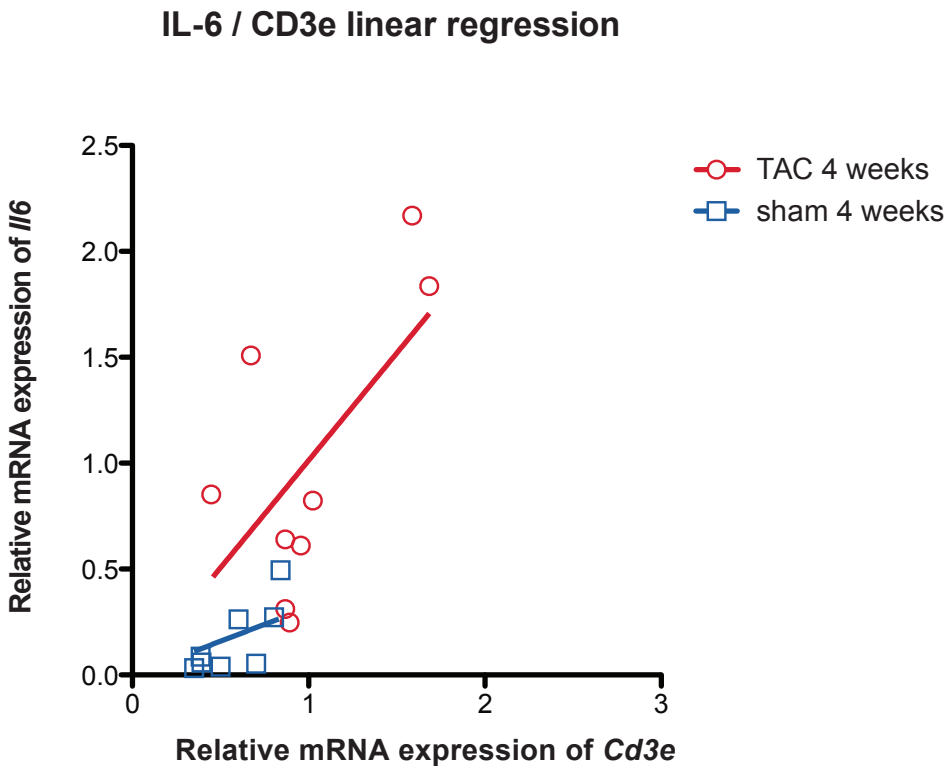

Figure 10: Correlation between relative mRNA expression of IL-6 and CD3e in left ventricles of sham- and TAC-operated mice. Each red circle represents one C57BL6/J TAC-operated mouse 4 weeks after surgery (n=9). Red line is the linear regression between Cd3e and Il6 expression. Each blue square represents a sham-operated mouse 4 weeks after surgery (n=7) and blue line is the linear regression between *Il6* and *Cd3e* expression. Linear regression test; p value = 0.0002 for TAC-mice ,p value = 0.0037 for sham mice.

TAC model, as it controls for any non-cardiac inflammatory components. The results of the correlation show that T cells could be recruited even by a low-grade inflammation, though obviously resulting in lower overall numbers, as shown in figure 8.

5.1.4.3 *T cell infiltration in human biopsies of HF patients*

In order to verify the clinical relevance of our findings, we performed IHC analysis of T cell infiltration in human biopsies of patients with two different forms of HF. Due to the nature of these biopsies the number of patients for this analysis is low, yet still significant.

First we examined the left ventricle biopsies of patients carrying laminin A/C mutations, which lead to a genetic form of dilated cardiomyopathy, as well as from patients with an additional mutation in tinin, leading to an even more severe form of cardiomyopathy. Laminin and tinin are both contractile and structural proteins of the sarcomeres (Roncarati et al., 2013). These biopsies were obtained during surgery for the implantation of Left Ventricular Assist Devices (LVAD). This genetic form of HF is not caused by infection or autommunity, thus any sign of inflammation would confirm that an immune response is associated to the cardiac pathology per se. T cells in the LV of patients with 1 mutation (LVAD 1M) were significantly more abundant compared to healthy donors. Patients with 2 mutations (LVAD 2 M) showed an even greater infiltration of T cells (**Fig.11**). The presence of T cells in the myocardium thus positively correlates with the severity of the pathology.

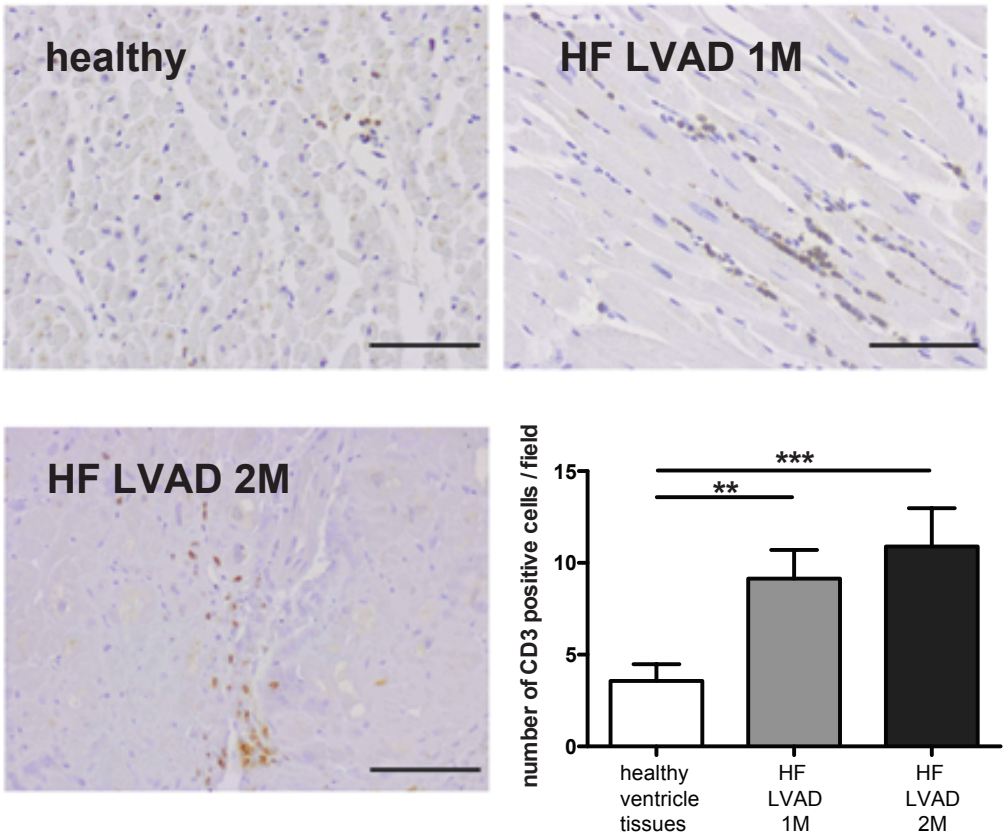

Figure 11: T cell infiltration in human cardiac biopsies of a genetic form of HF. Representative images of anti-CD3e staining (brown coloration) of left ventricular biopsies from patients with severe dilated cardiomyopathy due to a mutation in lamin A/C (HF LVAD 1M) (n=4), and patients carrying a second mutation in titin (HF LVAD 2M) (n=2) patients compared to healthy ventricles (n=3).. All the biopsies were obtained prior to Left Ventricular Assist Device (LVAD) placement. Number of positive CD3e cells are plotted as mean ± SEM for each group analyzed. One-way ANOVA with Dunn's post-test: *, p-value <0.05.

These biopsies we also analyzed for the presence of fibrosis via Azan's trichrome staining. The results obtained for the analysis of the presence of fibrotic tissue in the biopsies reflected the same trend as those obtained for T cell infiltration. Indeed, patients with HF of both groups had a higher percentage of fibrosis compared to healthy donors and also, as for T cell infiltration, there was a positive linear trend with increasing severity of the condition (**Fig.12**).

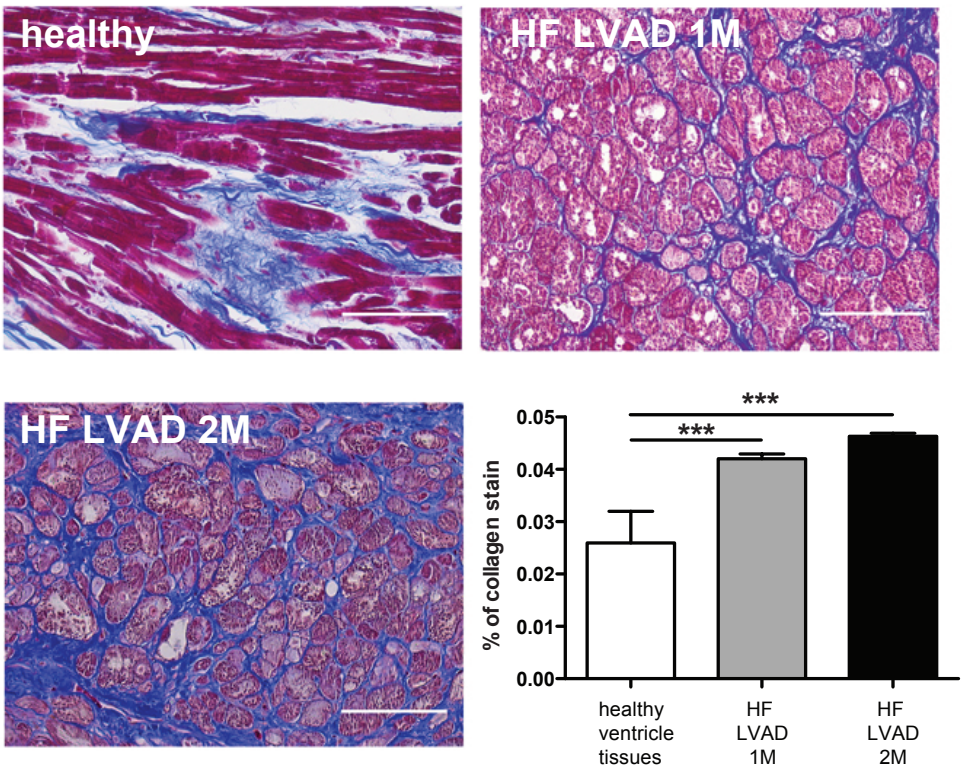

Figure 12: Collagen quantification in human cardiac biopsies of a genetic form of HF. Representative images of Azan's trichrome staining (blue coloration) of left ventricular biopsies from patients with severe dilated cardiomyopathy due to a mutation in lamin A/C (HF LVAD 1M) (n=4), and patients carrying a second mutation in titin (HF LVAD 2M) (n=2) patients compared to healthy ventricles (n=3). All the biopsies were obtained prior to Left Ventricular Assist Device (LVAD) placement. Percentage of collagen of 10 ROIs for each biopsy are plotted as mean ± SEM. Fisher's exact test for the presence versus absence of fibrosis: *, p-value <0.05; **, p-value <0.01. The amount of collagen significantly correlated with the severity of disease (one-way ANOVA with post-test for linear trend: p<0.001).

Patients with laminin mutations suffer from HF with a reduced ejection fraction (HFrEF). This is matched by the cardiac pathology in TAC-operated mice. However, the initial stimulus in the TAC model is pressure overload. Thus, to further assess the clinical relevance of our findings, we analyzed a second group of patients with aortic stenosis, which can lead to HF (Ross and Braunwald, 1968). Patients with aortic stenosis develop HF induced by pressure overload, hence sharing the etiology of their cardiac dysfunction with the TAC model. We found that patients

with aortic stenosis did indeed have increased levels of T cells infiltrating the left ventricle, as well as displaying significantly augmented presence of fibrosis (**Fig.13**).

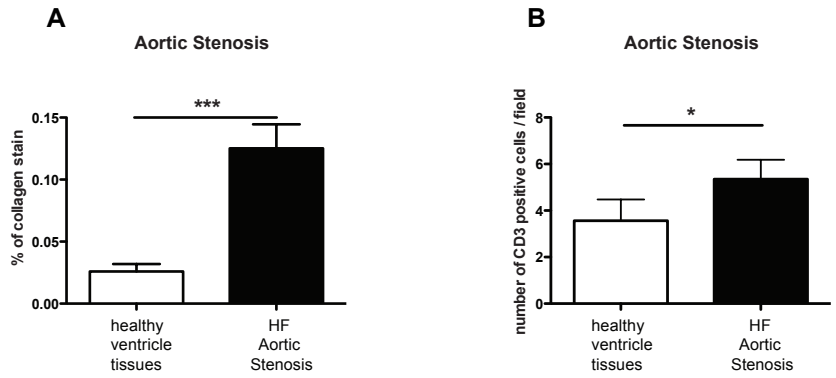

Figure 13: Collagen and T cells quantification in cardiac human biopsies of patients with aortic stenosis. (A) Cardiac biopsies of healthy ventricles (white bars, n=3) and patients with aortic stenosis induced-HF (black bars, n=2) stained with Azan's trichrome. Statistical analysis of the percentage of collagen in ROIs. Values are expressed as mean ± SEM. Fisher's exact test for presence or absence of collagen. ***, p-value <0.001. **(B)** Cardiac biopsies of healthy ventricles (white bars, n=3) and patients with aortic stenosis induced-HF (black bars, n=2) stained with anti-CD3e. Statistical analysis of the number of $CD3e^{+}$cells. Values are expressed as mean ± SEM. Mann-Whitney test. *, p-value <0.05.

These findings, taken together, support the hypothesis that a connection between T cells and fibrosis exists in pathological cardiac hypertrophy.

5.2 *Therapeutic approach in PO-induced HF*

Our mRNA expression analysis results and the immunohistochemical analysis of T cell infiltration, in both mouse models and in patients, suggest that pathological HF is characterized by T cell presence. In the past the inhibition of inflammation in HF patients has been attempted via the use of biological modifiers targeting pro-inflammatory cytokines (Mann, 2002). Since this approach failed, most likely due to the redundancy of cytokine functions, we hypothesized that using T cells, as therapeutic target could possibly be a more promising target, enabling a greater control of inflammation. T cells are required for the maintenance of long-term immune responses. Hence inhibiting T cell function could be a promising therapeutic strategy. One way

of controlling T cell function is via the adoptive cell transfer of Treg, which has already been performed in TAC-operated mice with encouraging results (Kanellakis et al., 2011). We could detect a significant increase of Foxp3 expression in the myocardium of TAC mice 8 weeks after TAC-surgery (**Fig.14**). The increase in Foxp3 indicates the presence of Treg; we hypothesized that, as in other immunological contexts (Garetto et al., 2015), Treg recruitment could be an attempt of the immune system to block an unwanted immune response.

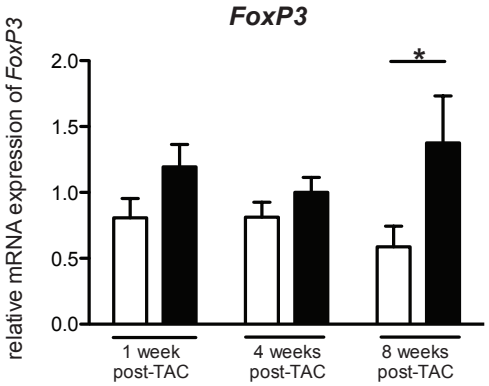

Figure 14: increase of regulatory T cells in TAC-operated mice. Gene expression analysis, via real-time TaqMan qPCR, of *Foxp3* internally normalized on 18s rRNA in the left ventricle of C57BL6/J mice TAC- and sham-operated. *Foxp3*, Treg specific marker, significantly increase in TAC mice 8 weeks after surgery. White bars represent sham-opertaed mice and black bars TAC-operated mice. Values are plotted as mean ± SEM (n=7–9). Two-way ANOVA with Bonferroni post-test; *, p-value <0.05.

As adoptive cell therapy is still in need of substantial development before becoming widely applicable in the clinic, we decided to intervene by inhibiting T cell function via the use of reagents that are currently approved for clinical use. We chose to use a reagent derived from molecules naturally used by Treg to control inflammation, CTLA4. We injected TAC-operated mice with the FDA-approved drug CTLA4-Ig (abatacept). Abatacept has been already discussed in the Section 2.3.

5.2.*1 Inhibition of T cell costimulation preserves heart functionality in TAC-operated mice*

TAC-operated mice 2 days after surgery already show significant changes in cardiac function (Souders et al., 2012). We assessed the T cell activation at this early timepoint in the heart-draining lymph nodes. We analyzed the median fluorescence intensity (MFI), via flow cytometry, of the T activation marker CD25 among $CD3e^+$ cells in heart-draining lymph nodes (mediastinal lymph nodes), non-draining lymph nodes (inguinal lymph nodes) and spleen. We found a significant upregulation of CD25 on T cells in the mediastinal lymph nodes (**Fig.15**).

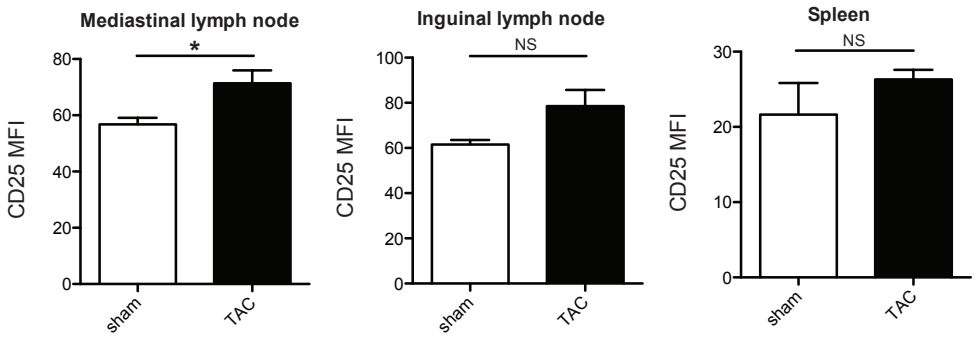

Figure 15: T cell activation occurs 2 days after TAC-operation in heart-darining lymph nodes. T cell activation in mediastinal (heart-draining) lymph nodes, inguinal lymph nodes and spleens of sham- (white bars, n=4) or TAC-operated (black bars, n=4) 2 days after surgery analyzed via flow cytometry. The mean fluorescence intensity (MFI) of CD25 expressed by $CD3e^+$ live T cells is plotted as mean ± SEM. Unpaired t-test. *, p-value <0.05.

Accordingly, we decided to start the treatment with abatacept at 2 days after TAC-operation, as this was the earliest timepoint in which the pathology is macroscopically measurable and the target of our treatment (activated T cell-dependent processes) is present. To this end, 8 week old C57BL6/J male mice, after pre-treatment echocardiography screening, underwent TAC or sham surgery. Starting 2 days after surgery, the mice were injected for 4 weeks, 3 times a week, with 200 µg of abatacept, resuspended in 100 µl of PBS or with 100µl with PBS (**Fig.16**). In a separate set of experiments, we also performed the treatment starting 2 weeks after TAC surgery,

in order to verify whether the effects of the drug on the progression of the disease could be achieved when the ailment was already at a more advanced state.

5.2.1.1 *Assessment of heart functionality after early treatment*

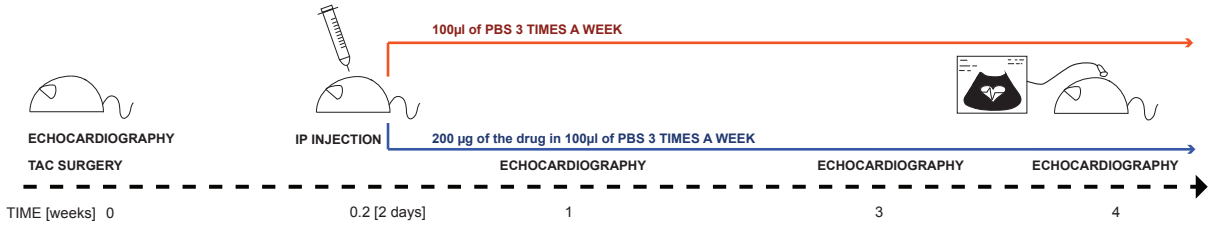

Figure 16: schematic representation of the therapeutic protocol applied to TAC-operated mice. C57BL6/J 8-10 weeks old male mice were screened via echocardiography. Starting 2 days (for the early treatment protocol) or 2 weeks (for the late treatment protocol) after surgery mice received 200µg of Abatacept in 100µl of PBS or 100µl of PBS 3 times a week for up-to 4 weeks. Heart functionality was analyzed via echocardiography during the duration of the experiment.

TAC- and sham-operated mice were monitored via echocardiography for the duration of the experiment. Mice from all groups did not display significant differences at the baseline for all the echocardiographic parameters analyzed (**Fig.17**). As expected, starting from week 1, TAC-mice injected with PBS had a significant reduction of %FS and %EF compared to PBS-injected sham controls. In abatacept-injected TAC mice, on the contrary, no difference at 1 and 4 weeks compared to sham-operated mice was observed. Abatacept-injected TAC mice showed a transient but significant difference compared to sham controls at 3 weeks after operation; however this difference, was lost by 4 weeks. Furthermore, there was a significant difference in %FS and %EF between abatacept-injected and PBS-injected TAC-operated mice. The difference in %FS between abatacept-injected and PBS-injected TAC-operated mice was evident starting at 1 week post-operation whilst the significance of difference in %EF between these two groups increases over time. The beneficial effects of abatacept on the myocardium were evident also in other echocardiography parameters, such as end-diastolic left ventricular internal diameter

(LVIDd) and end-systolic left ventricular internal diameter (LVIDs). These results suggest that abatacept administration reduces cardiac dysfunction and delays the progression induced by pressure-overload. The effects on heart functionality may seem of small magnitude but it has an important effect due to the crucial role of heart pump function for the survival of the organism. Even a small decrease in percentage can have a negative and important effect on the quality of life of the individual.

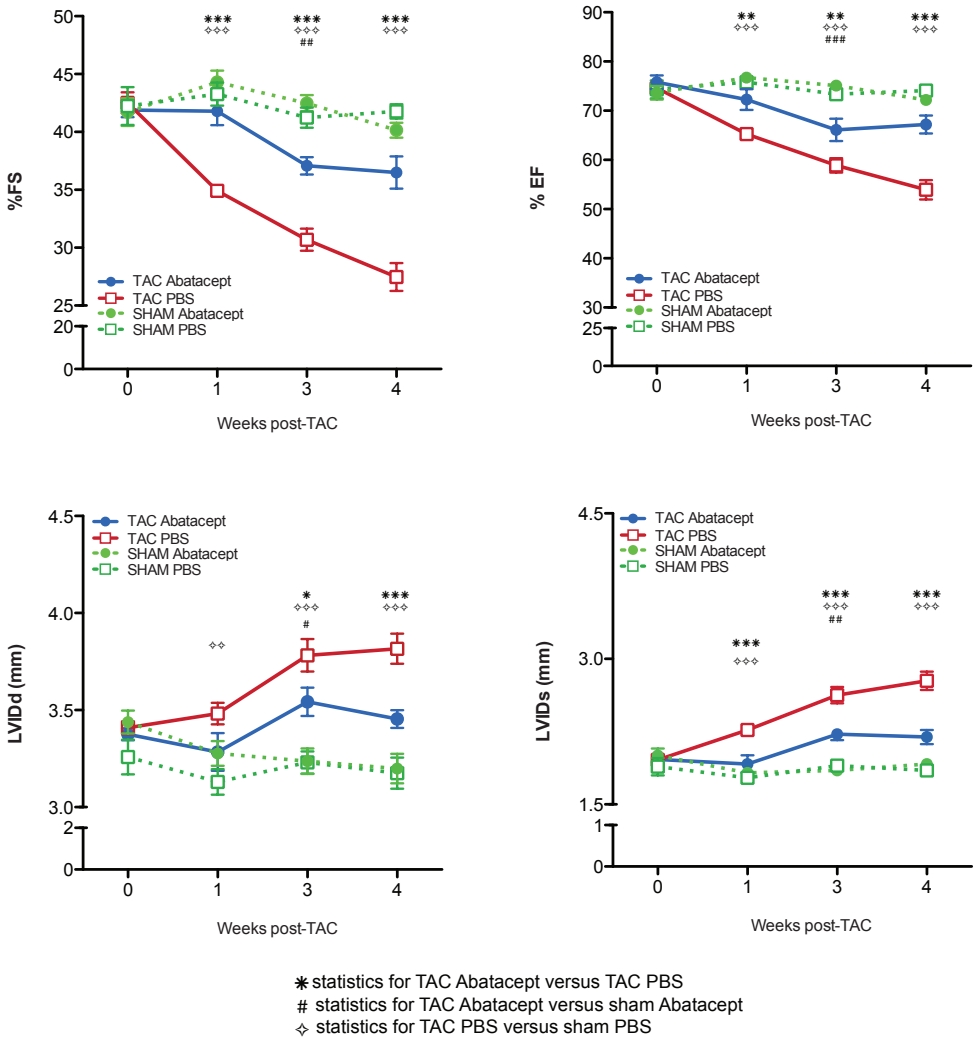

Figure 17: Abatacept reduces cardiac dysfunction and delays the progression induced by pressure-overload. C57BL6/J male mice, starting 2 days after sham- or TAC-operation, received three times per week 200µg of abatacept or PBS, for 4 weeks. At baseline, 1, 3 and 4 weeks after operation Fractional Shortening (A, %FS), Ejection Fraction (B, %EF), Left Ventricle Internal Dimension in Diastole (C, LVIDd) and Left Ventricle Internal Dimension in Systole (LVIDs) were measured via echocardiography. In the graphs are plotted the mean ± SEM (n=7–9) for each experimental group. Two-way ANOVA with Bonferroni post-test was applied and p-values are shown in the panel.

5.2.1.2 *Assessment of heart functionality after late treatment*

We performed echocardiography analyses on TAC-operated mice that received their first abatacept treatment 2 weeks after surgery, in order to assess the effects of the drug on more advanced-stage cardiac pathology. The late administration of abatacept did indeed have significant beneficial effects on heart functionality. As the treatment started 2 weeks after the TAC operation, heart functionality was already reduced compared to the baseline, yet in abatacept-treated TAC-operated mice further reduction in heart functionality was blocked. %FS and %EF of abatacept-treated mice were significantly different compared to PBS-treated mice, thus suggesting that abatacept is able to delay pressure overload-derived detrimental effects on heart functionality even is first administered 2 weeks after the TAC surgery (**Fig.18**).

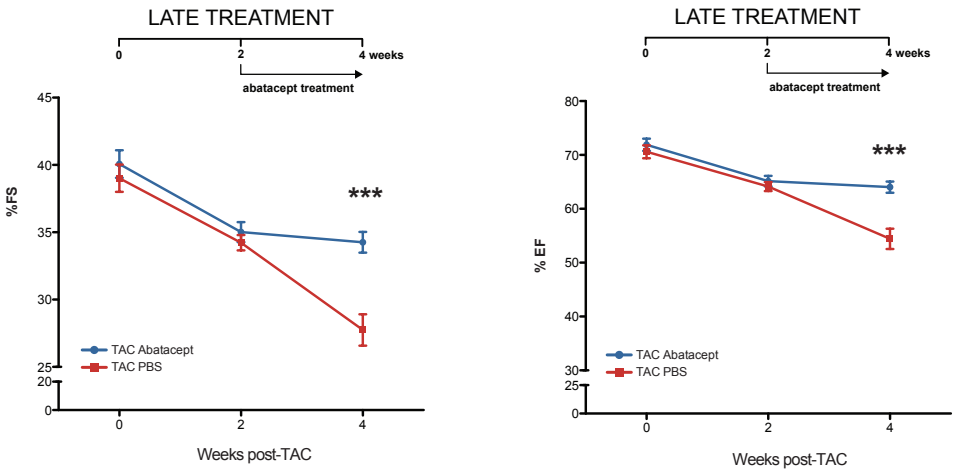

Figure 18: Abatacept treatment starting 2 weeks after operation improves FS and EF. C57BL6/J male mice, starting 2 weeks after TAC-operation, received three times per week 200µg of abatacept or PBS, for 2 weeks. At baseline, 2 and 4 weeks after operation Fractional Shortening (A, %FS) and Ejection Fraction (B, %EF) were measured via echocardiography. In the graphs are plotted the mean ± SEM (n=7) for each experimental group. Two-way ANOVA with Bonferroni post-test. ***; p-value < 0.001.

The beneficial effect on LVIDs was also maintained with the late treatment protocol whilst LVIDd did not show a significant difference between abatacept- and PBS-injected TAC mice (**Fig.19**).

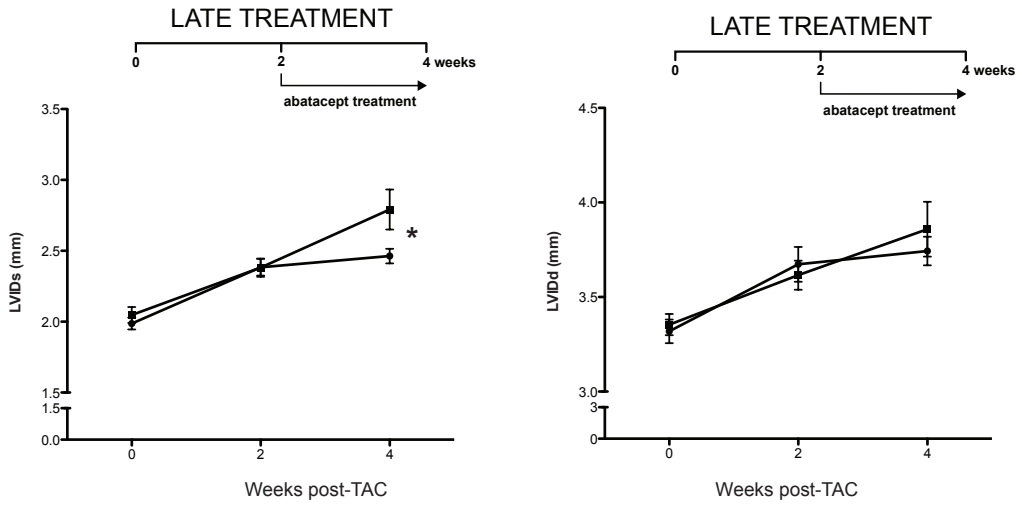

Figure 19: Effects of abatacept treatment starting 2 weeks after operation on LVIDd and LVIDs. C57BL6/J male mice, starting 2 weeks after TAC-operation, received three times per week 200μg of abatacept or PBS, for 2 weeks. At baseline, 2 and 4 weeks after operation Left Ventricle Internal Dimension in Diastole (A, LVIDd) and Left Ventricle Internal Dimension in Systole (B, LVIDs) were measured via echocardiography. In the graphs are plotted the mean ± SEM (n=7) for each experimental group. Two-way ANOVA with Bonferroni post-test. *; p-value < 0.05.

5.2.2 *Assessment of heart hypertrophy after abatacept treatment*

Besides impaired heart functionality, cardiac hypertrophy is one of the key features of HF in the TAC mouse model. Focusing on the early-treatment protocol, we examined the hypertrophic state of the TAC-operated mice at the end of the fourth week post-surgery. At this timepoint, we weighed the whole heart and the left ventricle post-sacrifice, so as to calculate the ratios HW/BW, LW/BW and HW/TL, as indicators of cardiac enlargement (**Fig.20**) (see above, section 5.1.2.2). For two of these morphometric parameters, HW/BW and HW/TL, abatacept-treated TAC-operated mice showed a significant reduction in cardiac hypertrophy compared to PBS-

treated mice. LW/BW of abatacept-injected TAC mice was not different compared to PBS-treated TAC-operated mice; we speculate that the left ventricular growth in the two groups of TAC mice was similar but the overall cardiac enlargement was impaired in the abatacept-treated group.

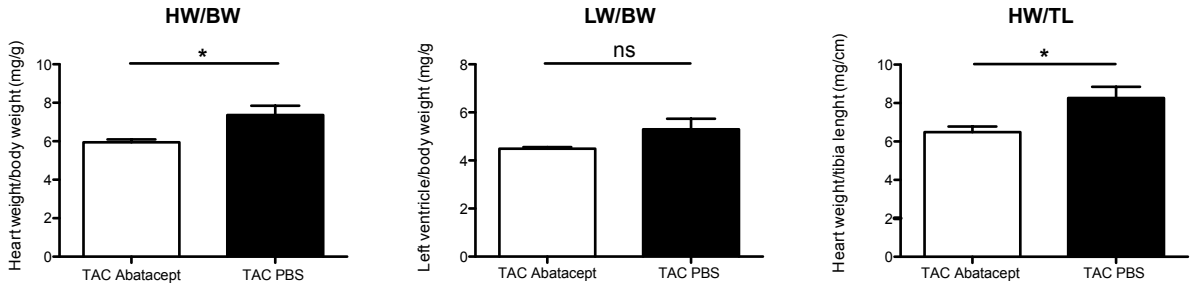

Figure 20: Heart hypertrophy is limited by abatacept administration in TAC-operated mice. TAC-operated mice injected, starting 2 days after operation, with abatacpet or PBS were sacrificed after 4 weeks. Ratios of (A) heart weight body weight (HW/BW, mg/g), (B) left ventricle body weight (LW/BW, mg/g) and (C) heart weight tibia length (HW/TL, mg/cm). Values are plotted as mean ± SEM (n=5-7). White bars represent TAC-operated mice injected with abatacept. Black bars represent TAC-operated mice injected with PBS. Unpaired t-test: *, p-value <0.05

Moreover we also analyzed gene expression, via qPCR, of genes belonging to the fetal gene program that is commonly reactivated in pathological cardiac hypertrophy (Dirkx et al., 2013) (**Fig.21**). *Mhy7, Nppb* and *Nppa* upregulation in TAC-operated mice treated with PBS was significantly increased compared to sham control; this upregulation was not present in abatacept-injected TAC mice.

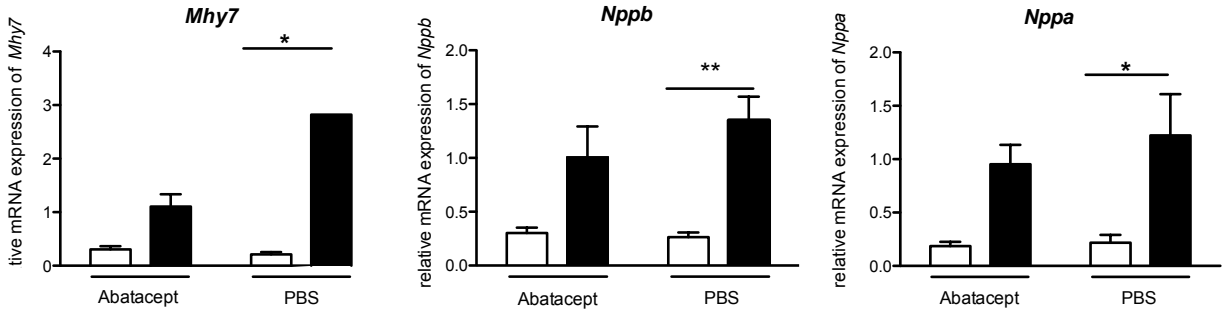

Figure 21: Fetal gene program reactivation is blunted in TAC-operated mice after abatacept treatment. TAC-operated mice were injected, starting 2 days after operation, with abatacpet or PBS for 4 weeks. Relative gene expression, in left ventricles, of (A) β-myosin (*Mhy7*), (B) brain natriuretic peptide (*Nppb*) and (C) atrial natriuretic factor (*Nppa*) were analyzed by real-time qPCR and internally normalized to 18S. Values are plotted as mean ± SEM (n=4-7). Two-way ANOVA with Bonferroni post-test; *, p-value <0.05; **, p-value <0.01. White bars represent sham mice and black bars represent TAC-operated mice.

5.2.3 *Analysis of fibrosis and cardiac infiltration in TAC mice treated with abatacept*

To further investigate the effects of abatacept on TAC-operated mice, we evaluated the fibrosis present in the myocardium, as fibrosis is one of the main features that distinguish pathological cardiac hypertrophy from physiological cardiac hypertrophy. Moreover, we examined the presence of immune cells infiltrating the myocardium after the treatment.

5.2.3.1 *Abatacept inhibits fibrosis formation in the myocardium of TAC-operated mice*

To achieve this, at the end of the fourth week of experiments (using the early treatment protocol), mice were sacrificed and hearts were collected for histological analyses. Hearts were paraffin-embedded and slides were cut longitudinally along the heart, in order to enable full view of the 4 chambers of the organ. We then stained with Azan's trichrome to enable analysis for fibrosis. Collagen staining intensity in abatacept-treated TAC-operated mice did not show increase compared to sham controls, whilst TAC-operated mice treated with PBS showed a

significant increase in fibrosis in the myocardium. Abatacept treatment was thus able to block cardiac fibrosis formation. (**Fig.22**).

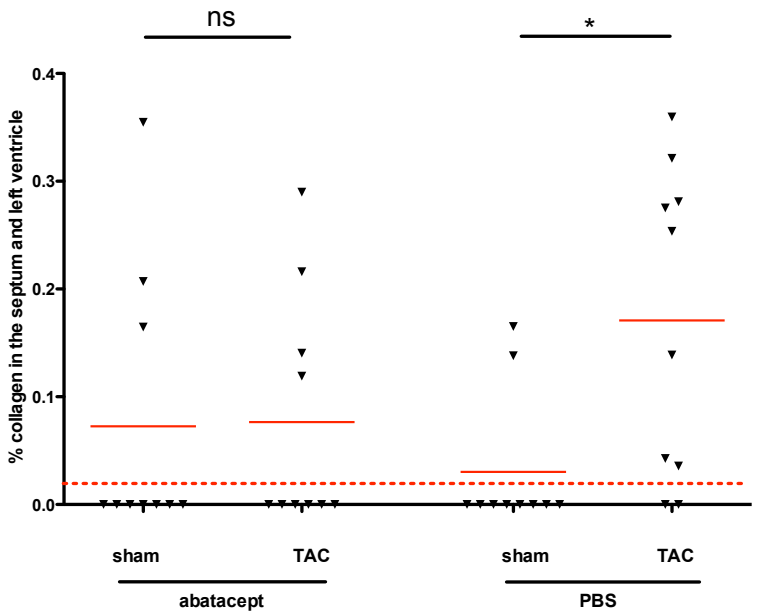

Figure 22: Abatacept administration reduces fibrosis in myocardium of TAC-operated mice. Sections of heart of sham- or TAC-operated mice, 4 weeks after operation and abatacept or PBS administration, were stained with Azan's trichrome (n=2). Five ROIs were selected in each sample and collagen staining intensity was quantified by image acquisition software. In the graphs each point represents the percentage of collagen in each ROI analyzed. The red lines represent the mean of each experimental group. The dotted red line is the threshold between collagen positive and negative ROIs. Fisher's exact test for the presence or absence of fibrosis was applied to sham versus TAC-operated for each treatment group. *, p-value<0.05.

5.2.3.2 *Abatacept administration reduces heart infiltration of T cells and macrophages*

Infiltration of the myocardium by immune cells has been shown to have detrimental effects on cardiac injury and repair, also is associated with fibrosis and cardiomyocytes apoptosis. Abatacept targets CD80/CD86, the ligands for CD28, which are necessary for T cell costimulation (Sharpe, 2009). As abatacept is known to block T cell activation, we wondered if it affected T cell accumulation in the ailing myocardium. We analyzed, via IHC with anti-CD3e, hearts of TAC mice, at 4 weeks after TAC operation, having undergone treatment with either abatacept or PBS (**Fig.23**). The number of $CD3e^{+}$ cells in TAC mice treated with abatacept was

significantly lower compared to PBS-treated mice. This suggests that T cell recruitment and/or expansion that occurs during the progression of TAC towards HF is blunted by the administration of abatacept.

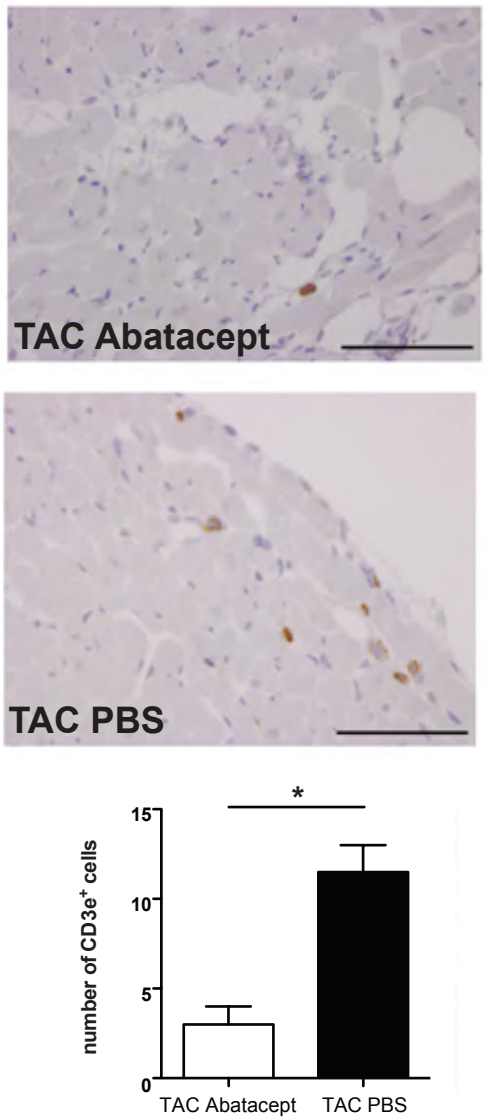

Figure 23: Abatacept reduces T cell expansion in the myocardium of TAC-operated mice. Hearts of TAC-operated mice treated with abatacept or injected with PBS were stained with anti-CD3e 4 weeks after operation. Statistical analysis was applied on number of $CD3e^+$ cells; data are plotted as mean ± SEM (n=2). White bar represents TAC-operated mice treated with abatacept and black bar represents TAC-operated mice injected with PBS. Unpaired t-test; *, p-value < 0.05. Representative images of the immunohistochemical staining with anti-CD3e (brown coloration; original magnification 40X; scale bar = 50 µm).

One of the known mechanisms of action of abatacept is the inhibition of T cell-dependent activation of monocytes and macrophages (Cutolo et al., 2009). T cells receive costimulation via CD80/CD86 and can thus subsequently enhance the activation of APC cells, including B cells, monocytes and macrophages. We thus analyzed, via IHC, the presence of AIF-1^{+} cells in TAC-operated mice, 1 week after operation (**Fig.24**). AIF-1 (Iba-1) is a marker for T cell-depednent macrophage activation (Utans et al., 1995). The presence of macrophages 1 week after TAC is consistent with our gene expression analysis showing an increase of CD11b, which is a marker for monocytes and macrophages, at the same timepoint. Abatacept administration significantly reduced the presence of macrophages in the myocardium of TAC-operated mice.

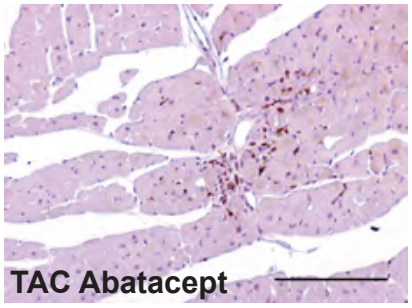

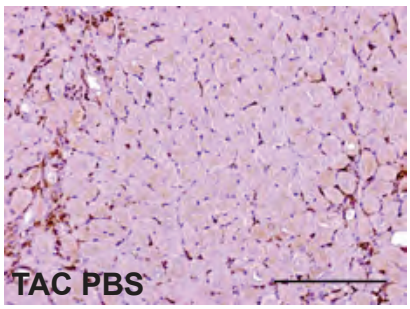

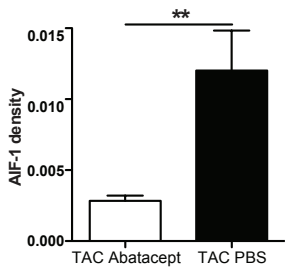

Figure 24: Abatacept inhibits macrophages infiltration in hearts of TAC-operated mice. Hearts of TAC-operated mice treated with abatacept or injected with PBS were stained with anti-AIF-1 (Iba-1) 1 week after operation. Statistical analysis was applied on number of AIF-1^{+} cells; data are plotted as mean ± SEM (n=2). White bar represents TAC-operated mice treated with abatacept and black bar represents TAC-operated mice injected with PBS. Unpaired t-test; **, p-value < 0.01. Representative images of the immunohistochemical staining with anti-AIF-1 (brown coloration; original magnification

At 4 weeks after TAC, the difference in percentage of macrophages in the myocardium was not significant (**Fig.25**); these results match the reduction in CD11b expression between 1 and 4 weeks, as identified in our mRNA expression assays

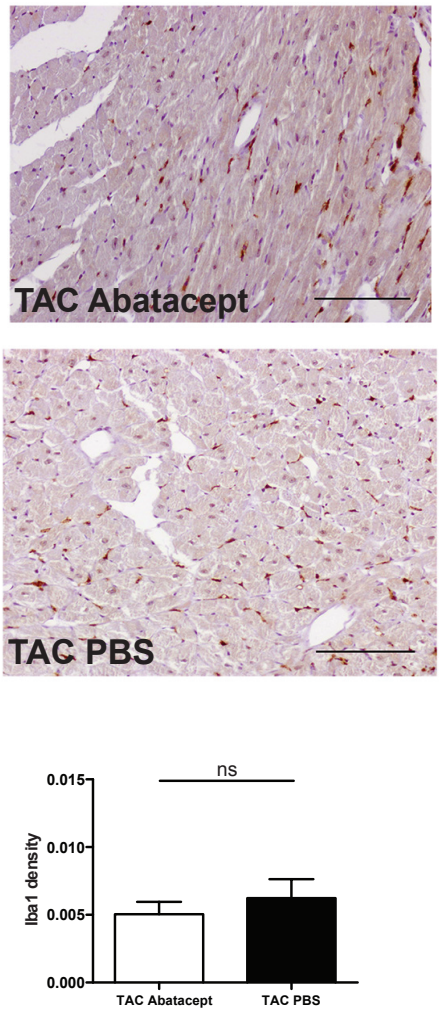

Figure 25: Macrophage presence in the myocardium of TAC-operated mice treated with abatacept does not change after 4 weeks. Hearts of TAC-operated mice treated with abatacept or injected with PBS were stained with anti-AIF-1 (Iba-1) 4 weeks after operation. Representative images of the immunohistochemical staining with anti-AIF-1 (brown coloration; original magnification 20X; scale bar = 100 μm). Statistical analysis was applied on number of AIF-1^{+} cells; data are plotted as mean ± SEM (n=2). White bar represents TAC-operated mice treated with abatacept and black bar represents TAC-operated mice injected with PBS. Unpaired t-test.

5.2.3.3 *Analysis of monocyte and macrophage maturation in the myocardium*

In order to further characterize the macrophages and monocytes infiltrating the myocardium, we sought to identify and distinguish, via flow cytometry analysis, the different populations present. At 1 week after surgery, hearts of TAC-operated mice treated with abatacept or PBS were collected and single cell suspensions were stained for flow cytometry analysis.

We identified the cell populations via side and forward scatter gating, followed by identification of single cell populations. We then discriminated dead from live cells using the a cell viability dye. Finally we detected the $CD45^+$ population in our samples. In order to distinguish the different degrees of maturation, ranging from monocytes to mature macrophages, we identified among the $CD45^+$ $CD11b^+$ cells three distinct populations: $Ly6C^{hi}$ F4-80^- monocytes, $Ly6C^{hi}$ F4-80^+ maturing macrophages and finally $Ly6C^-$ F4-80^+ mature macrophages (**Fig.26**) (Epelman et al., 2014).

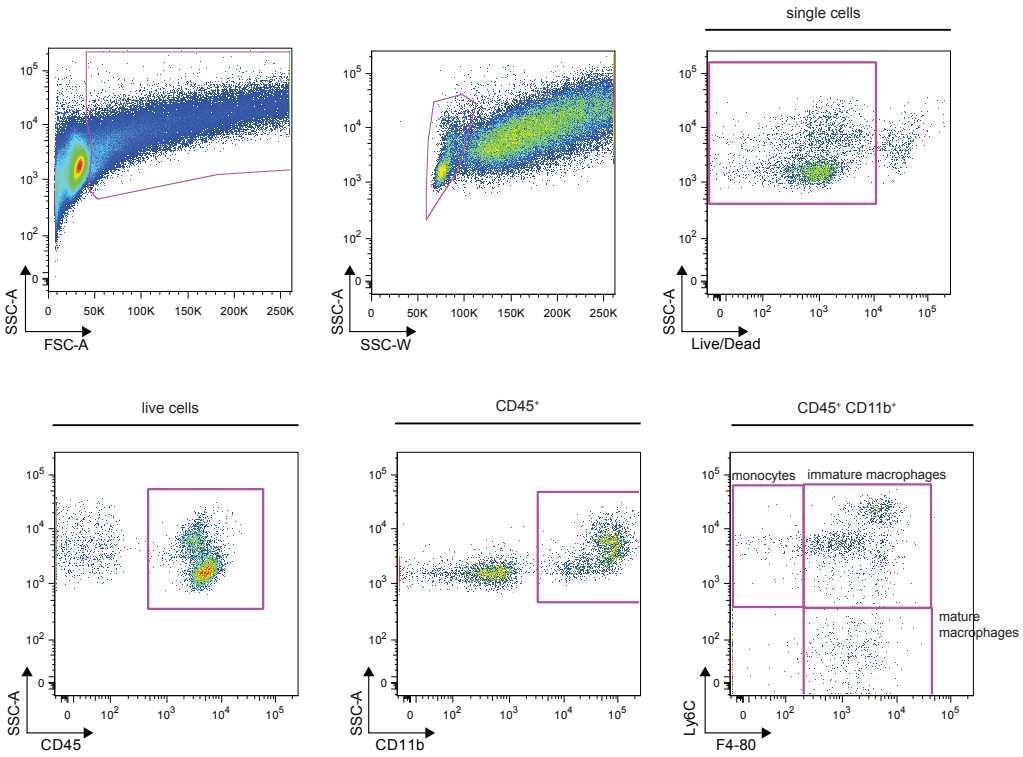

Figure 26: Gating strategy for flow cytometry analysis of macrophages infiltrating the myocardium. Cardiac single cell suspensions from TAC operated mice 1 week after operation were stained for flow cytometry. Cells were first gated based on forward (FSC) and side scatter (SSC), doublets were excluded and live single cells were discriminated from dead cells using Live/Dead dye. Among single live cells $CD45^+$ and $CD11b^+$ cells were selected. Further discrimination was based on Ly6C and F4-80 expression: $Ly6C^+$ $F4\text{-}80^-$ monocytes, $Ly6C^+$ $F4\text{-}80^+$ immature macrophages and $Ly6C^-$ $F4\text{-}80^+$ mature macrophages.

In PBS-treated mouse hearts, the mature population was significantly higher whilst the immature significantly lower, whilst the opposite was true in abatacept-treated mouse hearts. These results suggest that abatacept is able to limit transition from immature monocytes to mature macrophages in the myocardium (**Fig. 27**), though we cannot formally distinguish this effect from a differential recruitment of the two populations.

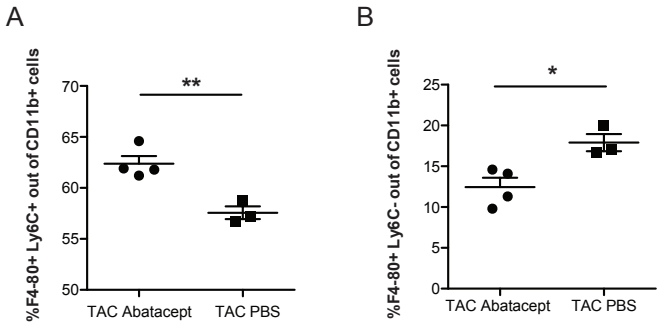

Figure 27: Abatacept inhibits cardiac macrophage maturation. Cardiac single cell suspensions of TAC operated mice treated with abatacept or injected with PBS 1 week after the operation were stained and analyzed by flow cytometry. Cells were gated as in Fig.26. Percentage of (A) F4-80$^+$ Ly6C$^+$ out of CD11b$^+$ CD45$^+$ live cells and (B) percentage of F4-80$^+$ Ly6C$^-$ out of CD11b$^+$ CD45$^+$ live cells are plotted as mean ± SEM. Black circles represent TAC-operated mice injected with abatacept and black squares represent TAC-operated mice injected with PBS. Unpaired t-test; *, p-value < 0.05; **, p-value < 0.01 (n=4, 3).

5.2.4 *Administration of human IgG Isotype has no effects on murine heart functionality, whilst it has detrimental effects on TAC-operated mice cardiac contractility*

Abatacept is a fusion protein of human CTLA4 and human IgG immunoglobulin. Although it has been shown to have effects on mouse models (Dhirapong et al., 2013), we performed additional controls in order to assess if abatacept could have immunogenic effects on mice.

A group of non-TAC-operated mice received abatacept, using the same administration protocol applied to the experimental group. Moreover, we also injected another group of non-operated mice with human IgG isotype control, to verify if the human immunoglobulin portion per se could have negative effects on mice. Neither of these two groups of mice showed a significant change in heart functionality compared to sham-operated, untreated mice (**Fig.28**). Thus the administration of abatacept per se had no effects, beneficial or detrimental, on heart functionality. Moreover abatacept is a human fusion protein with an extracellular portion of a

human IgG1. The lack of effects on heart functionality in non-TAC-operated mice injected with IgG isotype control suggested that even if abatacept is a human molecule it is well tolerated by mice.

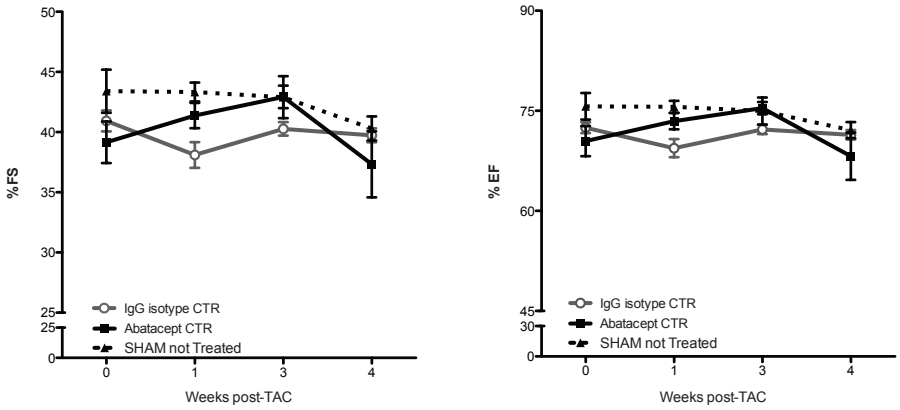

Figure 28: Abatacept or human IgG isotype do not affect heart functionality of non-operated mice. Fractional shortening (%FS) and ejection fraction (%EF) of non-operated mice injected with abatacept or human IgG isotype control three times per week for 4 weeks did not change compared to sham-operated mice not injected. Values are plotted as mean ± SEM (n=3–4). Two-way ANOVA with Bonferroni post-test.

However, when we administered IgG isotype control to TAC-operated mice, the outcome was worsened heart functionality; as early as 1 week after TAC, IgG-injected TAC mice had a significant decrease in %FS and %EF compared to PBS-injected TAC-operated mice. The worse cardiac conditions of IgG-injected TAC mice were evident also when we compared LVIDd and LVIDs to PBS-injected TAC mice (**Fig.29**). These results confirmed that the beneficial effects of the administration of abatacpet in independent from the immunoglobulin portion of the molecule.

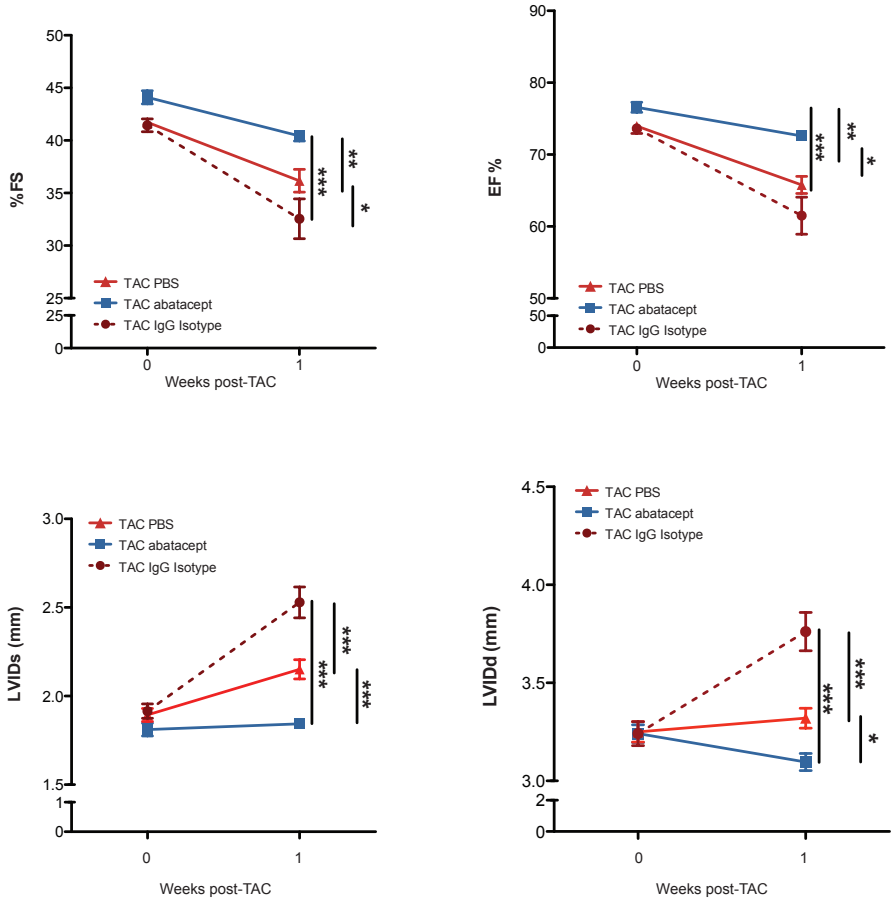

Figure 29: IgG isotype administration in TAC-operated mice worsen cardiac dysfunction. Heart functionality of TAC-operated mice treated with abatacept, PBS or human IgG isotype control for 1 week starting 2 days after operation was assessed via echocardiography. Fractional shortening (%FS), ejection fraction (%EF), left ventricle internal dimension in systole (LVIDs) and left ventricle internal dimension in diastole (LVIDd) are plotted as mean ± SEM for each experimental group (n=6-9). Two-way ANOVA with Bonferroni post-test; *, p-value <0.05; **, p-value <0.01; ***, p-value <0.001.

5.3 *Further characterization of the mechanisms of action of abatacept*

The mechanisms of function of CTLA4 and abatacept have been extensively studied in many contexts, especially for abatacept in RA. Nonetheless we sought to understand how these mechanisms may be acting in our treatment of pathological cardiac hypertrophy.

5.3.1 *Abatacept effects on T cell proliferation and activation*

Abatacept binds to CD80/CD86 on APC, hence blocking T cell costimulation. This can lead to T cell anergy and cell death. We first confirmed the abatacept effects on T cell expansion *in vitro*. We cultured total splenocytes, in plates previously coated with anti-CD3e, for 48 hours in the presence of 20ng/ml of abatacept or IgG isotype control. We then collected the cells and stained for flow cytometry analysis. Anti-CD3 stimulation led to an expansion in the percentage of $CD3^+$ T cells. The addition of abatacept, though not its isotype control, to the medium was able to reduce this expansion of T cells (**Fig.30**).

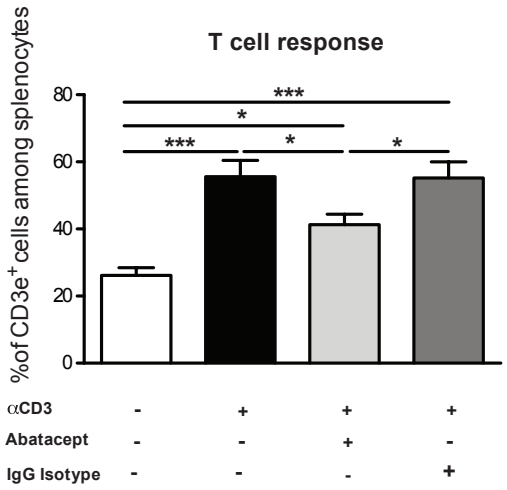

Figure 30: Abatcaept reduces T cell proliferation. Total splenocytes of 8 week-old C57BL/6J mice were activated with anti-CD3 and cultured with 20µg/ml abatacept or IgG isotype control for 72 hours. Splenocytes were stained with anti-CD3e and analyzed by FACS. Values are plotted as mean ± SEM of 4 independent experiments (n=4). One way-ANOVA repeated measurements test with Tukey's post-test. *, p-value <0.05; ***, p-value <0.001.

We then sought to understand whether the effects of abatacept occurred locally at the site of pathology and its draining lymph nodes or systemically. We analyzed T cells from TAC-operated mice treated with abatacept or PBS and or sham-operated mice at 1 week after surgery, by flow cytometry for the expression of CD25. We examined T cells harvested from mediastinal lymph nodes (which drain the heart), inguinal lymph nodes and spleen (**Fig.31**). The percentage of $CD25^+$ T cells in all these three tissues was significantly reduced in abatacept-injected TAC mice, thus suggesting that the suppression of T cell activation occurs systemically. The heart-infiltrating T cells were too few to enable a robust assessment of CD25 expression levels. As T cell suppression will limit their ability to proliferate, the reduced T cell presence in the heart at 4 weeks after TAC (Fig.23) is compatible with the possible consequences of this suppression.

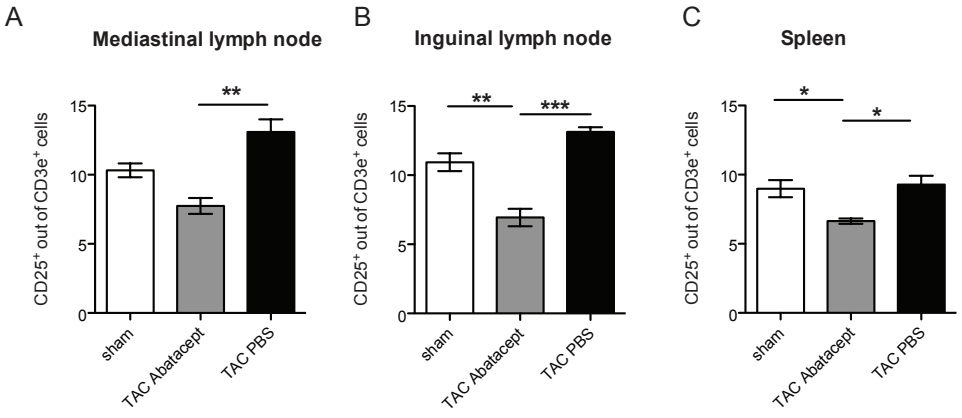

Figure 31: Abatacept systemically suppresses T cell activation. Single cell suspensions of (A) mediastinal (heart-draining) lymph nodes, inguinal lymph nodes and spleens, 1 week after TAC or sham-operation, were stained for flow cytometry analysis. Percentage of $CD25^+$ cells out of $CD3e^+$ cells are plotted as mean ± SEM. White bars represent sham mice not injected, grey bars represent TAC-operated mice treated with abatacept black bars represent TAC-operated mice injected with PBS (n=3). One-way ANOVA with Tukey's post-test: *, p-value <0.05; **, p-value <0.01, ***, p-value<0.001.

5.3.2 *Therapeutic effects of abatacept on PO-induce HF are mediated by the anti-inflammatory cytokine IL-10*

5.3.2.1 *Abatacept administration induces upregulation of IL-10 gene expression*

We analyzed the presence of soluble factors in the left ventricle of TAC mice treated with abatacept. We analyzed, using qPCR, the gene expression of several cytokines and chemokines 1 week post-surgery, when therapeutic effects were already evident. In TAC-operated mice treated with PBS we found a significant increase of IL-6 expression compared to sham controls, confirming the data shown above (Fig.1); we also found a significant increase of IL-6 in abatacept-treated mice. Yet abatacept treated TAC-operated mice displayed a significant increase of IL-10, the immunosuppressive cytokine (**Fig. 32**).

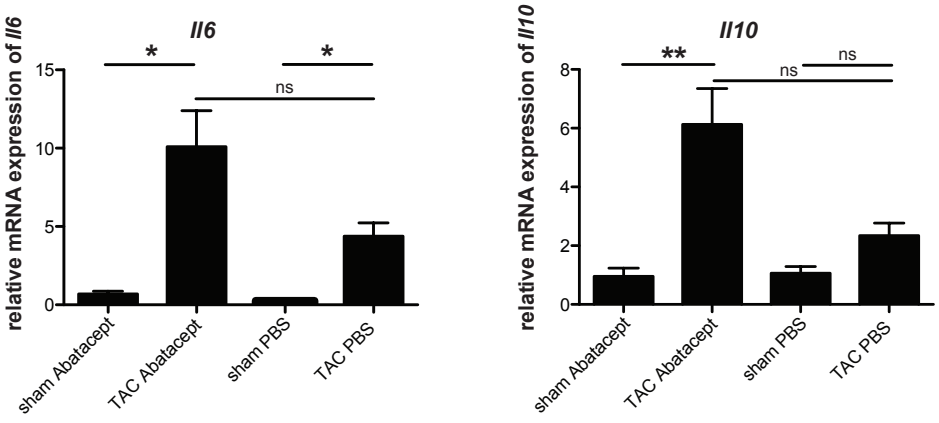

Figure 32: *Il10* expression in left ventricle of TAC-operated mice treated with abatacept is upregulated. Gene expression analysis, by real-time qPCR and internally normalized with 18s rRNA, of *Il6* and *Il10* in left ventricle of sham- or TAC-operated mice injected with abatacept or PBS 1 week after operation. Bars represent mean ± SEM (n=5, 8) of relative gene expression of *Il6* and *Il10*. One-way ANOVA, Dunn's post-test *, p-value <0.05.

This was not the case for PBS-treated animals. Given the important immunoregulatory role of IL-10, we thus investigated both *in-vitro* and *in-vivo* the effects of this cytokine in the myocardium and sought to identify the immune population primarily responsible for its production.

5.3.2.2 *B cells produce IL-10 in response to Abatacept in a T-cell independent manner*

We wanted to identify which immune population is the main source of IL-10 in response to abatacept. We cultured *in* total splenocytes *vitro* on plates coated with anti-CD3e, having added 20ng/ml of abatacept to the medium. After 48 hours, we analyzed the splenocytes, previously stained with antibodies against population-specific surface markers and against IL-10, via flow cytometry. Although T cells and macrophages did produce IL-10 in response to abatacept, the main source of the cytokine appeared to be B cells (**Fig. 33**).

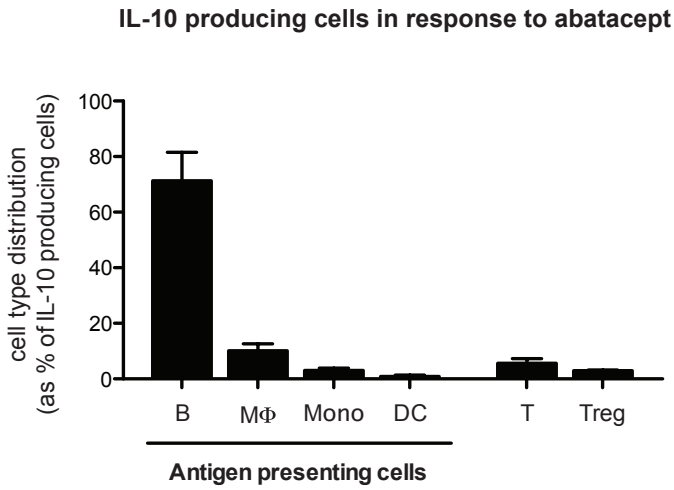

Figure 33: Abatacept *in-vitro* induces IL-10 production by B cells. Total splenocytes of 8 week-old C57BL/6J mice were activated with anti-CD3. Splenocytes were cultured with 20µg/ml abatacept for 72 hours and stained for flow cytometry analysis. Among IL-10^{+} cells were analyzed the percentage of cells expressing population-specific markers (CD19+ B cells, CD11c+ dendritic cells, CD11b+ monocytes and myeloid-derived cells, F4/80+ macrophages, CD3e+ T cells, and CD3e+ Foxp3+ Treg cells). Values are plotted as mean ± SEM of 3 independent experiments (n=3).

In the absence of Abatacept or in the presence of IgG isotype the percentage of IL-10 producing B cells was significantly decreased (**Fig. 34**).

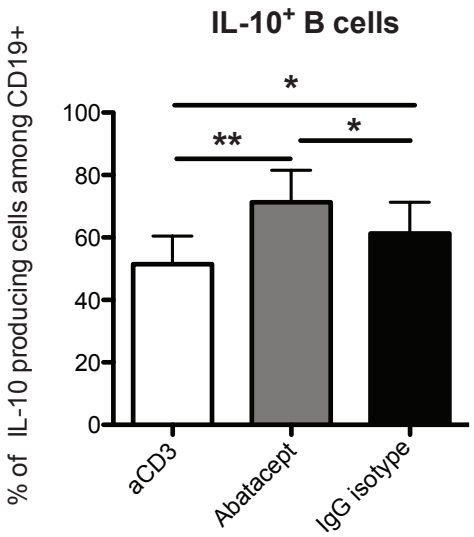

Figure 34: Abatacept *in-vitro* induces IL-10 production by B cells. Total splenocytes of 8 week-old C57BL/6J mice were activated with anti-CD3. Splenocytes were cultured with 20µg/ml abatacept or IgG isotype for 72 hours and stained for flow cytometry analysis. IL-10-producing cells among $CD19^+$ (B cels) were analyzed by flow cytometry and plotted as mean ± SEM of 3 independent experiments (n=3). White bar represents activated splenocytes with no addition to the medium, grey bar represents activated splenocytes cultured with abatacept and black bar represents activated splenocytes cultured with IgG Isotype. One-way ANOVA, Tukey's post-test. *, p-value <0.05; **, p-value <0.01.

Finally to assess whether the production of IL-10 by B cells was dependent on T cell function, as the drug is known to inhibit T cell-dependent B cell functions, we cultured either total splenocytes or T cell-depleted splenocytes. The cells were activated with anti-CD3e and LPS, in order to be able to activate both T and B cells; abatacept was also present in the medium. We assessed the percentage of $CD45^+$ cells producing IL-10 in the different conditions. The absence of T cells had no significant effects on the production of IL-10 (Fig.35), suggesting that B cells production of IL-10 happens in a T cell-independent manner.

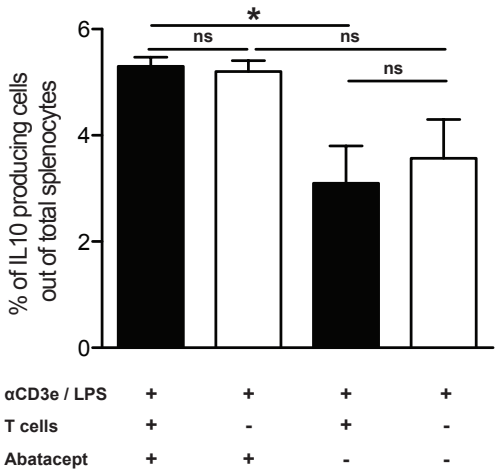

Figure 35: Abatacept induces IL-10 production in a T cell-independent manner. Total splenocytes or T cell-depleted splenocytes were isolated from 8 week-old C57BL/6J mice. Cells were activated with 2µg/ml anti-CD3 and 5 µg/ml of LPS. Splenocytes were cultured for 48 hours with or without 20µg/ml abatacept. Cells stained and analyzed by flow cytometry to assess IL-10 production. The percentage of $CD45^+$ cells producing IL-10 are plotted as mean ± SEM (n=3). Black bars represent total splenocytes and black bars represent T-cell depleted splenocytes. Two-way ANOVA with Bonferroni post-test.*, p-value <0.05.

5.3.2.3 *Direct effects of IL-10 and abatacept on cardiomyocytes*

In order to verify whether IL-10 had any direct effects on cardiomyocytes, we used an *in vitro* model of cardiac hypertrophy. We isolated neonatal cardiomyocytes and, after an overnight starvation, we added PE that, as already mentioned above, is a potent inducer of cardiac hypertrophy. We cultured neonatal cardiomyocytes in presence of PE for 48 hours; 4 hours after the addition of PE were added either IL-10 or IL-6. At the end of the experiment, cells were collected for gene expression analysis of *Mhy7, Nppb* and *Npp*a. In the presence PE cardiomyocytes cultured with IL-6 showed a higher upregulation of *Mhy7* and *Nppa* compared to

cardiomyocytes cultured with PE and IL-10. The beneficial effects of IL-10 on cardiomyocytes have been already shown (Verma et al., 2012); these results also support, though not conclusively, that IL-10 could have a direct, although limited, inhibitory effect on hypertrophy (**Fig.36**).

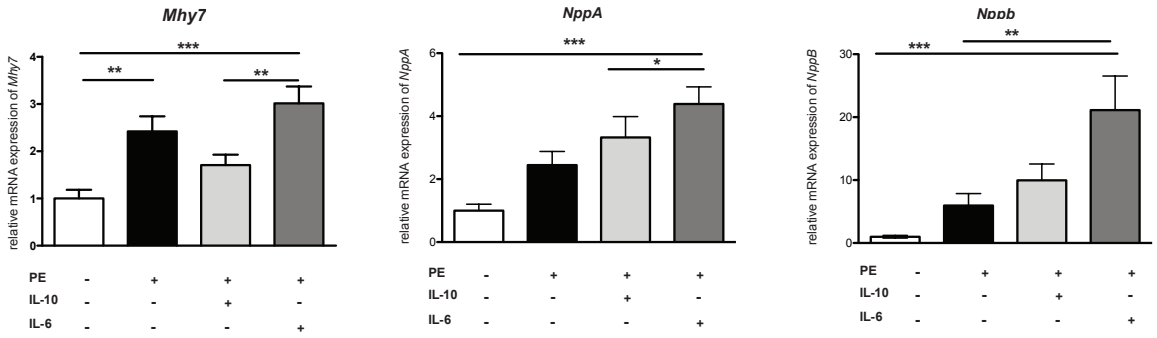

Figure 36: Effects of IL-10 on neonatal cardiomyocytes treated with phenylephrine. Gene expression of *Mhy7, NppA* and *NppB* mRNA relative expression assessed by real-time qPCR in mouse neonatal cardiomyocytes 48 hours after addition of 100 µM of phenylephrine (PE) and either IL-10 or IL-6. Bars show relative mean ± SEM mRNA expression, internally normalized to 18s rRNA expression of 4 independent experiments in triplicates (n=12). One way-ANOVA Tukey's post-test; *, p-value <0.05; **, p-value <0.01; ***, p-value <0.001.

We thus wondered whether Abatacept could have a direct effect on cardiomyocytes. We cultured neonatal cardiomyocytes with PE for 48 hours in presence of 20µg/ml of Abatacept. After 48 hours we collected the cells and analyzed the gene expression of hypertrophic genes.

We observed a significant dowregulation of *Mhy7* in cardiomyocytes cultured in presence of PE and abatacept compared to cardiomyocytes culture with PE, *Nppa* and *Nppb* did not show a significant change in gene expression (**Fig.37**). As this data was inconclusive, we cannot formally exclude a direct effect of abatacept on cardiomyocytes.

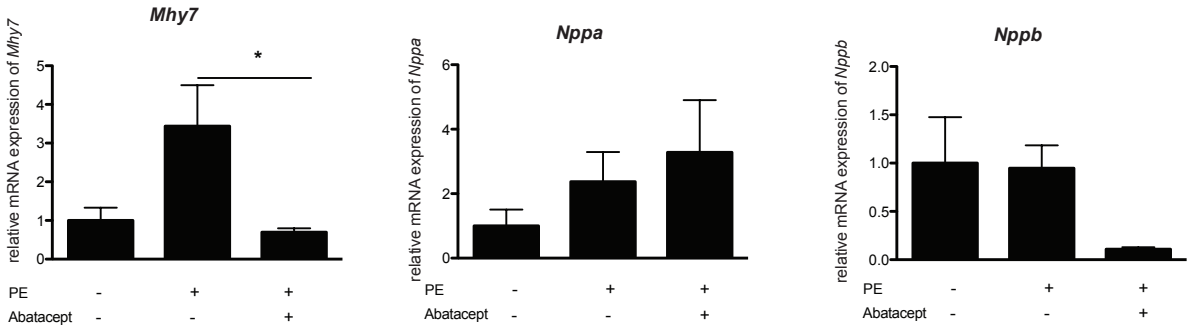

Figure 37 Effects of abatacept on neonatal cardiomyocytes treated with phenylephrine. Gene expression of *Mhy7, NppA* and *NppB* mRNA relative expression assessed by real-time qPCR in mouse neonatal cardiomyocytes 48 hours after addition of 100 μM of phenylephrine (PE) and 20μg/ml of abatacept. Bars show relative mean ± SEM mRNA expression, internally normalized to 18s rRNA expression of 4 independent experiments in triplicates (n=12). One way-ANOVA Tukey's post-test; *, p-value <0.05.

5.3.2.4 *IL-10 deficient mice are refractive to abatacept treatment*

In order to examine the possible role of IL-10 in the therapeutic effects of abatacept we performed TAC or sham operation in C57BL6/J male IL-10 deficient mice (*Il10* KO). We performed the same therapeutic protocol in IL-10KO mice as in Fig. 16 and we assessed the heart functionality by echocardiography. We found a significant decrease in heart functionality in *Il10* KO mice subjected to TAC and treated with PBS compared to WT TAC-operated mice that received the same treatment; *Il10* KO sham controls had no significant differences in any echocardiographic parameter compared to WT sham controls. Importantly, our data demonstrated that the absence of IL-10 completely abolished the therapeutic effects of abatacept. Indeed %FS, %EF, LVIDd and LVIDs in *Il10* KO mice treated with abatacept did not show any improvement compared to PBS injected TAC mice, both WT and *Il10* KO (**Fig.38**). This is consistent with previous reports showing that absence of IL-10 in pressure-overload induced heart damage results in more severe disease (Verma et al., 2012).

Thus our results demonstrate that the improvement in cardiac contractility in mice subjected to pressure-overload treated with abatacept is mediated by IL-10.

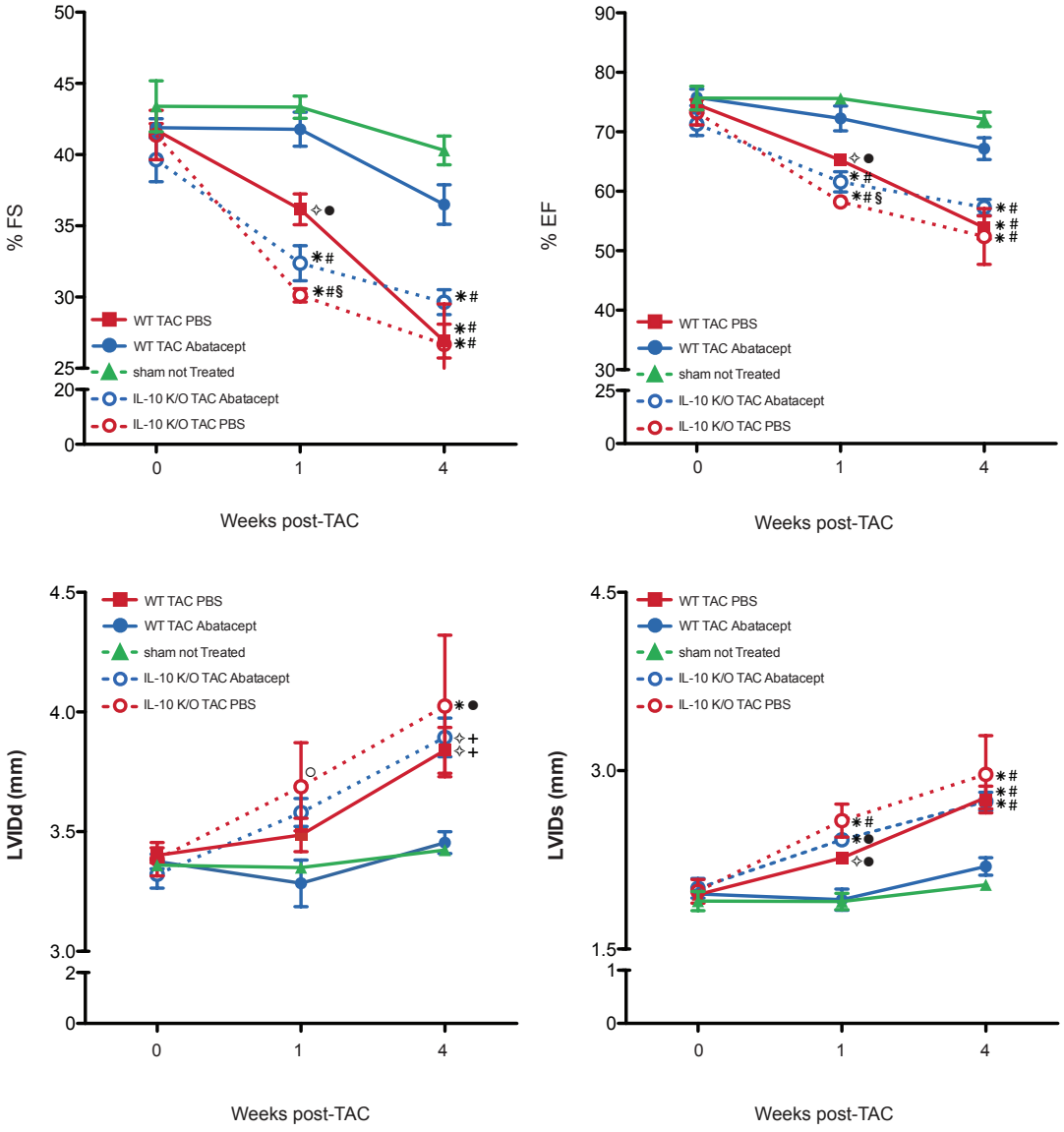

Figure 38: Abatacept treatment is ineffective on heart functionality of TAC-operated mice IL-10 deficient. C57BL6/J male mice WT and IL-10 KO underwent TAC or sham operation and received, starting 2 days post-operation, injections of 200µg of abatacept or PBS three times per week, for 4 weeks. (A) Fractional shortening (%FS). (B) Ejection fraction (%EF), (C) Left ventricle internal dimension in diastole (LVIDd) and (D) Left ventricle internal dimension in systole (LVIDs) were measured by echocardiography at baseline, 1 and 4 weeks after operation. Data are plotted as mean ± SEM (n=5–9). Two-way ANOVA with Bonferroni post-test. Statistics are indicated as follow: **O**, p-value <0.05 versus TAC WT abatacept; ✧, p-value <0.01 versus TAC WT abatacept; *, p-value <0.001 versus TAC WT abatacept; +, p-value <0.05 versus sham not-treated; ●, p-value <0.01 versus sham not-treated; #, p-value <0.001 versus sham not-treated; §, p-value <0.01 versus TAC WT PBS.

5.3.2.5 *IL-10 is required for the abatacept mediated block of T cell proliferation in the myocardium*

One of the mechanisms of action of abatacept is to block T cell activation and expansion; as we found a significant decrease of T cell presence in the myocardium of TAC-operated mice treated with the drug we wondered if this effect was dependent on IL-10. We stained via immunohistochemistry with anti-CD3e cardiac sections of *Il10* KO mice TAC-operated and treated with abatacept or PBS. T cell expansion in the myocardium of *Il10* KO TAC-operated mice was not inhibited by abatacept administration (**Fig.39**). This finding suggests that IL-10 is required to inhibit T cell expansion; moreover this result also further supports the conclusion that T cell presence correlates with worse cardiac function.

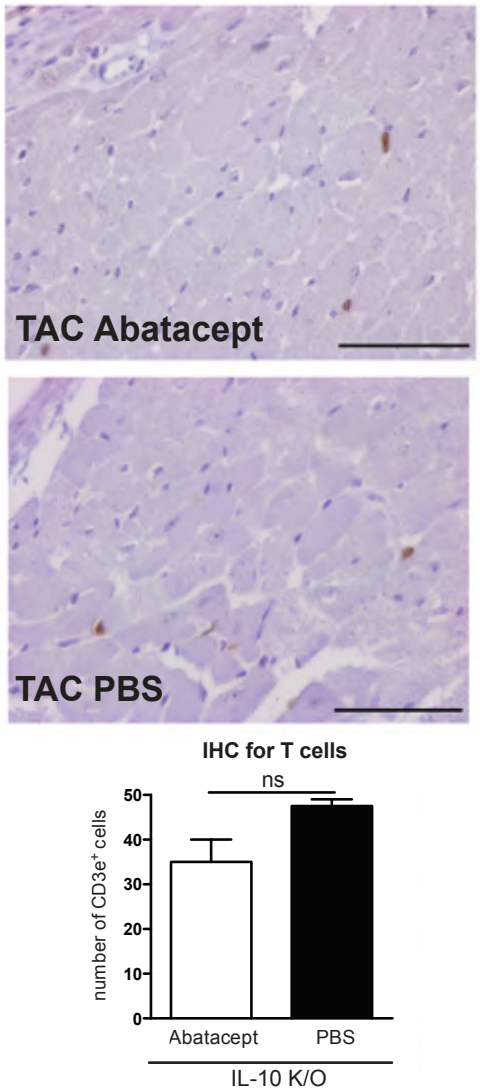

Figure 39: Abatacept-mediated inhibition of T cell expansion is IL-10 dependent. IL-10KO mice underwent TAC-operation and received abatacept or PBS three times per week, starting 2 days after operation. Heart sections of TAC-operated IL-10 KO mice, 4 weeks after operation, were stained via immunohistochemistry with anti-CD3e. Number of $CD3e^+$ per sections is plotted as mean ± SEM (n=2). Unpaired t-test. ns, not significant. White bar represents TAC-operated mice injected with abatacept and black bar represents TAC-operated mice injected with PBS. Representative images of the staining for CD3e (brown coloration; image acquisition with 20x magnification; scale bar = 100 µm).

5.3.2.6 *IL-10 inhibits cardiomyocyte apoptosis*

Cardiomyocytes cell death can occur as consequence of PO-induced cardiac stress (Condorelli et al., 1999). We thus wondered if abatacept-treated TAC-operated mice preserved heart functionality due to preserved cardiomyocyte viability. We stained heart sections with TUNEL-staining kit in order to quantify the percentage of apoptotic cardiomyocytes in TAC mice (**Fig.40**). Abatacept-treated WT TAC-operated mice had significantly reduced apoptosis of cardiomyocytes, thus potentially explaining the improved heart functionality in this group of mice. IL-10 deficiency, as above, eliminated this protective effect of abatacept administration. In fact *Il10* KO TAC-operated mice that received abatacept had no difference in cardiomyocyte apoptosis compared to PBS-treated animals.

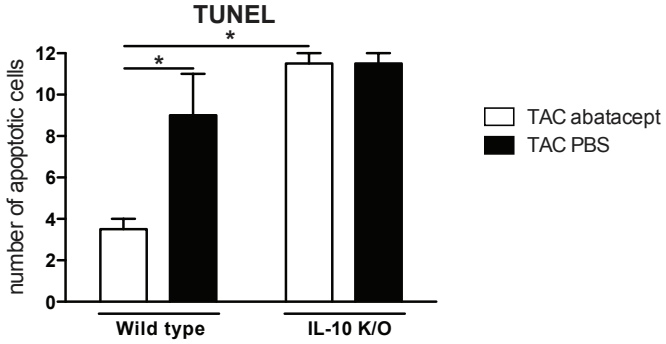

Figure 40: Abatacept inhibition of cardiomyocytes apoptosis is mediated by IL-10. C57BL6/J male mice WT and IL-10KO underwent TAC operation and received abatacept or PBS three times a week starting 2 days after operation. After 4 weeks heart sections were stained with TUNEL assay for assessment of cardiomyocytes apoptosis. Number of apoptotic cells for each section is plotted as mean ± SEM (n=2). White bars represent abatacept-treated TAC-operated mice and black bars represent PBS-injected TAC-operated mice. Two-way ANOVA with Bonferroni post-test; *, p-value <0.05.

5.3.2.7 *Transfer of WT B cells in IL-10KO TAC mice can restore the therapeutic effects of abatacept*

Finally we sought to investigate whether the adoptive transfer of IL-10-sufficient immune cells was sufficient to restore the abatacept-mediated therapeutic effects. *Il10* KO recipients received $2*10^6$ B cells or $2*10^6$ T cells via intravenal transfer from IL-10 sufficient donors, two days prior to TAC operation. WT B and T cells were isolated from C57BL6/J WT male mice age-matched with the recipients. T and B cells purity was assessed by flow cytometry and cells were injected intravenously. The next day mice were screened for baseline echocardiography analysis and the day after TAC was performed. Starting 2 days after the TAC operation, mice received abatacept injections three times a week for 1 week (**Fig.41**). Transfer of WT B cells was sufficient to restore the beneficial effects on heart functionality; *Il10* KO TAC-operated mice that received WT B cells had %FS and %EF values that did not differ from sham controls or from WT TAC-operated mice that received abatacept. Thus the therapeutic effects that abatacept exerts on heart functionality may be dependent on IL-10 production by B cells.

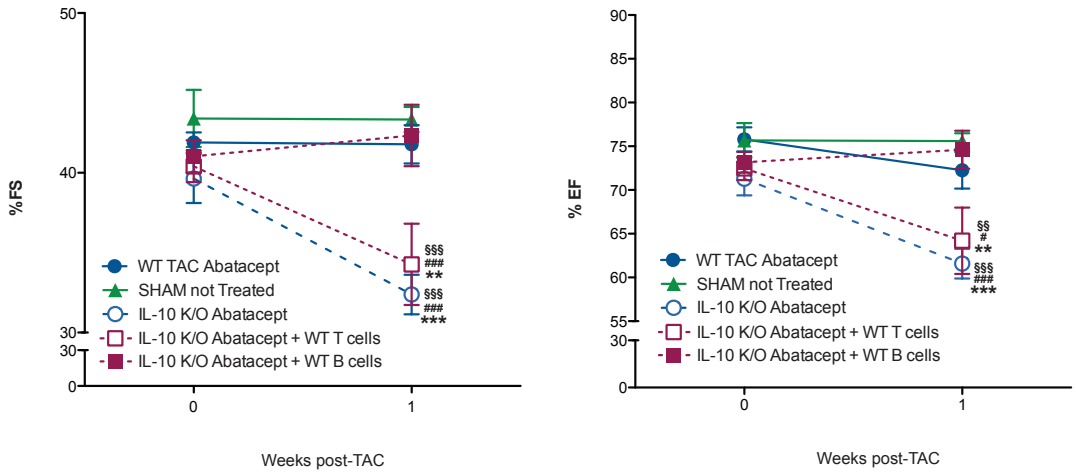

Figure 41: Transfer of IL-10 sufficient B cell restores abatacept therapeutic effects in IL-10KO mice. IL-10KO mice received wild-type T or B cells prior to TAC-operation and baseline echocardiographic screening. TAC-operated mice 2 days post-operation were injected three time per week with 200µg of abatacept for 1 week. Heart functionality was assessed via echocardiography and measurement of (A) Fractional shortening (%FS) and (B) ejection fraction (%EF). Data are plotted as mean ± SEM for each experimental group at all time-points (n=3-7). Two-way ANOVA with Bonferroni post-test. *, statistics for IL10 KO TAC abatacept + WT B cells; #, statistics for WT TAC abatacept; §, statistics for sham not treated.

6. *DISCUSSION*

Pathological cardiac hypertrophy progression and HF pathogenesis are linked to the activation of a cardiac inflammatory response (Hofmann and Frantz, 2013). This inflammatory response has been already extensively investigated, especially regarding the involvement of pro-inflammatory cytokines such IL-6, IL-1b and TNFα (Mann, 2002). Indeed, according to the cytokine hypothesis, pro-inflammatory cytokines trigger a cascade of events that lead to HF pathogenesis (Seta et al., 1996). Several clinical trials targeting these cytokines were conducted with no successful outcome (Mann, 2015). The lack of success of clinical trials targeting pro-inflammatory cytokines could be related to their redundancy (Yndestad et al., 2006). Pro-inflammatory cytokines activate and sustain the cellular mediators of the immune system. Yet many studies have shown that in the pathogenesis of HF cells of both the innate (Epelman et al., 2014; Kuwahara et al., 2012) and the adaptive immune system (Laroumanie et al., 2014) are involved. Inflammation seems to be involved in many different processes that characterize HF, thus the search of a therapeutic target better than individual pro-inflammatory cytokines could be very useful. In this study we show that targeting the adaptive immune response has beneficial effects on HF development and therapeutic potential, rendering adaptive response mediators a potentially utilizable target.

In order to identify a target for a novel immunotherapeutic approach in HF, we characterized the immune response in the gold-standard HF mouse model at different time points after the induction of disease via surgical generation of pressure overload. At an early time point (1 week post-operation) we identified an increased presence of the innate immune response accompanied by M1-related chemokines and cytokines. At a later timepoint, 4 weeks post-operation, we identified a decrease in CD11b expression, a marker innate immunity, with a simultaneous increase of CD3e expression, a marker for T cell presence. It has been shown that T cells are necessary to sustain chronic immune responses (Loke et al., 2007). The increased presence of T

cells 4 weeks post-operation in the left ventricle of TAC-operated mice allowed us to speculate that T cells could be sustaining the chronic inflammatory response that underlies the pathogenesis of HF. The increase in T cells presence was accompanied by a reduction of the expression of M1-polarized chemokines and cytokines and the concomitant increase of Th2-polarized cytokine IL-4 (Zhu, 2015).

The role of type 2 immune responses in the progression of HF has been already investigated in a recent study comparing two strains of mice, C57BL6/J and Balb/c. Balb/c mice, that are more prone to type 2 polarized immune responses, develop a more severe form of HF (Yu et al., 2006). The role of Th2 cells in fibrosis formation has been proposed in many different pathological contexts (Wynn, 2004). Thus the simultaneous increase of IL-4 expression and upregulation of markers indicative of T cell presence supports the idea that Th2 cells may be actively promoting fibrosis formation in TAC-operated mice. Th2-associated cytokines (Zhu and Paul, 2010) were absent in the physiological cardiac hypertrophy models that we analyzed. Further, fibrosis is a hallmark of pathological cardiac hypertrophy (Daskalopoulos et al., 2016) but absent in physiological cardiac hypertrophy, we speculated that the switch towards a Th2 response in TAC-operated mice could be a driver for fibrosis formation.

However our speculation are based on gene expression analysis, thus to better understand the polarization of the inflammatory response in the myocardium would be necessary to isolate cardiac infiltrating T cells. On isolated T cells would be possible to perform ex-vivo analysis of cytokine production and also GATA-3 expression should be addressed.

In addition to Th2 cells, other inflammatory mediators are linked to fibrosis. TGFβ is known to activate fibroblasts and to support their differentiation into myoFb (Kong et al., 2014). The observed increase of TGFβ in the left ventricle of TAC-operated mice may be a reflection of an ongoing activation of fibroblasts and the consequent fibrosis formation. This hypothesis is further supported by the fact that TGFβ is absent in the left ventricle of AKt-tg mice, which develop physiological cardiac hypertrophy and do not develop fibrosis (Condorelli et al., 2002).

TAC-operated mice lacking T cells develop a milder form of HF (Laroumanie et al., 2014; Nevers et al., 2015). Yet, from our data it also seems reasonable to speculate that the role of T cells in the progression of HF is not exclusively restricted to their involvement in fibrosis formation, as we observed significant differences in aspects unrelated to fibrosis, such as cardiomyocyte cell death.

In the myocardium of TAC-operated mice, T cells are present starting at 1 week post-operation. T cells were subsequently expanded or further recruited leading to a significant increase in their presence by 4 weeks post-operation. The presence of T cells is not restricted to HF animal models, thus supporting the clinical relevance to the above findings. We showed that T cells are present also in the cardiac biopsies of patients with two different non-immunological types of HF. We chose two different types of HF: HF due to a genetic form of dilated cardiomyopathy with laminin mutation as well as HF caused by aortic stenosis. These two groups of patients share respectively the pathological effects on heart functionality or the initial pathological stimulus with TAC-operated mice. Patients with laminin mutation A/C develop HF with reduced EF (HFrEF) (Roncarati et al., 2013), like the TAC animal model, although differing in the initial causes of the disease. On the other hand, patients with aortic stenosis, which develop HF (Ross and Braunwald, 1968) with preserved EF (HFpEF) (Drazner, 2011), share the same etiology with the TAC-operated mice. The presence of T cells in both groups of patients, independently from the etiology and/or the status of their EF, confirms that the involvement of T cells is a ubiquitous characteristic in the pathogenesis of HF. Moreover, these findings suggest that the manner in which they are recruited and/or expanded in the myocardium is independent from the identity of the initial stress stimulus. The connection between T cells and fibrosis was also evident in the human biopsies, as T cell presence correlated with collagen deposition. All these findings, taken together, are compatible with the hypothesis that T cells are important for the pathogenesis of HF.

T cells sustain chronic long-lasting immune responses (Loke et al.,2007). Yet even long-lasting responses have to be physiologically terminated. Treg cells are the natural immune regulators of detrimental or unwanted immune responses (Sakaguchi et al., 2008). In pathological contexts, Treg are recruited to the site of inflammation in the attempt to control and block the inflammatory response (Garetto et al., 2015); in many cases this recruitment may happen too late to successfully control the inflammatory response. This may be the case in the myocardium, as our results show. Nevertheless, an artificial boost in Treg numbers has beneficial effects, as demonstrated in Treg adoptive transfer studies in HF animal models (Kvakan et al., 2009; Kanellakis et al., 2011). Adoptive cell transfer (ACT) is, indeed, a promising approach for many different pathological contexts, yet it currently is an expensive and complex therapeutic strategy, in need of substantial development before becoming clinically applicable. In order to overcome these intrinsic limitations, we sought a more immediate, less demanding and more readily applicable approach that can achieve similar effects as Treg cells without the involvement of cell transfer.

Treg mediate their suppressive effects via different means, already discussed in section 2.3.2. These include CTLA4-mediated APC suppression. CTLA4 is a co-inhibitory molecule that specifically blocks full activation of T cells, via competitive binding to CD80/CD86, limiting the access of CD28 (Frauwirth and Thompson, 2002). CTLA4 has been used in clinic for over 20 years as a CTLA4-Ig fusion protein (abatacept). Abatacept is an FDA-approved drug for the treatment of RA (Moreland et al., 2006). Even though abatacept is a human protein, its efficacy in mice has been already demonstrated (Dhirapong et al., 2013), rendering it also suitable for mouse studies.

The animal model chosen for this study, the TAC-operated mouse model, is considered the gold standard for HF research. The induction of the model requires that the mice undergo a surgical procedure. This raises the possible criticism that the inflammatory response identified in the left ventricle of TAC-operated mice could be derived from the procedure per se and not related to the

cardiac pathogenesis. Yet the sham controls, which undergo the same surgical process with the only exception of the absence of final aortic ligation, did show a low –but present- degree of inflammation. This demonstrates that the sham group is a valid control for any non-cardiac inflammatory component in the TAC model.

We developed two therapeutic protocols for PO-induce HF mice utilizing abatacept. As abatacept targets activated T cells and these are detectable in the heart-draining lymph nodes as early as 2 days after-operation, in the first therapeutic protocol we started the administration of the drug at this timepoint. Although 2 days is a very premature timepoint, the effects of the TAC-surgery on mice are already detectable via echocardiography, which is a clinically-relevant measurement (Souders et al., 2012).

We demonstrated that abatacept delays the progression and reduces the severity of HF in TAC-operated mice. One of the main effects of PO is the reduced heart functionality and contractility; abatacept had significant beneficial effects on several echocardiography parameters used as indication of the heart functionality. Significant effects on heart functionality, even if of smaller magnitude, were obtained also with administration of abatacept starting 2 weeks after the TAC surgery. Other important features of the PO-induced HF reduced by abatacept administration are cardiac hypertrophy and "fetal-gene program" reexpression (Dirkx et al., 2013).

Abatacept, despite being a human fusion protein with a human immunoglobulin Fc domain, did not cause any detrimental effect on heart functionality of non-operated mice, thus demonstrating that the drug is not immunogenic and despite the presence of a human Fc domain. This could be due to the immunosuppressive effect of CTLA-4. Non-specific immunoglobulin administration to HF patients in the past has led to encouraging clinical results (Gullestad et al., 2001), through an unknown mechanism. This finding could lead to the criticism that the therapeutic effects obtained by abatacept administration could be due to a beneficial effect of the Ig-portion of the drug. However the administration of human IgG isotype control to TAC-operated mice

drastically worsened the heart functionality. This renders it unlikely that the IgG alone has any beneficial effects. This finding further confirmed the validity of choosing PBS administration as a more robust and reliable control for the experiments featuring abatacept administration.

We detected a systemic suppression of T cell activation after the administration of abatacept in TAC-operated mice. Further, T cell presence in the myocardium was also reduced. The decrease of T cell infiltration was accompanied by the reduction of fibrosis, thus further supporting the connection between T cells and fibrosis. As abatacept directly binds APC, it is not unexpected that the drug also affected macrophage expansion/recruitment and monocyte maturation (Wenink et al., 2012; Cutolo et al., 2009). Indeed, in the myocardium, abatacept inhibited the maturation of monocytes to macrophages and consequently reduced macrophage infiltration in the heart.

Even though the physiological functions of CTLA4 have been already extensively studied, we sought to characterize the mechanisms of action of abatacept in HF. Although it has been reported that cultured neonatal cardiomyocytes can express CD80 (Nengwen et al., 2014), the target of the drug, we did not detect a direct effect on neonatal cardiomyocytes. Yet we cannot formally exclude that a direct effect on cardiomyocytes may be contributing to the effects of abatacept, as we only assessed gene expression of fetal genes, indicative of the hypertrophic state.

In addition to the systemic suppression of T cell activation, abatacept induced expression of the anti-inflammatory and anti-fibrotic cytokine IL-10. As shown in the results section in Fig. 33, this was not accompanied by any downregulation of pro-inflammatory cytokine IL-6. IL-6 is induced by cardiac stress and it is one of the first cytokines to be produced by cardiomyocytes (Souders et al., 2012). IL-6 during the acute phase of cardiac stress has an anti-apoptotic effect on cardiomyocytes; yet its chronic activity eventually leads to detrimental effects (Fontes et al., 2015). Moreover with the administration of abatacept we were able to block T cell activation that

occurs downstream of IL-6 production, thus the lack of effects on IL-6 expression in TAC-operated mice abatacept-treated. We found that IL-10 was significantly increased only in TAC-operated abatacept-treated mice; and not in TAC-operated PBS-treated mice. From this we conclude that i) abatacept treatment does not affect the levels of potentially cardiotoxic cytokine IL-6; and ii) that the presence of the anti-inflammatory cytokine IL-10 in TAC-operated abatacept-treated mice may be counteracting the pro-inflammatory function of IL-6. In other words, it is possible that the balance between these two cytokines will determine the overall inflammatory response. Another potentially relevant issue is that IL-6 requires to bind to its soluble receptor sIL-6R in order to activate pro-fibrotic and pro-hypertrophic responses (Szabo-Fresnais et al., 2010). An assessment of sIL-6R levels in the different treatment groups would have been informative.

From the above results, we thus identified a correlation between the ratio of pro- versus anti-inflammatory cytokine expression and the magnitude of the cardiac dysfunction. In order to quantify this correlation, we calculated two indexes, one indicative of inflammation and one indicative of heart dysfunction. The inflammation index was calculated as the mRNA level of the pro-inflammatory cytokine IL-6 divided by mRNA level of the anti-inflammatory cytokine IL-10. The heart dysfunction index (HDI) was calculated as (-1) x (% fractional shortening), for all mouse models analyzed in this study and normalized to their matching control group.

These two indexes show that improvement of heart functionality after abatacept administration is accompanied by decreased inflammation. Not only does this give insights on the mechanism of action of abatacept, it also further links HF-related decrease of heart functionality to inflammation.

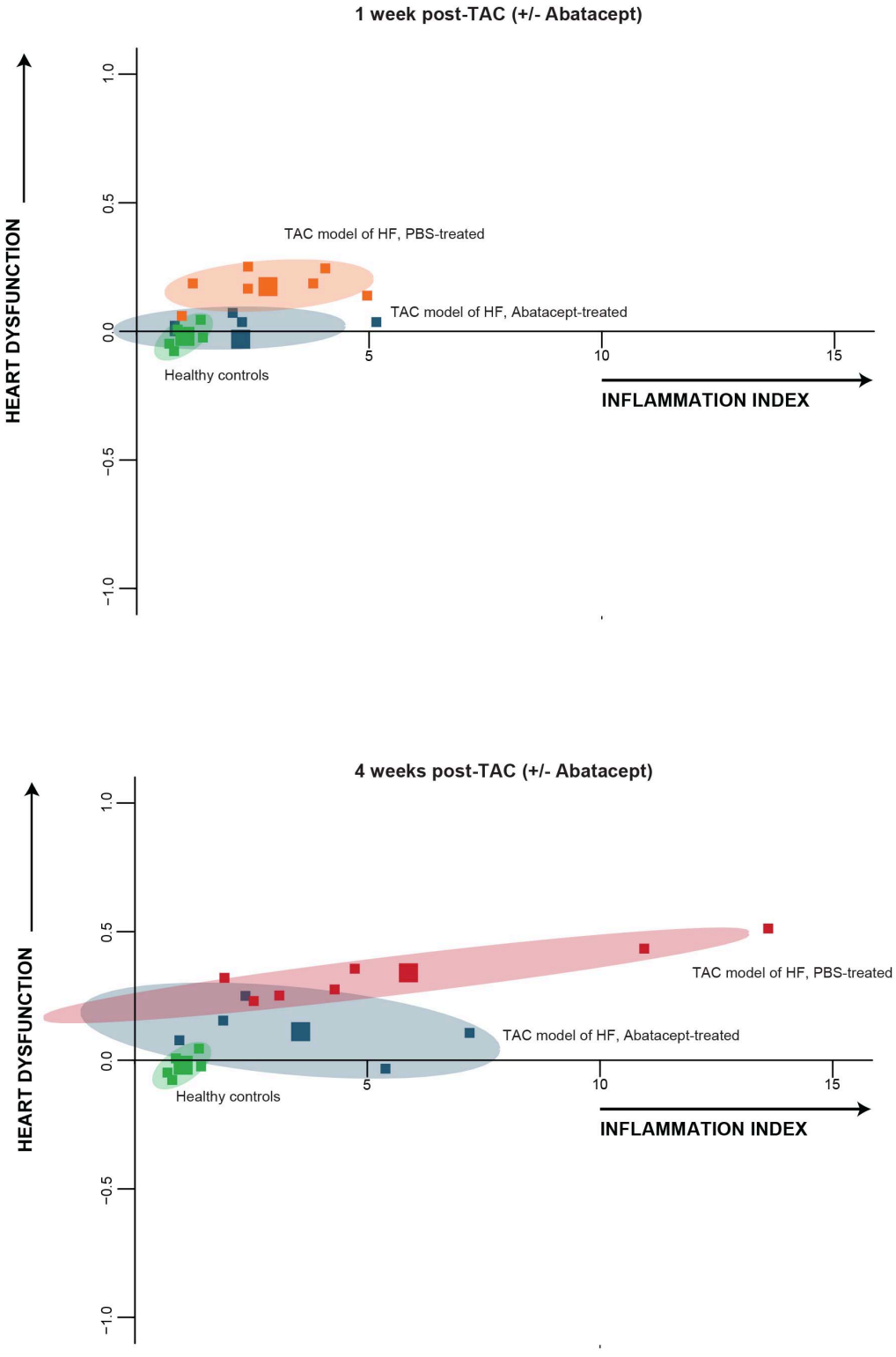

Figure 42: Realtionship between inflammation index and heart dysfucntion. Heart dysfunction index (HDI) plotted on the y axis versus an inflammation index on the x axis. Each point represents data from one mouse. Larger points indicate the mean of each group and the shaded ellipses represent one standard deviation from the mean. HDI values were internally normalized. Healthy refers to sham-operated control (PBS-treated) mice. TAC model of HF refers to TAC-operated control (PBS-treated) mice. TAC model of HF abatacept –treated refers to TAC-operated treated with abatacept three times per week starting 2 days post-operation. All groups are represented at 1 (above graph) and 4 weeks (bottom graph) post-operation. The normalization of the HDI for each mouse was calculated with the following formula: [[HDI of sample − mean HDI of matching control] / mean HDI of matching control]. The following groups were used as matching controls for normalization: for TAC-operated mice at 1 or 4 weeks post-operation: sham-operated mice prior to operation (basal reading); for healthy mice (sham-operated): sham operated prior to operation (basal reading).

Compatible with the above results, TAC-operated IL-10-deficient mice were refractive to the treatment. The cardio-protective effects of IL-10 have been previously demonstrated (Verma et al., 2012) rendering further support to the interpretation that abatacept exerts its therapeutic functions on the myocardium throughout this cytokine. Moreover, for the same reasons, the reduced heart functionality in TAC-operated IL-10-deficient mice treated with PBS is not surprising.

Abatacept targets APC by binding to CD80/CD86, yet it has been reported to not have any direct effects on DC phenotype or gene expression (Carman et al., 2009), while it has been shown to directly modulate macrophages and B cells (Mihara et al., 2000; Cutolo et al., 2009). Indeed B cells are the main source of IL-10 in response to abatacept administration. We were able to detect a low-level production of IL-10 from T cells and Treg after abatacept administration *in vitro*. Nonetheless, only the transfer of IL-10-sufficient B cells, not IL-10-sufficient T cells, prior to treatment, in TAC-operated mice lacking IL-10 was able to restore the therapeutic effects of abatacept on cardiac functionality.

Abatacept is known to exert its effects exclusively on T cell-dependent APC functions (Wenink et al., 2012; Mihara et al., 2000). Yet, *in vitro* IL-10 production by B cells in response to the drug occured in a T cell-independent manner. We can thus speculate that abatacept, via the binding of CD80/CD86 on B cells, may possibly activate intracellular signaling that induces IL-10 production in B cells, independently from T cell presence.

Another way of action of abatacept is through the induction of Treg expansion (Ko et al., 2010). However, we did not observe an increase of Treg in the left ventricle of TAC-mice treated with the drug, thus –at least in our system- there is no concrete evidence for such an effect.

In conclusion, our results show, as a consequence of abatacept treatment, IL-10 blocks the deterioration of heart functionality in TAC-operated mice. In response to abatacept administration, we detected a reduction of T cell expansion and macrophage recruitment/expansion. This may lead to reduced fibrosis and cardiomyocyte apoptosis, enabling

the preservation of heart functionality.

We have summarized our findings in a scheme (**Fig. 43**) depicting the effects of abatacept on the myocardium. In response to pressure overload-induced stress signals in the myocardium, an inflammatory response is generated, featuring increased pro-inflammatory cytokines. This inflammatory response activates and recruits macrophages. Macrophages, and B cells, acting as APC, fully activate T cells via costimulation. The T cells may then become responsible for the maintenance of the long-lasting response that ensues (Loke et al., 2007). As a consequence of this immune cell infiltration, fibrosis formation and increased cardiomyocyte cell death occurs, leading to reduced heart functionality. Abatacept administration enabled us to control this inflammatory response and thus to inhibit these three hallmarks of cardiac pathology, by impeding T cell costimulation. Moreover, abatacept induces an increased production of IL-10, mainly by B cells, which further blocks T cell expansion. IL-10 production by B cells is essential for the therapeutic effects of abatacept in the myocardium and it occurs in a T cell-independent manner. As a caveat, it is important to stress that this is not the only way to modulate HF; rather this therapeutic approach could be integrated with other therapeutic strategies. The main advantage of our approach is that abatacept is an FDA-approved drug and which been in clinical practice for more than 10 years (Moreland et al., 2006). Thus the adverse effects of the drug are limited, and its toxicological profile is well-studied. Hence, our proof-of-principle approach may have substantial translational potential.

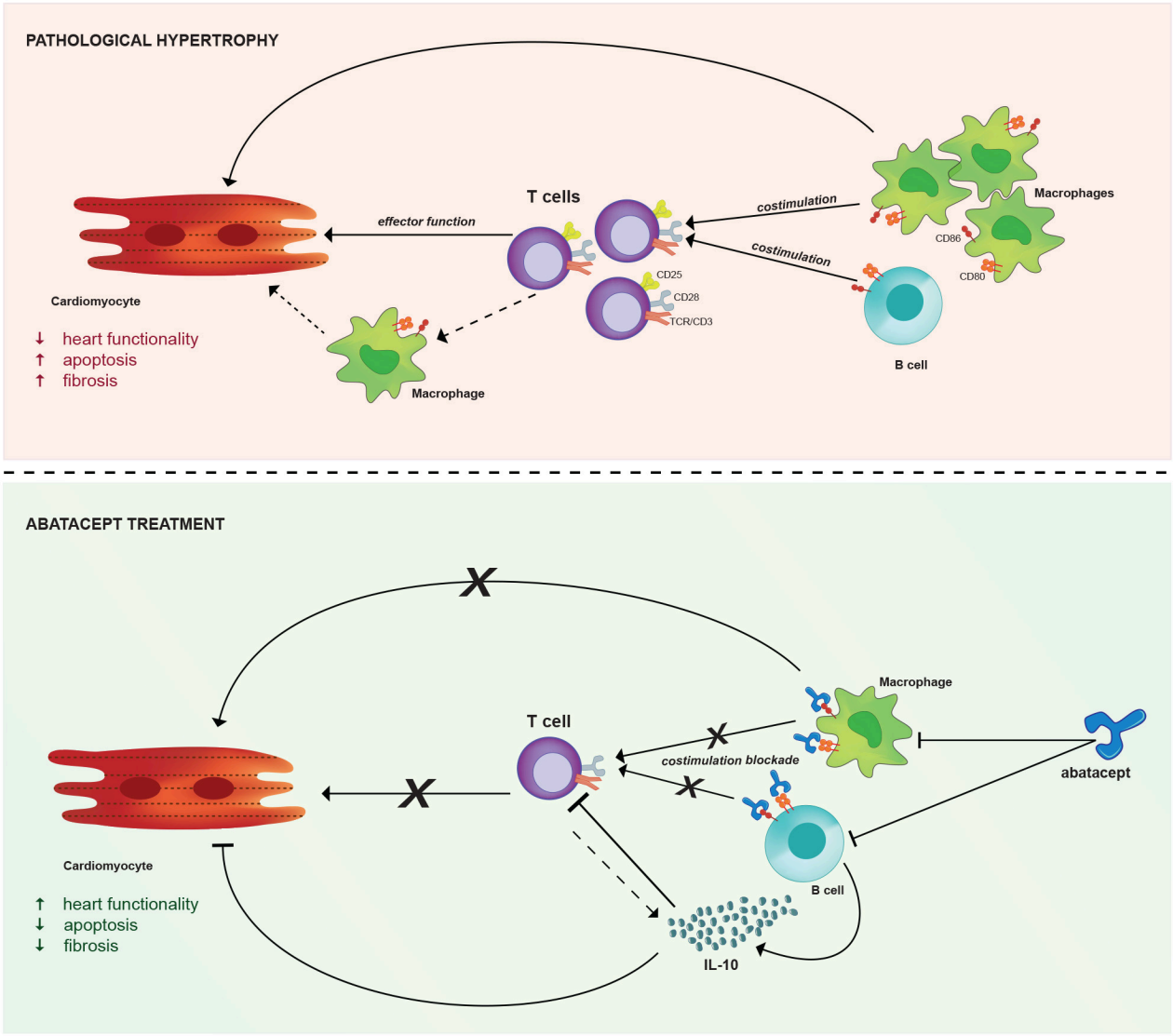

Figure 43: Summary of abatacept administration therapeutic effects in PO-induced HF. During pathological cardiac hypertrophy increase of pro-inflammatory cytokines that recruit and activate macrophages and B cells, which can act as antigen-presenting cells (APCs). T cells receive costimulation from APC via CD28 binding to CD80/CD86 and increase CD25 expression. Fully activated T cells maintain chronic inflammatory response in the myocardium responsible for increased fibrosis, apoptosis and decreased heart functionality. Administration of abatacept, which bind to CD80/CD86 expressed on APCs, blocks T cell costimulation thus reduces their activation and expansion. Direct effect on macrophages reduces their maturation and on B cells induces IL-10 production. As result of the above apoptosis and fibrosis are reduced whilst heart functionality is maintained.

7. CONCLUSIONS AND FUTURE PERSPECTIVES

The results presented in this study demonstrate that abatacept, an FDA-approved drug, that block T cell costimulation can significantly reduce the severity and delay the progression of HF in a PO-induced HF mouse model. These results taken together underline the importance of adaptive immune responses in the pathogenesis of cardiac hypertrophy and HF progression. The activation of adaptive immunity in response to cardiac stress signals could be an unwanted consequence of the immune system's inability to distinguish between pathogen-induced signals and pressure-overload induced cardiac injury. Indeed, it will be interesting to deepen our understanding in the future of the exact nature of the triggers of adaptive immune activation in HF. Above all it is necessary to assess the source of the pro-inflammatory cytokines and chemokines expressed in the left ventricle of TAC-operated mice. Although it has been reported in literature (Souders et al., 2012) and suggested from our *in-vitro* experiments on neonatal cardiomyocytes (Section 5.1.3, figure 7) that cardiomyocytes produce pro-inflammatory cytokines, it is necessary in the future perform gene expression analysis on different cell populations isolated form TAC-operated mice. It is essential in fact to notice that in this study we did not analyzed the involvement of the stromal component and of fibroblasts, which are the most abundant cell component of the myocardium (Fujiu and Nagai, 2013). Since abatacept administration reduces fibrosis formation in TAC-operated mice we hypothesized that the reduction of fibrosis is dependent on T cell activation, however it is necessary unveil the effects on fibroblasts.

Several important further analyses would be needed before usage of this therapy for HF patients in the clinic can be proposed. Although the TAC-operated mouse model is the gold-standard experimental model for HF studies, it still presents experimental limitations, as it does not completely reflect the pathogenesis of some forms of HF. Yet, our data show that T cells are

present in the myocardium of patients with different types of HF: patients with laminin A/C mutations, developing HFrEF as well as patients with aortic stenosis, mostly developing HFpEF. The TAC-operated mouse model displays HFrEF, thus resembling the symptoms of patients with laminin mutations. On the other hand, the TAC-operated mouse model is driven by the same mechanistic cause as that found in patients with aortic stenosis. The biggest limitation of the mouse model used in this study is that even if it resembles the human pathological for what concerns the triggering pathological cardiac hypertrophy, it does not match the clinical symptoms. Our therapeutic approach should be evaluated in an experimental model of HFpEF in order to add further support to its eventual applicability in the clinic. Unfortunately, currently such an experimental model has not yet been fully validated. Clinical trials in humans would have to be performed in order to validate the clinical applicability and efficacy of the approach. It is hoped that such efforts may aid in bringing a novel and greatly needed therapeutic solution to the urgent clinical burden of HF.

Finally, despites the further analyses above mentioned, this study highlights the importance of finding new pathological applications for existing drugs. Indeed, as for other pathological contexts (Marschallinger et al., 2015), validated immune-mediated therapy reagents could be suitable for novel therapeutic applications in chronic pathologies where inflammation has an active role in the progression of the disease.

8. REFERENCES

Ait-Oufella, H., Salomon, B. L., Potteaux, S., Robertson, A. K., Gourdy, P., Zoll, J., Merval, R., Esposito, B., Cohen, J. L., Fisson, S., Flavell, R. A., Hansson, G. K., Klatzmann, D., Tedgui, A., Mallat, Z. (2006). "Natural regulatory T cells control the development of atherosclerosis in mice." Nat Med 12(2): 178-180.

Alberts, B. J., A; Lewis, J; Morgan, D; Raff, M; Roberts, K; Walter, P (2007). "Molecular Biology of the Cell."

Aluvihare, V. R., Kallikourdis, M., Betz, A. G. (2005). "Tolerance, suppression and the fetal allograft." J Mol Med 83(2):88-96

Ancey, C., Corbi, P., Froger, J., Delwail, A., Wijdenes, J., Gascan, H., Potreau, D., Lecron, J. C. (2002). "Secretion of Il-6, Il-11 and Lif by Human Cardiomyocytes in Primary Culture." Cytokine 18(4): 199-205.

Andersen, K. G., Nissen, J.K., Betz, A.G. (2012). "Comparative Genomics Reveals Key Gain-of-Function Events in Foxp3 during Regulatory T Cell Evolution." Front Immunol. 3: 113

Anker, S. D. (2004). "Inflammatory mediators in chronic heart failure: an overview." Heart 90(4): 464-470.

Aoyagi, T., Matsui, T. (2012). "The Cardiomyocyte as a Source of Cytokines in Cardiac Injury." J Cell Sci Ther. (0): 003

Askling, J.; Baecklund, E.; Granath, F.; Geborek, P.; Fored, M.; Backlin, C.; Bertilsson, L.; Cöster, L.; Jacobsson, L. T.; Lindblad, S.; Lysholm, J.; Rantapää-Dahlqvist, S.; Saxne, T.; van Vollenhoven, R.; Klareskog, L.; Feltelius, N. (2009). "Anti-tumour necrosis factor therapy in rheumatoid arthritis and risk of malignant lymphomas: relative risks and time trends in the Swedish Biologics Register." Ann Rheum Dis. 68(5): 648-53.

Badenhorst, D., Maseko, M., Tsotetsi, O. J., Naidoo, A., Brooksbank, R., Norton, G. R., Woodiwiss, A. J. (2003). "Cross-linking influences the impact of quantitative changes in myocardial collagen on cardiac stiffness and remodelling in hypertension in rats." Cardiovasc Res 57(3):632-41.

Barhoumi, T., Kasal, D. A., Li, M. W., Shbat, L., Laurant, P., Neves, M. F., Paradis, P., Schiffrin, E. L. (2011). "T regulatory lymphocytes prevent angiotensin II-induced hypertension and vascular injury." Hypertension 57(3): 469-476.

Baudino, T. A., Carver, W., Giles, W., Borg, T. K. (2006). "Cardiac fibroblasts: friend or foe?" Am J Physiol Heart Circ Physiol 291(3): H1015-1026.

Bennett, C. L., Christie, J., Ramsdell, F., Brunkow, M.E., Ferguson, P.J., Whitesell, L., Kelly, T.E., Saulsbury, F.T., Chance, P.F., Ochs, H.D. (2001). "The immune dysregulation,

polyendocrinopathy, enteropathy, X-linked syndrome (IPEX) is caused by mutations of FOXP3." Nat Genet 27(1):20-1.

Berenji, K., Drazner, M. H., Rothermel, B. A., Hill, J. A. (2005). "Does load-induced ventricular hypertrophy progress to systolic heart failure?" Am J Physiol Heart Circ Physiol 289(1): H8-H16.

Berk, B. C., Fujiwara, K., Lehoux, S. (2007). "ECM remodeling in hypertensive heart disease." Journal of Clinical Investigation 117(3): 568-575.

Bopp, T., Becker, C., Klein, M., Klein-Hessling, S., Palmetshofer, A., Serfling, E., Heib, V., Becker, M., Kubach, J., Schmitt, S., Stoll, S., Schild, H., Staege, M. S., Stassen, M., Jonuleit, H., Schmitt, E. (2007). "Cyclic adenosine monophosphate is a key component of regulatory T cell-mediated suppression." J Exp Med 204(6): 1303-1310.

Bozkurt, B., Kribbs, S. B., Clubb, F. J. J., Michael, L. H., Didenko, V. V., Hornsby, P.J., Seta, Y., Oral, H., Spinale, F. G., Mann, D. L. (1998). "Pathophysiologically Relevant Concentrations of Tumor Necrosis Factor-a Promote Progressive Left Ventricular Dysfunction and Remodeling in Rats." Circulation: 1382-1391.

Buchbinder, E. I., Desai, A. (2016). "CTLA-4 and PD-1 Pathways Similarities, Differences, and Implications of Their Inhibition." American Journal of Clinical Oncology 39(1):98-106.

Carman, J. A., Davis, P.M., Yang, W.P., Zhu, J., Chang, H., He, A., Truong, A., Suchard, S.J., Nadler, S.G. (2009). "Abatacept does not induce direct gene expression changes in antigen-presenting cells." J Clin Immunol 29(4):479-89.

Carnevale, D., Pallante, F., Fardella, V., Fardella, S., Iacobucci, R., Federici, M., Cifelli, G., De Lucia, M., Lembo, G. (2014). "The angiogenic factor PlGF mediates a neuroimmune interaction in the spleen to allow the onset of hypertension." Immunity 41(5): 737-752.

Carter, N. A., Vasconcellos, R., Rosser, E.C., Tulone, C., Muñoz-Suano, A., Kamanaka, M., Ehrenstein, M.R., Flavell, R.A., Mauri C. (2011). "Mice lacking endogenous IL-10-producing regulatory B cells develop exacerbated disease and present with an increased frequency of Th1/Th17 but a decrease in regulatory T cells." J Immunol 186(10): 5569-5579.

Cerutti, A., Puga, I., Cols, M. (2013). "New helping friends for B cells." Eur J Immunol 42(8): 1956–1968.

Condorelli, G., Drusco, A., Stassi, G., Bellacosa, A., Roncarati, R., Iaccarino, G., Russo, M. A., Gu, Y., Dalton, N., Chung, C., Latronico, M. V., Napoli, C., Sadoshima, J., Croce, C. M., Ross, J. Jr. (2002). "Akt induces enhanced myocardial contractility and cell size in vivo in transgenic mice." Proc Natl Acad Sci U S A 99(19): 12333-12338.

Condorelli, G., Morisco, C., Stassi, G., Notte, A., Farina, F., Sgaramella, G., de Rienzo, A., Roncarati, R., Trimarco, B., Lembo, G. (1999). "Increased cardiomyocyte apoptosis and changes in proapoptotic and antiapoptotic genes bax and bcl-2 during left ventricular adaptations to chronic pressure overload in the rat." Circulation 99(23):3071-8.

Cosmi, L., Maggi, L., Santarlasci, V., Liotta, F., Annunziato, F. (2014). "T helper cells plasticity in inflammation." Cytometry Part A 85(1): 36-42.

Cutolo, M., Soldano, S., Montagna, P., Sulli, A., Seriolo, B., Villaggio, B., Triolo, P., Clerico, P., Felli, L., Brizzolara, R. (2009). "CTLA4-Ig interacts with cultured synovial macrophages from rheumatoid arthritis patients and downregulates cytokine production." Arthritis Res Ther 11(6): R176.

Damas, J. K., Eiken, H. G., Oie, E., Bjerkeli, V., Yndestad, A., Ueland, T., Tonnessen, T., Geiran, O. R., Aass, H., Simonsen, S., Christensen, G., Froland, S. S., Attramadal, H., Gullestad, L., Aukrust, P. (2000). "Myocardial expression of CC- and CXC-chemokines and their receptors in human end-stage heart failure " Cardiovascular Research 47(4):778-8.

Daskalopoulos, E. P., Dufeys, C., Bertrand, L., Beauloye, C., Horman, S. (2016). "AMPK in cardiac fibrosis and repair: Actions beyond metabolic regulation." J Mol Cell Cardiol 91: 188-200.

Davis, J., Molkentin, J. D. (2014). "Myofibroblasts: Trust your heart and let fate decide." Journal of Molecular and Cellular Cardiology 70: 9-18.

de Jong, S., van Veen, T. A., de Bakker, J. M., Vos, M. A., van Rijen, H. V. (2011). "Biomarkers of myocardial fibrosis." J Cardiovasc Pharmacol 57(5): 522-535.

Dhirapong, A., Yang, G.X., Nadler, S., Zhang, W., Tsuneyama, K., Leung, P., Knechtle, S., Ansari, A.A., Coppel, R.L., Liu, F.T., He, X.S., Gershwin, M.E. (2013). "Therapeutic effect of cytotoxic T lymphocyte antigen 4/immunoglobulin on a murine model of primary biliary cirrhosis." Hepatology 57(2):708-15.

Dick, S. A., Epelman, S. (2016). "Chronic Heart Failure and Inflammation. What Do We Really Know?" Circulation Research 119(1):159-76.

Dirkx, E., da Costa Martins, P. A., De Windt, L. J. (2013). "Regulation of fetal gene expression in heart failure." Biochim Biophys Acta 1832(12): 2414-2424.

Dobaczewski, M., Chen, W., Frangogiannis, N. G. (2011). "Transforming growth factor (TGF)-beta signaling in cardiac remodeling." J Mol Cell Cardiol 51(4): 600-606.

Dorn, G. W., 2nd, J. Robbins and P. H. Sugden (2003). "Phenotyping hypertrophy: eschew obfuscation." Circ Res 92(11): 1171-1175.

Drazner, M. H. (2011). "The progression of hypertensive heart disease." Circulation 123(3): 327-334.

Epelman, S., Lavine, K.J., Beaudin, A.E., Sojka, D.K., Carrero, J.A., Calderon, B., Brija, T., Gautier, E.L., Ivanov, S., Satpathy, A.T., Schilling, J.D., Schwendener, R., Sergin, I., Razani, B., Forsberg, E.C., Yokoyama, W.M., Unanue, E.R., Colonna, M., Randolph, G.J., Mann, D.L. (2014). "Embryonic and adult-derived resident cardiac macrophages are maintained through distinct mechanisms at steady state and during inflammation." Immunity 40(1): 91-104.

Floudas, A., Amu, S., Fallon, P.G. (2016). "New Insights into IL-10 Dependent and IL-10 Independent Mechanisms of Regulatory B Cell Immune Suppression." J Clin Immunol 36 Suppl 1:25-33.

Fontes, J. A., Rose, N. R., Cihakova, D. (2015). "The varying faces of IL-6: From cardiac protection to cardiac failure." Cytokine 74(1):62-8.

Forteza-Alberti, J. F., Sanchis-Gomar, F., Lippi, G., Cervellin, G., Lucia, A., Calderon-Montero, F. J. (2016). "Limits of ventricular function: from athlete's heart to a failing heart." Clin Physiol Funct Imaging doi: 10.1111/cpf.12341.

Frauwirth, K. A., Thompson, C.B. (2002). "Activation and inhibition of lymphocytes by costimulation." J Clin Invest 109(3): 295–299.

Frieler, R. A., Mortensen, R. M. (2015). "Immune Cell and Other Non-Cardiomyocyte Regulation of Cardiac Hypertrophy and Remodeling." Circulation 131(11): 1019–1030.

Fujio, Y., Nguyen, T.;, Wencker, D., Kitsis, R. N., Walsh, K. (2000). "Akt Promotes Survival of Cardiomyocytes In Vitro and Protects Against Ischemia-Reperfusion Injury in Mouse Heart." Circulation 101(6): 660–667.

Fujiu, K., Nagai, R. (2013). "Contributions of cardiomyocyte–cardiac fibroblast–immune cell interactions in heart failure development." Basic Research in Cardiology 108(4).

Garetto, S., Trovato, A.E., Lleo, A., Sala, F., Martini, E., Betz, A. G., Norata, G. D., Invernizzi, P., Kallikourdis, M. (2015). "Peak inflammation in atherosclerosis, primary biliary cirrhosis and autoimmune arthritis is counter-intuitively associated with regulatory T cell enrichment." Immunobiology 220(8):1025-9.

Gershon, R. K., Kondo, K. (1970). "Cell Interactions in the Induction of Tolerance: The Role of Thymic Lymphocytes." Immunology 18(5):723-37.

Ghigo, A., Franco, I., Morello, F., Hirsch, E. (2014). "Myocyte signalling in leucocyte recruitment to the heart." Cardiovasc Res 102(2): 270-280.

Gjesdal, O., Bluemke, D. A., Lima, J. A. (2011). "Cardiac remodeling at the population level--risk factors, screening, and outcomes." Nat Rev Cardiol 8(12): 673-685.

Gourdie, R. G., Dimmeler, S., Kohl, P. (2016). "Novel therapeutic strategies targeting fibroblasts and fibrosis in heart disease." Nat Rev Drug Discov 15(9): 620-638.

Gratz, I. K., Rosenblum, M. D., Abbas, A. K. (2013). "The life of regulatory T cells." Annals of the New York Academy of Sciences 10.1111/nyas.12011.

Grohmann, U., Orabona, C., Fallarino, F., Vacca, C., Calcinaro, F., Falorni, A., Candeloro, P., Belladonna, M.L., Bianchi, R., Fioretti, M.C., Puccetti, P. (2002). " CTLA-4-Ig regulates tryptophan catabolism in vivo." Nat Immunol 3(11):1097-101.

Grossman, W., Jones D., and McLaurin L. P. (1975). "Wall Stress and Patterns of Hypertrophy in the Human Left Ventricle." Journal of Clinical Investigation 56(1): 56–64.

Grossman, W., Paulus, W. J. (2013). "Myocardial stress and hypertrophy: a complex interface between biophysics and cardiac remodeling." J Clin Invest 123(9): 3701-3703.

Gullestad, L., Aass, H., Fjeld, J. G., Wikeby, L., Andreassen, A. K., Ihlen, H., Simonsen, S., Kjekshus, J., Nitter-Hauge, S., Ueland, T., Lien, E., Frøland, S. S., Aukrust, P. (2001). "Immunomodulating Therapy With Intravenous Immunoglobulin in Patients With Chronic Heart Failure." Circulation 103(2):220-5.

Gullestad, L., Ueland, T., Vinge, L. E., Finsen, A., Yndestad, A., Aukrust, P. (2012). "Inflammatory Cytokines in Heart Failure: Mediators and Markers." Cardiology 122(1):23-35.

Guzik, T. J., Hoch, N. E., Brown, K. A., McCann, L. A., Rahman, A., Dikalov, S., Goronzy, J., Weyand, C., Harrison, D. G. (2007). "Role of the T cell in the genesis of angiotensin II induced hypertension and vascular dysfunction." J Exp Med 204(10): 2449-2460.

Hartupee, J., Mann, D. L. (2013). "Positioning of inflammatory biomarkers in the heart failure landscape." J Cardiovasc Transl Res 6(4): 485-492.

Hasenfuss, G. (1998). "Animal models of human cardiovascular disease, heart failure and hypertrophy." Cardiovascular Research: 60–76.

Hashimoto, D., Chow, A., Noizat, C., Teo, P., Beasley, M. B., Leboeuf, M., Becker, C.D., See, P., Price, J., Lucas, D., Greter, M., Mortha, A., Boyer, S.W., Forsberg, E.C., Tanaka, M., van Rooijen, N., García-Sastre, A., Stanley, E.R., Ginhoux, F., Frenette, P.S., Merad, M. (2013). "Tissue-resident macrophages self-maintain locally throughout adult life with minimal contribution from circulating monocytes." Immunity 38(4): 792-804.

Heineke, J. and Molkentin, J. D. (2006). "Regulation of cardiac hypertrophy by intracellular signalling pathways." Nat Rev Mol Cell Biol 7(8): 589-600.

Heymans, S., González, A., Pizard, A., Papageorgiou, A. P., López-Andrés, N., Jaisser, F., Thum, T., Zannad, F., Díez, J. (2015). "Searching for new mechanisms of myocardial fibrosis with diagnostic and/or therapeutic potential." European Journal of Heart Failure 17(8): 764-771.

Hirota, H., Yoshida, K., Kishimoto, T., Taga, T. (1995). "Continuous activation of gpl30, a signal-transducing receptor component for interleukin 6-related cytokines, causes myocardial hypertrophy in mice." Proc. Natl. Acad. Sci 92 (11): 4862-4866.

Hofmann, U. and S. Frantz (2013). "How can we cure a heart "in flame"? A translational view on inflammation in heart failure." Basic Res Cardiol 108(4): 356.

Hori, S., Nomura, T., Sakaguchi, S. (2003). "Control of regulatory T cell development by the transcription factor Foxp3." Science 299(5609): 1057-1061.

Hunter, J. J. and Chien, K. R. (1999). "Signaling pathways for cardiac hypertrophy and failure." N Engl J Med 341(17): 1276-1283.

Ishibashi, M., Hiasa, K., Zhao, Q., Inoue, S., Ohtani, K., Kitamoto, S., Tsuchihashi, M., Sugaya, T., Charo, I. F., Kura, S., Tsuzuki, T., Ishibashi, T., Takeshita, A., Egashira, K. (2004). "Critical role of monocyte chemoattractant protein-1 receptor CCR2 on monocytes in

hypertension-induced vascular inflammation and remodeling." Circ Res 94(9): 1203-1210.

Janeway, C. A., Travers, P., Walport, M., Shlomchik, M. J. (2001). "Immunobiology (5th ed.)." New York and London: Garland Science.

Josefowicz, S. Z., Lu, L. F., Rudensky, A. Y. (2012). "Regulatory T cells: mechanisms of differentiation and function." Annu Rev Immunol 30: 531-564.

Kakkar, R., Lee, R. T. (2010). "Intramyocardial Fibroblast Myocyte Communication." Circulation Research 106(1): 47-57.

Kanellakis, P., Dinh, T. N., Agrotis, A., Bobik, A. (2011). "CD4(+)CD25(+)Foxp3(+) regulatory T cells suppress cardiac fibrosis in the hypertensive heart." J Hypertens 29(9): 1820-1828.

Kassan, M., Galan, M., Partyka, M., Trebak, M., Matrougui, K. (2011). "Interleukin-10 Released by CD4+CD25+ Natural Regulatory T Cells Improves Microvascular Endothelial Function Through Inhibition of NADPH Oxidase Activity in Hypertensive Mice." Arterioscler Thromb Vasc Biol 31(11):2534-42.

Kemi, O. J., Ceci, M., Wisloff, U., Grimaldi, S., Gallo, P., Smith, G. L., Condorelli, G., Ellingsen, O. (2008). "Activation or Inactivation of Cardiac Akt/mTOR Signaling Diverges Physiological From Pathological Hypertrophy." Journal of Cellular Physiology(214): 316-321.

Ko, H. J., Cho, M.L., Lee, S.Y., Oh, H.J., Heo, Y.J., Moon, Y.M., Kang, C.M., Kwok, S.K., Ju, J.H., Park, S.H., Park, K.S., Kim, H.Y. (2010). "CTLA4-Ig modifies dendritic cells from mice with collagen-induced arthritis to increase the CD4+CD25+Foxp3+ regulatory T cell population." J Autoimmun 34(2): 111-120.

Kohl, P., Camelliti, P., Burton, F. L., Smith, G. L. (2005). "Electrical coupling of fibroblasts and myocytes: relevance for cardiac propagation." Journal of Electrocardiology 38(4): 45-50.

Kong, P., Christia, P., Frangogiannis, N. G. (2014). "The pathogenesis of cardiac fibrosis." Cell Mol Life Sci 71(4): 549-574.

Kong, S. W., Bodyak, N., Yue, P., Liu, Z., Brown, J., Izumo, S., Kang, P. M. (2005). "Genetic expression profiles during physiological and pathological cardiac hypertrophy and heart failure in rats." Physiol Genomics 21(1): 34-42.

Korganow, A. S., Ji, H., Mangialaio, S., Duchatelle, V., Pelanda, R., Martin, T., Degott, C., Kikutani, H., Rajewsky, K., Pasquali, J. L., Benoist, C., Mathis, D. (1999). "From Systemic T Cell Self-Reactivity to Organ-Specific Autoimmune Disease via Immunoglobulins." Immunity 10(4): 451-461.

Kremer, J. M., Westhovens, R., Leon, M., Di Giorgio, E., Alten, R., Steinfeld, S., Russell, A., Dougados, M., Emery, P., Nuamah, I. F., Williams, G. R., Becker, J. C., Hagerty, D. T., Moreland, L. W. (2003). "Treatment of rheumatoid arthritis by selective inhibition of T-cell activation with fusion protein CTLA4Ig." N Engl J Med 349(20):1907-15.

Kubota, T., Bounoutas, G. S., Miyagishima, M., Kadokami, T., Sanders, V. J., Bruton, C., Robbins, P. D., McTiernan, C. F., Feldman, A. M. (2000). "Soluble Tumor Necrosis Factor Receptor Abrogates Myocardial Inflammation but Not Hypertrophy in Cytokine-Induced Cardiomyopathy." Circulation 101(21):2518-25.

Kubota, T., McTiernan, C. F., Frye, C. S., Slawson, S. E., Lemster, B. H., Koretsky, A. P., Demetris, A. J., Feldman, A. M. (1997). "Dilated Cardiomyopathy in Transgenic Mice With Cardiac-Specific Overexpression of Tumor Necrosis Factor-α." Circulation Research 81(4):627-35.

Kunisada, K., Negoro, S., Tone, E., Funamoto, M., Osugi, T., Yamada, S., Okabe, M., Kishimoto, T., Yamauchi-Takihara, K. (1999). "Signal transducer and activator of transcription 3 in the heart transduces not only a hypertrophic signal but a protective signal against doxorubicin-induced cardiomyopathy." PNAS 97(1):315-9.

Kuwahara, F., Kai, H., Tokuda, K., Takeya, M., Takeshita, A., Egashira, K., Imaizumi, T. (2004). "Hypertensive Myocardial Fibrosis and Diastolic Dysfunction: Another Model of Inflammation?" Hypertension 43(4): 739-745.

Kuwahara, K., Nishikimi, T., Nakao, K. (2012). "Transcriptional Regulation of the Fetal Cardiac Gene Program." Journal of Pharmacological Sciences 119(3): 198-203.

Kvakan, H., Kleinewietfeld, M., Qadri, F., Park, J.K., Fischer, R., Schwarz, I., Rahn, H.P., Plehm, R., Wellner, M., Elitok, S., Gratze, P., Dechend, R., Luft, F. C., Muller, D. N. (2009). "Regulatory T cells ameliorate angiotensin II-induced cardiac damage." Circulation 119(22): 2904-2912.

Kwon, W. Y., Cha, H. N., Heo, J. Y., Choi, J. H., Jang, B. I., Lee, I. K., Park, S. Y. (2016). "Interleukin-10 deficiency aggravates angiotensin II-induced cardiac remodeling in mice." Life Sci 146: 214-221.

Lahl, K., Loddenkemper, C., Drouin, C., Freyer, J., Arnason, J., Eberl, G., Hamann, A., Wagner, H., Huehn, J., Sparwasser, T. (2007). "Selective depletion of Foxp3+ regulatory T cells induces a scurfy-like disease." J Exp Med 204(1): 57-63.

Lai, N. C., Gao, M. H., Tang, E., Tang, R., Guo, T., Dalton, N. D., Deng, A., Tang, T. (2012). "Pressure overload-induced cardiac remodeling and dysfunction in the absence of interleukin 6 in mice." Lab Invest 92(11): 1518-1526.

Laroumanie, F., Douin-Echinard, V., Pozzo, J., Lairez, O., Tortosa, F., Vinel, C., Delage, C., Calise, D., Dutaur, M., Parini, A., Pizzinat, N. (2014). "CD4+ T cells promote the transition from hypertrophy to heart failure during chronic pressure overload." Circulation 129(21): 2111-2124.

Latronico, M. V., Elia, L., Condorelli, G., Catalucci, D. (2008). "Heart failure: targeting transcriptional and post-transcriptional control mechanisms of hypertrophy for treatment." Int J Biochem Cell Biol 40(9): 1643-1648.

Levine, B., Kalman, J., Mayer, L., Fillit, H.M., Packer, M. (1990). "Elevated Circulating Levels of Tumor Necrosis Factor in Severe Chronic Heart Failure." N Engl J Med 323(4):236-41.

Loke, P., Gallagher, I., Nair, M. G., Zang, X., Brombacher, F., Mohrs, M., Allison, J. P., Allen, J. E. (2007). "Alternative Activation Is an Innate Response to Injury That Requires CD4+ T Cells to be Sustained during Chronic Infection." The Journal of Immunology 179(6): 3926-3936.

Maisel, A. (2001). "B-type natriuretic peptide levels: a potential novel "white count" for congestive heart failure." J Card Fail 7(2): 183-193.

Manis, J. P., Tian, M., Alt, F. W. (2002). "Mechanism and control of class-switch recombination." Trends in Immunology 23 (1): 31-39.

Mann, D. L. (2002). "Inflammatory Mediators and the Failing Heart: Past, Present, and the Foreseeable Future." Circulation Research 91(11): 988-998.

Mann, D. L. (2015). "Innate immunity and the failing heart: the cytokine hypothesis revisited." Circ Res 116(7): 1254-1268.

Mann, M. K., Maresz, K., Shriver, L. P., Tan, Y., Dittel, B. N. (2007). "B Cell Regulation of CD4+CD25+ T Regulatory Cells and IL-10 Via B7 is Essential for Recovery From Experimental Autoimmune Encephalomyelitis." The Journal of Immunology 178(6): 3447-3456.

Marschallinger, J., Schäffner, I., Klein, B., Gelfert, R., Rivera, F. J., Illes, S., Grassner, L., Janssen, M., Rotheneichner, P., Schmuckermair, C., Coras, R., Boccazzi, M., Chishty, M., Lagler, F. B., Renic, M., Bauer, H. C., Singewald, N., Blümcke, I., Bogdahn, U., Couillard-Despres, S., Lie, D. C., Abbracchio, M. P., Aigner, L. (2015). "Structural and functional rejuvenation of the aged brain by an approved anti-asthmatic drug." Nat Commun 6: 8466.

Matrougui, K., Abd Elmageed, Z., Kassan, M., Choi, S., Nair, D., Gonzalez-Villalobos, R. A., Chentoufi, A. A., Kadowitz, P., Belmadani, S., Partyka, M. (2011). "Natural regulatory T cells control coronary arteriolar endothelial dysfunction in hypertensive mice." Am J Pathol 178(1): 434-441.

Matsumoto, K., Ogawa, M., Suzuki, J., Hirata, Y., Nagai, R., Isobe, M. (2011). "Regulatory T lymphocytes attenuate myocardial infarction-induced ventricular remodeling in mice." Int Heart J 52(6): 382-387.

Mauri, M., Bosma, A. (2012). "Immune Regulatory Function of B Cells." Annu. Rev. Immunol 30:221-41.

McMullen, J. R., Shioi, T., Huang, W. Y., Zhang, L., Tarnavski, O., Bisping, E., Schinke, M., Kong, S., Sherwood, M. C., Brown, J., Riggi, L., Kang, P. M., Izumo, S. (2004). "The insulin-like growth factor 1 receptor induces physiological heart growth via the phosphoinositide 3-kinase(p110alpha) pathway." J Biol Chem 279(6): 4782-4793.

Melendez, G. C., McLarty, J. L., Levick, S. P., Du, Y., Janicki, J. S., Brower, G. L. (2010). "Interleukin 6 mediates myocardial fibrosis, concentric hypertrophy, and diastolic dysfunction in rats." Hypertension 56(2): 225-231.

Meng, X., Yang, J., Dong, M., Zhang, K., Tu, E., Gao, Q., Chen, W., Zhang, C., Zhang, Y. (2015). "Regulatory T cells in cardiovascular diseases." Nature Reviews cardiology 1 3(3):167-79.

Mian, M. O., Barhoumi, T., Briet, M., Paradis, P., Schiffrin, E. L. (2016). "Deficiency of T-regulatory cells exaggerates angiotensin II-induced microvascular injury by enhancing immune responses." J Hypertens 34(1): 97-108.

Mihara, M., Tan, I., Chuzhin,Y., Reddy, B., Budha, L., Holzer, A., Gu, Y., Davidson, A. (2000). "CTLA4Ig inhibits T cell-dependent B-cell maturation in murine systemic lupus erythematosus." J Clin Immunol 106(1):91-101.

Mihl, C., Dassen, W.R.M., Kuipers H. (2008). "Cardiac remodelling: concentric versus eccentric hypertrophy in strength and endurance athletes." Netherlands Heart Journal 6(4): 129–133.

Mizoguchi, A., Mizoguchi, E., Takedatsu, H., Blumberg, R. S., Bhan, A. K. (2002). "Chronic Intestinal Inflammatory Condition Generates IL-10-Producing Regulatory B Cell Subset Characterized by CD1d Upregulation." Immunity 16: 219-230.

Moreland, L., Bate, G., Kirkpatrick, P. (2006). "Abatacept." Nat Rev Drug Discov. 5(3):185-6.

Mosmann, T. R., Cherwinski, H., Bond, M. W., Giedlin, M. A., Coffman, R. L. (1986). "Two types of murine helper T cell clone. I. Definition according to profiles of lymphokine activities and secreted proteins." J Immunol 175(1):5-14.

Murakami, N., Riella, L. V. (2014). "Co-inhibitory pathways and their importance in immune regulation." Transplantation 98(1):3-14.

Naugle, J. E., Olson, E. R., Zhang, X., Mase, S. E., Pilati, C. F., Maron, M. B., Folkesson, H. G., Horne, W. I., Doane, K. J. and Meszaros, J. G. (2006). "Type VI collagen induces cardiac myofibroblast differentiation: implications for postinfarction remodeling." Am J Physiol Heart Circ Physiol 10.1152/ajpheart.00321.2005.

Nengwen, K., Su, A., Youping, L. (2014). "Expression of CD80 on cultured neonatal mice cardiomyocytes and attenuation of cytotoxic T lymphocyte-mediated lysis." Transplant Proc 46(1):266-70.

Nevers, T., Salvador, A. M., Grodecki-Pena, A., Knapp, A., Velazquez, F., Aronovitz, M., Kapur, N. K., Karas, R. H., Blanton, R. M., Alcaide, P. (2015). "Left Ventricular T-Cell Recruitment Contributes to the Pathogenesis of Heart Failure." Circ Heart Fail 8(4): 776-787.

Oh, S., Hwang, E. S. (2014). "The role of protein modifications of T-bet in cytokine production and differentiation of T helper cells." J Immunol Res 2014: 589672.

Pandiyan, P., Zheng, L., Ishihara, S., Reed, J., Lenardo, M. J. (2007). "CD4+CD25+Foxp3+ regulatory T cells induce cytokine deprivation-mediated apoptosis of effector CD4+ T cells." Nat Immunol 8(12): 1353-1362.

Peng, H., Yang, X. P., Carretero, O. A., Nakagawa, P., D'Ambrosio, M., Leung, P., Xu, J., Peterson, E. L., Gonzalez, G. E., Harding, P., Rhaleb, N. E. (2011). "Angiotensin II-induced dilated cardiomyopathy in Balb/c but not C57BL/6J mice." Exp Physiol 96(8): 756-764.

Perrino, C., Naga Prasad, S. V., Mao, L., Noma, T., Yan, Z., Kim, H. S., Smithies, O., Rockman, H. A. (2006). "Intermittent pressure overload triggers hypertrophy-independent cardiac dysfunction and vascular rarefaction." J Clin Invest 116(6): 1547-1560.

Porter, K. E., Turner, N. A. (2009). "Cardiac fibroblasts: at the heart of myocardial remodeling." Pharmacol Ther 123(2): 255-278.

Rai, V., Sharma, P., Agrawal, S., Agrawal, D. K. (2016). "Relevance of mouse models of cardiac fibrosis and hypertrophy in cardiac research." Mol Cell Biochem 424(1-2):123-145.

Ren, J., Samsonb, W. K., Sowersc, J. R. (1999). "Insulin-like Growth Factor I as a Cardiac Hormone: Physiological and Pathophysiological Implications in Heart Disease." Journal of Molecular and Cellular Cardiology 31(11):2049-61.

Rockman, H. A., Koch, W. J., Lefkowitz, R. J. (1997). "Cardiac function in genetically engineered mice with altered adrenergic receptor signaling." Am. J. Physiol. 272(4 Pt 2):H1553-9.

Rockman, H. A., Ross, R.S., Harris, A.N., Knowlton, K.U., Steinhelper, M.E., Field, L.J., Ross, J. Jr., Chien, K.R. (1991). "Segregation of atrial-specific and inducible expression of an atrial natriuretic factor transgene in an in vivo murine model of cardiac hypertrophy." Proc. Natl. Acad. Sci. 88(18): 8277–8281.

Roncarati, R., Viviani Anselmi, C., Krawitz, P., Lattanzi, G., von Kodolitsch, Y., Perrot, A., di Pasquale, E., Papa, L., Portararo, P., Columbaro, M., Forni, A., Faggian, G., Condorelli, G., Robinson, P. N. (2013). "Doubly heterozygous LMNA and TTN mutations revealed by exome sequencing in a severe form of dilated cardiomyopathy." Eur J Hum Genet. 21(10):1105-11.

Ross, J. J., Braunwald, E. (1968). "Aortic stenosis." Circulation. 38(1 Suppl):61-7.

Rost, R. (1997). "The athlete's heart. Historical perspectives--solved and unsolved problems." Cardiol Clin: 493-512.

Rubtsov, Y. P., Rasmussen, J. P., Chi, E. Y., Fontenot, J., Castelli, L., Ye, X., Treuting, P., Siewe, L., Roers, A., Henderson, W. R., Jr., Muller, W., Rudensky, A. Y. (2008). "Regulatory T cell-derived interleukin-10 limits inflammation at environmental interfaces." Immunity 28(4): 546-558.

Rudd, C. E., Taylor, A., Schneider, H. (2009). "CD28 and CTLA-4 coreceptor expression and signal transduction." Immunol Rev. 229(1):12-26.

Sakaguchi, S., Sakaguchi, N., Asano, M., Itoh, M., Toda, M. (1995). "Immunologic self-tolerance maintained by activated T cells expressing IL-2 receptor alpha-chains (CD25). Breakdown of a single mechanism of self-tolerance causes various autoimmune diseases." J Immunol 155(3): 1151-1164.

Sakaguchi, S., Yamaguchi, T., Nomura, T., Ono, M. (2008). "Regulatory T cells and immune tolerance." Cell 133(5): 775-787.

Sallusto, F., Lanzavecchia, A., Mackay, C. R. (1998). "Chemokines and chemokine receptors in T-cell priming and Th1/Th2-mediated responses." Immunol Today 19(12):568-74.

Samak, M., Fatullayev, J., Sabashnikov, A., Zeriouh, M., Schmack, B., Farag, M., Popov, A. F., Dohmen, P. M., Choi, Y. H., Wahlers, T., Weymann, A. (2016). "Cardiac Hypertrophy: An Introduction to Molecular and Cellular Basis." Med Sci Monit Basic Res 22: 75-79.

Sarris, M., Andersen, K. G., Randow, F., Mayr, L., Betz, A. G. (2008). "Neuropilin-1 expression on regulatory T cells enhances their interactions with dendritic cells during antigen recognition." Immunity 28(3):402-13.

Sasayama, S., Okada, M., Matsumori, A. (2000). "Chemokines and cardiovascular diseases." Cardiovascular Research 45(2):267-9.

Seta, Y., Shan, K., Bozkurt, B., Oral, H., Mann, D. L. (1996). "Basic Mechanisms in Heart Failure: The Cytokine Hypothesis." Journal of Cardiac Failure 2(3): 243-249.

Sharpe, A. H. (2009). "Mechanisms of costimulation." Immunol Rev 229(1):5-11.

Sharpe, A. H., Freeman, G. J. (2002). "The B7-CD28 superfamily." Nat Rev Immunol. 2(2):116-26.

Shevach, E. M. (2009). "Mechanisms of foxp3+ T regulatory cell-mediated suppression." Immunity 30(5): 636-645.

Shevach, E. M. (2011). "Biological functions of regulatory T cells." Advances in immunology 112: 137-176.

Shevach, E. M., Thornton, A. M. (2014). "tTregs, pTregs, and iTregs: similarities and differences." Immunol Rev 259(1): 88-102.

Shi, J. and Wei, L. (2012). "Regulation of JAK/STAT signalling by SOCS in the myocardium." Cardiovasc Res 96(3):345-7.

Shimizu, I. and Minamino, T. (2016). "Physiological and pathological cardiac hypertrophy." J Mol Cell Cardiol 97: 245-262.

Silverthorn, D. U. (2007). "Human Physiology: An Integrated Approach with Interactive Physiology." Pearson Education 4th Edition.

Souders, C. A., Borg, T. K., Banerjee, I., Baudino, T. A. (2012). "Pressure overload induces early morphological changes in the heart." Am J Pathol 181(4): 1226-1235.

Stavnezera, J., Amemiya, C. T. (2004). "Evolution of isotype switching." Seminars in Immunology 16(4):257-75.

Stølen, T. O., Høydal, M. A., Kemi, O. J., Catalucci, D., Ceci, M., Aasum, E., Larsen, T., Rolim, N., Condorelli, G., Smith, G. L., Wisløff, U. (2009). "Interval training normalizes

cardiomyocyte function, diastolic Ca2+ control, and SR Ca2+ release synchronicity in a mouse model of diabetic cardiomyopathy." Circ Res. 105(6):527-36.

Szabo, S. J., Kim, S. T., Costa, G. L., Zhang, X., Fathman, C. G., Glimcher, L. H. (2000). "A Novel Transcription Factor, T-bet, directs Th1 Lineage Commitment." Cell. 100(6):655-69.

Szabo-Fresnais, N., Lefebvre, F., Germain, A., Fischmeister, R., Pomerance, M. (2010). "A new regulation of IL-6 production in adult cardiomyocytes by beta-adrenergic and IL-1 beta receptors and induction of cellular hypertrophy by IL-6 trans-signalling." Cell Signal 22(7): 1143-1152.

Tadokoro, C. E., Shakhar, G., Shen, S., Ding, Y., Lino, A. C., Maraver, A., Lafaille, J. J., Dustin, M. L. (2006). "Regulatory T cells inhibit stable contacts between CD4+ T cells and dendritic cells in vivo." J Exp Med 203(3): 505-511.

Takahashi, T., Tagami, T., Yamazaki, S., Uede, T., Shimizu, J., Sakaguchi, N., Mak, T. W., Sakaguchi, S. (2000). "Immunologic self-tolerance maintained by CD25(+)CD4(+) regulatory T cells constitutively expressing cytotoxic T lymphocyte-associated antigen 4." J Ex Med. 192(2):303-10.

Tan, S. M.; Zhang, Y.; Connelly, K. A.; Gilbert, R. E.; Kelly, D. J. (2010). "Targeted inhibition of activin receptor-like kinase 5 signaling attenuates cardiac dysfunction following myocardial infarction." Am J Physiol Heart Circ Physiol 298: H1415–H1425.

Tang, T. T., Yuan, J., Zhu, Z.F., Zhang, W.C., Xiao, H., Xia, N., Yan, X.X., Nie, S.F., Liu, J., Zhou, S.F., Li, J.J., Yao, R., Liao, M.Y., Tu, X., Liao, Y.H., Cheng, X. (2012). "Regulatory T cells ameliorate cardiac remodeling after myocardial infarction." Basic Res Cardiol 107(1): 232.

Taylor, C. T., Pouyssegur, J. (2007). "Oxygen, hypoxia, and stress." Ann N Y Acad Sci 1113: 87-94.

Terrell, A. M., Crisostomo, P. R., Wairiuko, G. M., Wang, M., Morrell, E. D., Meldrum, D. R. (2006). "Jak/STAT/SOCS signaling circuits and associated cytokine-mediated inflammation and hypertrophy in the heart." Shock 26(3): 226-234.

Tham, Y. K., Bernardo, B. C., Ooi, J. Y., Weeks, K. L., McMullen, J. R. (2015). "Pathophysiology of cardiac hypertrophy and heart failure: signaling pathways and novel therapeutic targets." Arch Toxicol 89(9): 1401-1438.

Tomasek, J. J., Gabbiani, G., Hinz, B., Chaponnier, C., Brown, R. A. (2002). "Myofibroblasts and mechano-regulation of connective tissue remodelling." Nature Reviews Molecular Cell Biology 3(5): 349-363.

Utans, U., Arceci, R. J., Yamashita, Y., Russell, M. E. (1995). "Cloning and characterization of allograft inflammatory factor-1: a novel macrophage factor identified in rat cardiac allografts with chronic rejection." J Clin Immunol. 95(6):2954-62.

Van Linthout, S., Miteva, K., Tschope, C. (2014). "Crosstalk between fibroblasts and inflammatory cells." Cardiovasc Res 102(2): 258-269.

Van Tassell, B. W., Seropian, I. M., Toldo, S., Mezzaroma, E., Abbate, A. (2013). "Interleukin-1beta induces a reversible cardiomyopathy in the mouse." Inflamm Res 62(7): 637-640.

Van Tassell, B. W., Valle Raleigh, J. M., Abbate, A. (2014). "Targeting Interleukine-1 in Heart Failure and Inflammatory Heart Disease." Curr Heart Fail Rep. 12(1):33-41.

Vazquez, M. I., Catalan-Dibene, J., Zlotnik, A. (2015). "B cells responses and cytokine production are regulated by their immune microenvironment." Cytokine. 74(2):318-26.

Verma, S. K., Krishnamurthy, P., Barefield, D., Singh, N., Gupta, R., Lambers, E., Thal, M., Mackie, A., Hoxha, E., Ramirez, V., Qin, G., Sadayappan, S., Ghosh, A. K., Kishore, R. (2012). "Interleukin-10 treatment attenuates pressure overload-induced hypertrophic remodeling and improves heart function via signal transducers and activators of transcription 3-dependent inhibition of nuclear factor-kappaB." Circulation 126(4): 418-429.

Vignali, D. A., Collison, L. W., Workman, C. J. (2008). "How regulatory T cells work." Nat Rev Immunol 8(7): 523-532.

Walker, L. S., Sansom, D. M. (2011). "The emerging role of CTLA4 as a cell-extrinsic regulator of T cell responses." Nat Rev Immunol. 11(12):852-63.

Wang, M., Markel, T., Crisostomo, P., Herring, C., Meldrum, K. K., Lillemoe, K. D., Meldrum, D. R. (2007). "Deficiency of TNFR1 protects myocardium through SOCS3 and IL-6 but not p38 MAPK or IL-1beta." Am J Physiol Heart Circ Physiol. 292(4):H1694-9.

Waterhouse, P., Penninger, J. M., Timms, E., Wakeham, A., Shahinian, A., Lee, K. P., Thompson, C. B., Griesser, H., Mak, T. W. (1995). "Lymphoproliferative disorders with early lethality in mice deficient in Ctla-4." Science. 270(5238):985-8.

Weirather, J., Hofmann, U. D., Beyersdorf, N., Ramos, G. C., Vogel, B., Frey, A., Ertl, G., Kerkau, T., Frantz, S. (2014). "Foxp3+ CD4+ T cells improve healing after myocardial infarction by modulating monocyte/macrophage differentiation." Circ Res 115(1): 55-67.

Wenink, M. H., Santegoets, K. C., Platt, A. M., van den Berg, W. B., van Riel, P. L., Garside, P., Radstake, T. R., McInnes, I. B. (2012). "Abatacept modulates proinflammatory macrophage responses upon cytokine-activated T cell and Toll-like receptor ligand stimulation." Ann Rheum Dis. 71(1):80-3.

Weinblatt, M. E., Moreland, L. W., Westhovens, R., Cohen, R. B., Kelly, S. M., Khan, N. Pappu, R., Delaet, I., Luo, A., Gujrathi, S., Hochberg, M. C. (2013). "Safety of abatacept administered intravenously in treatment of rheumatoid arthritis: integrated analyses of up to 8 years of treatment from the abatacept clinical trial program." J Rheumatol. 40(6): 787-97.

Wing, K., Onishi, Y., Prieto-Martin, P., Yamaguchi, T., Miyara, M., Fehervari, Z., Nomura, T., Sakaguchi, S. (2008). "CTLA-4 control over Foxp3+ regulatory T cell function." Science. 322(5899):271-5.

Wing, K., Sakaguchi, S. (2010). "Regulatory T cells exert checks and balances on self tolerance and autoimmunity." Nat Immunol 11(1): 7-13.

Wu, Y. L., Liang, J., Zhang, W., Tanaka, Y., Sugiyama, H. (2012). "Immunotherapies: the blockade of inhibitory signals." Int J Biol Sci 8(10): 1420 - 1430.

Wynn, T. A. (2004). "Fibrotic disease and the T(H)1/T(H)2 paradigm." Nat Rev Immunol 4(8):583-94.

Yang, F., Dong, A., Mueller, P., Caicedo, J., Sutton, A. M., Odetunde, J., Barrick, C. J., Klyachkin, Y. M., Abdel-Latif, A., Smyth, S. S. (2012). "Coronary artery remodeling in a model of left ventricular pressure overload is influenced by platelets and inflammatory cells." PLoS One 7(8): e40196.

Ying, X., Lee, K., Li, N., Corbett, D., Mendoza, L., Frangogiannis, N. G. (2009). "Characterization of the Inflammatory and Fibrotic Response in a Mouse Model of Cardiac Pressure Overload." Histochem Cell Biol. 131(4):471-81.

Yndestad, A., Damas, J. K., Oie, E., Ueland, T., Gullestad, L., Aukrust, P. (2006). "Systemic inflammation in heart failure--the whys and wherefores." Heart Fail Rev 11(1): 83-92.

Yu, Q., Horak, K., Larson, D. F. (2006). "Role of T lymphocytes in hypertension-induced cardiac extracellular matrix remodeling." Hypertension 48(1): 98-104.

Zandbergen, H. R., Sharma, U.C., Gupta, S., Verjans, J.W., van den Borne, S., Pokharel, S., van Brakel, T., Duijvestijn, A., van Rooijen, N., Maessen, J.G., Reutelingsperger, C., Pinto, Y.M., Narula, J., Hofstra, L. (2009). "Macrophage Depletion in Hypertensive Rats Accelerates Development of Cardiomyopathy." Journal of Cardiovascular Pharmacology and Therapeutics. 14(1):68-75.

Zhang, D. H., Cohn, L., Ray, L., Bottomly, K., Ray, A. (1997). "Transcription Factor GATA-3 Is Differentially Expressed in Murine Th1 and Th2 Cells and Controls Th2-specific Expression of the Interleukin-5 Gene." The Journal of Biological Chemistry. 272(34):21597-603.

Zhu, J. (2015). "T helper 2 (Th2) cell differentiation, type 2 innate lymphoid cell (ILC2) development and regulation of interleukin-4 (IL-4) and IL-13 production." Cytokine. 75(1):14-24.

Zhu, J., Paul, W. E. (2010). "Heterogeneity and plasticity of T helper cells." Cell Res 20(1): 4-12.